INFORMATION TO USERS

This material was produced from a microfilm copy of the original document. While the most advanced technological means to photograph and reproduce this document have been used, the quality is heavily dependent upon the quality of the original submitted.

The following explanation of techniques is provided to help you understand markings or patterns which may appear on this reproduction.

1. The sign or "target" for pages apparently lacking from the document photographed is "Missing Page(s)". If it was possible to obtain the missing page(s) or section, they are spliced into the film along with adjacent pages. This may have necessitated cutting thru an image and duplicating adjacent pages to insure you complete continuity.

2. When an image on the film is obliterated with a large round black mark, it is an indication that the photographer suspected that the copy may have moved during exposure and thus cause a blurred image. You will find a good image of the page in the adjacent frame.

3. When a map, drawing or chart, etc., was part of the material being photographed the photographer followed a definite method in "sectioning" the material. It is customary to begin photoing at the upper left hand corner of a large sheet and to continue photoing from left to right in equal sections with a small overlap. If necessary, sectioning is continued again — beginning below the first row and continuing on until complete.

4. The majority of users indicate that the textual content is of greatest value, however, a somewhat higher quality reproduction could be made from "photographs" if essential to the understanding of the dissertation. Silver prints of "photographs" may be ordered at additional charge by writing the Order Department, giving the catalog number, title, author and specific pages you wish reproduced.

5. PLEASE NOTE: Some pages may have indistinct print. Filmed as received.

University Microfilms International
300 North Zeeb Road
Ann Arbor, Michigan 48106 USA
St. John's Road, Tyler's Green
High Wycombe, Bucks, England HP10 8HR

78-8696

SILVERSTEIN, Jeffrey Lester, 1947-
ASPECTS OF THE DESIGN AND CONTROL OF FIXED BED CATALYTIC REACTORS.

City University of New York, Ph.D., 1978
Engineering, chemical

University Microfilms International, Ann Arbor, Michigan 48106

ASPECTS OF THE DESIGN AND CONTROL OF FIXED BED CATALYTIC REACTORS

by

JEFFREY L. SILVERSTEIN

A dissertation submitted to the Graduate Faculty in Engineering in partial fulfillment of the requirements for the degree of Doctor of Philosophy, The City University of New York.

1977

This manuscript has been read and accepted for the Graduate Faculty in Engineering in satisfaction of the dissertation requirement for the degree of Doctor of Philosophy.

Jan 7 78
Date

Chairman of Examining Committee

January 4, 1978
Date

Executive Officer

Prof. R. A. Graff

Prof. F. Thau

Prof. R. Mekel

Supervisory Committee

The City University of New York

ABSTRACT

ASPECTS OF THE DESIGN AND CONTROL
OF FIXED BED CATALYTIC REACTORS

by

Jeffrey L. Silverstein

Adviser: Professor Reuel Shinnar

The study of catalytic reactions in micro reactors for purposes of scale-up is often hampered by the fact that backmixing and mass transfer effects are more pronounced than in large industrial reactors. A minimum reactor size is often needed for reliable scale-up. Section I of this dissertation describes some simplified design methods to compute it. It is shown that reasonable estimates for the minimum size can be obtained by computing the variance of the contact time distribution in the catalyst phase. The way in which the variance is related to the conversion and the selectivity in the reactor is described and the relationship between the variance and the design parameters of the reactor is discussed.

The design and control strategies for catalytic fixed bed reactors with external heat feedback are often difficult to develop because of the complex nature of the system behavior and that of its component units. Section II of this dissertation shows how much a system, with

inherent positive feedback, can be analyzed by generating the frequency responses of its component units separately, and then matching and suitably altering them to obtain a desired frequency response and stability margin for the entire system.

Two practical examples are offered to illustrate the technique and to show how alterations in the basic system design can sometimes simplify the control problem. The economic penalties of these alterations are discussed qualitatively and it is indicated that a compromise is often required between increased costs, improved steady state operation and easier control.

The nonlinear behavior of the reactor is also discussed. A simple method of nonlinear analysis is described which involves a series of computer simulations to generate the nonlinear frequency responses. The nonlinear behavior of the control loops are discussed in terms of their saturation limits when large disturbances are involved. It is shown how a simple alteration in the basic control strategy can significantly extend the range of control.

DEDICATION

To Christine, whose love and encouragement, more than anything else, contributed to the completion of this work.

ACKNOWLEDGEMENTS

The author wishes to express his gratitude to his family and friends for their support during the course of this work. Thanks are also offered to Prof. Reuel Shinnar for his assistance in this endeavor.

Financial assistance was made available at various times by the City College Fund, the National Science Foundation, and the American Chemical Society. This aid is gratefully acknowledged.

TABLE OF CONTENTS

TABLE OF CONTENTS (continued)

LIST OF TABLES - SECTION I

LIST OF TABLES - SECTION II

LIST OF FIGURES - SECTION I

LIST OF FIGURES - SECTION II

SECTION I - DESIGN OF FIXED BED CATALYTIC MICROREACTORS

INTRODUCTION

Due to increasing costs of large scale pilot plants and the delay involved in starting up the industrial plant while data is being taken, the need for fast, reliable and economical means of data gathering is taking on greater importance. Pigford (1972) recently expressed his concern regarding this problem and indicated that use of micro-scale equipment with scale-up factors of one million or more might offer a solution. Micro-equipment offers advantages over conventional pilot plant equipment because it is economical and fast and easy to construct.

This paper deals with the design of fixed bed catalytic micro-reactors. Several investigators (Mears, 1971; Bischoff, 1969; Edwards and Richardson, 1968; Aris and Amundson, 1957; McHenry and Wilhelm, 1967; Wehner and Wilhelm, 1956) have already dealt with some specific aspects of the problem--the effects of molecular and turbulent diffusion. However, there are other factors such as mass transfer to the catalyst particles and intraparticle transport processes which also affect the operation of small reactors. The result of these four effects on the reactor is to cause it to deviate from plug flow. Deviations from plug flow will reduce the conversion and affect the selectivity of the reactor giving unreliable estimates for the performance of the industrial reactor. It is well known that these effects can be diminished by increasing the length of the reactor or by decreasing the catalyst particle size.

It is recognized that plug flow conditions do not insure reliable kinetic results. It is just as important that the reactor be isothermal, because nonisothermal effects are often more important than mixing and diffusional effects in affecting kinetics. However, it is much easier to experimentally determine if the reactor is isothermal than it is to measure mixing effects. Thus, there is a justification for treating the case of mixing separately.

Often the different transport processes are treated separately, but really they have a cumulative effect on plug flow and, as we will show, they can be evaluated by a single criterion--the variance of the contact time distribution. Although this thesis was done specifically for the design of micro-reactors, the results are independent of reactor size. In this sense the study might also be useful for designing industrial packed bed reactors.

THEORY

General Reactor Model

This approach is based on the concept of the contact time distribution in the catalyst phase. Measurement of it has been discussed by Glasser, et.al. (1973), and its application to catalytic reactors has been discussed by several authors (Levenspiel and Kunii, 1969; Krambeck, et.al., 1969; Orcutt, et.al., 1962). The many questions that arose regarding the latest article (Glasser, et.al., 1973) indicate that a clarification of this concept might be in order.

In a homogeneous reactor we can clearly define a residence time distribution and show that it completely describes any first order kinetics. In a catalytic reactor, however, the definition is more difficult. For a first order reaction it is not sufficient to know how long a molecule has resided in the total system. Only the time spent near a reactive site is important. We cannot define or measure this time, just as we cannot measure local reaction rates. In this sense the concept of a contact time distribution is fictitious in the same way as is a reaction rate per unit volume of catalyst. These concepts involve the implicit assumption that if we grind the catalyst particles to a small enough size further reduction of size will not affect reaction rates. Consequently, nonuniformities and small scale transport processes can be ignored.

As a single molecule travels through a heterogeneous reactor it passes in and out of several catalyst particles. It is this cumulative sojourn time inside the particles which we define as the contact time. The mean contact time, τ_c, is just the total catalyst volume divided by the volumetric flow rate. If the contact time distribution is a delta function, then the reactor behaves as a pure plug flow reactor with mean residence time τ_c.

It is the idea of a uniform reaction rate per unit volume of catalyst that underlies the concept of the contact time distribution. Consider an isothermal reactor filled with finely ground catalyst that is long enough so that pure plug flow exists. Let us assume that we have a feedstock that contains a large number of compounds, A_i, with concentrations a_{i_o}, each undergoing an irreversible first order reaction

with rate constant k_i. The concentration of each compound at the outlet of the reactor will be:

$$a_i = a_{i_o} e^{-k_i \tau_c}$$

This relationship allows us to experimentally determine a set of $k_i \tau_c$ for the reactions. Now assume that the set of reactions occur in another reactor with large catalyst particles and with an arbitrary mixing pattern in the interstitial phase. The total catalyst volume remains the same. The concentration of each compound at the outlet of the reactor will be described by the following function:

$$\psi(k_i \tau_c) = \frac{a_i}{a_{i_o}} \tag{1}$$

where the $k_i \tau_c$ are those determined in the true plug flow reactor. If there are a large number of a_i and $k_i \tau_c$ then we can consider the values of $\psi(k_i \tau_c)$ as point values of a continuous function which characterizes the reactor. We define $\psi(k\tau_c)$ as the Laplace transform of the contact time distribution. We note that $\psi(k\tau_c)$ has all the properties of the Laplace transform of a probability density function. It is a decreasing positive function, and as $k\tau_c$ goes to zero, $\psi(k\tau_c)$ approaches unity and its derivatives are finite.

If the simplified description of uniform catalyst behavior is reasonable, then the contact time distribution has a clear physical meaning. It is the sojourn time distribution of molecules inside the catalyst phase. It should be emphasized that this physical interpretation of $\psi(t)$ is only correct to the extent that our assumptions about the catalyst behavior are correct. However, eq. (1) is a rigorous

definition regardless of the catalyst behavior. If the inverse transform operation is performed, the following is obtained.

$$\frac{a_i}{a_{i_o}} = \int_o^\infty e^{-k_i t} \psi(t)dt \qquad (2)$$

The contact time distribution can therefore be looked upon as an operator which shows in what way the probability of a molecule to react in a pure plug flow reactor is modified by mixing processes in a real reactor.

Since systems of many independently occurring reactions are seldom encountered, the problem now is to evaluate $\psi(k\tau_c)$ over a wide range of $k\tau_c$. Zahner (1971) and Glasser, et.al. (1973) describe a method whereby $\psi(k\tau_c)$ can be determined directly by experiment. It uses the successive exchange of deuterium with neopentane which involves twelve consecutive first order reactions with successively decreasing rate constants each in proportion to the number of hydrogens on the molecule. The rate constant of the first reaction might be designated by 12 k, then the second rate constant would be 11 k, and so on. A concentration measurement of all of the intermediate species enables one to estimate $\psi(k\tau_c)$ at each of the twelve values of the rate constants. To make this clear let us examine the following reaction with initial concentration a_o of A and no B present.

$$A \overset{k_1}{\rightarrow} B \overset{k_2}{\rightarrow} C$$

The concentrations of A and B are the following:

$$a = \int_o^\infty a_o e^{-k_1 t} \psi(t)dt$$

$$b = \int_o^\infty \frac{k_1 a_o}{k_1 - k_2} (e^{-k_2 t} - e^{-k_1 t}) \psi(t)dt$$

By definition of the Laplace transform we obtain the following:

$$\frac{a}{a_o} = \psi(k_1)$$

$$\frac{b}{a_o} = \frac{k_1}{k_1 - k_2} [\psi(k_2) - \psi(k_1)]$$

By knowing the rate constants, or at least their ratios, and measuring the concentrations, one can progressively construct a curve of $\psi(k\tau_c)$. The problem here, of course, is with the accuracy of the measurements, especially for species at low concentration. Glasser, et.al., also describes how measurements of the concentrations can lead to a construction of the first twelve terms of the Taylor Series expansion of $\psi(k\tau_c)$ using finite difference approximations of the derivatives. As will be shown later, an analytic approximation of $\psi(k\tau_c)$ can be useful in estimating how sensitive the selectivity is to closeness to plug flow.

A less rigorous method for determining $\psi(k\tau_c)$ would be a multiple tracer experiment as described by Shinnar, et.al., (1972). We need to find two tracers with identical behavior in the interstitial phase, but one that diffuses into the particles as would a reactant and the other that stays in the interstitial phase. Here too we can extract

$\psi(k\tau_c)$ from the experimental data as outlined in the paper. However, finding tracers with the described properties is extremely difficult.

Finally, if we had an exact flow model we could compute $\psi(k\tau_c)$ by the method given in the paper by Shinnar, et.al. This is the procedure we follow here. Of course an exact flow model is never known; we seldom know the exact values of the diffusivities, especially those inside the catalyst particles. However, since we are only interested in assuring conditions close to plug flow, these limitations do not present such a formidable obstacle, because useful limits on the values of the diffusivities can be approximated. The advantage of this procedure over the others is that a micro-reactor can be systematically designed to approach plug flow as closely as desired. The computational procedure is now described.

First we compute the Laplace transform of the residence time distribution in the inactive interstitial phase α:

$$\mathcal{L}[f(t)] = f(s)$$

Then we compute the Laplace transform of the conditional probability density $X(t/\tau)$:

$$\mathcal{L}[X(t/\tau)] = X(s/\tau) = e^{-\rho(s)\tau}$$

which is the sojourn time distribution of a particle in the intra-particle phase β given a total residence time τ in phase α. The function $\rho(s)$ depends on the particular model chosen for phase β.

The Laplace transform of the contact time distribution is then given by the following:

(3) $$\psi(s) = f(\rho(s))$$

whereas the Laplace transform of the residence time distribution in the total system is given by:

(4) $$g(s) = f(s + \rho(s))$$

Phase α

We model phase α as a tubular reactor with a longitudinal dispersion. All of the transport processes due to molecular and turbulent diffusion are described by a single diffusivity D, for which an empirical correlation has been developed by Edwards and Richardson (1968). This overall diffusivity is described as a linear combination of the molecular and turbulent diffusivities D_m and D_t respectively:

$$D = \gamma D_m + D_t$$

The coefficient γ is a tortuosity factor suggested by Edwards and Richardson to account for the tortuous nature of the passages between the particles.

The Laplace transform of the residence time distribution in phase α is given in any standard textbook (Kramers and Westerterp, 1963) as:

(5) $$f(s) = \frac{4q}{(1+q)^2 e^{\frac{Pe}{2}(q-1)} - (q-1)^2 e^{\frac{-Pe}{2}(1+q)}}$$

where $q = (1 + 4\tau_\alpha S/Pe)^{1/2}$.

The other terms of the equation are defined as follows:

$$\frac{1}{Pe} = \frac{1}{Pe_m} + \frac{1}{Pe_t} ; \quad Pe_m = \frac{uL}{\gamma D_m} ; \quad Pe_t = \frac{uL}{D_t} ; \quad \tau_\alpha = \frac{L}{u}$$

where u is the velocity, which is assumed constant across the catalyst bed, L is the length of the bed, τ_α is the mean residence time in phase α, Pe_m and Pe_t are Peclet numbers for molecular and turbulent diffusion, respectively, and Pe is an overall Peclet number.

Phase β

We neglect the shape of the catalyst particles and assume that they can be described as thin plates of thickness 2b. The transport of mass to the particle surface is described by a mass transfer coefficient h, and the internal transfer processes are described by a one dimensional diffusion model with diffusion coefficient D_β, and with diffusing length b, the catalyst volume per unit interfacial surface area. The function $\rho(s)$ for this case is given by:

$$\rho(s) = \frac{\frac{\lambda b}{h\theta} \sqrt{s\theta} \tanh \sqrt{s\theta}}{1 + \frac{b}{h\theta} \sqrt{s\theta} \tanh \sqrt{s\theta}} \tag{6}$$

where $\lambda = hc/A_\alpha$, c is the interfacial area per unit length of reactor, A_α is the cross-sectional area of phase α, and $\theta = b^2/D_\beta$, the Einstein diffusion time.

By utilizing eq. (3) together with eq. (5) and eq. (6), the following expression for the Laplace transform of the contact time distribution is obtained:

$$(7) \qquad \psi(s) = \frac{4q'}{(1+q')^2 \; e^{\frac{Pe}{2}(q'-1)} - (q'-1)^2 \; e^{-\frac{Pe}{2}(1+q')}}$$

where q' is defined as:

$$q = \left(1 + \frac{4\tau_\alpha}{Pe} \; \rho(s)\right)^{1/2}$$

To obtain a measure of the spread of $\psi(t)$ about the mean contact time, and hence a measure of the deviation from plug flow, we now compute the variance of $\psi(t)$. The moments of $\psi(t)$, which are represented by η_k, can be obtained by differentiation or by the less tedious method given by Shinnar, et.al. (1972) and described in the Appendix. The first and second moments of $\psi(t)$ are found to be:

$$(8a) \qquad \eta_1 = n\tau_\beta = \tau_c$$

$$(8b) \qquad \eta_2 = \tau_c^2 \left(1 + \frac{2}{Pe} + \frac{2e^{-Pe}}{Pe^2} - \frac{2}{Pe^2} + \frac{2}{n} + \frac{2\theta}{3\tau_c}\right)$$

where $n = \tau_\alpha hc/A_\alpha$ is a dimensionless group representing the average number of times a particle passes from phase α to phase β in a time interval of length τ_α. The term $\tau_\beta = b/h$. The term τ_c is the mean contact time defined as the catalyst volume divided by the fluid volumetric flow rate. The preceding mathematical development gives a result which is consistent with this, since $n\tau_\beta$, when appropriately manipulated, gives τ_c as defined.

The normalized variance is the following:

$$\frac{\sigma_\psi^2}{\tau_c^2} = 2\left(\frac{1}{Pe} + \frac{e^{-Pe}}{Pe^2} - \frac{1}{Pe^2} + \frac{1}{n} + \frac{\theta}{3\tau_c}\right)$$

For large values of the Peclet number (>20), the normalized variance can be closely approximated by:

$$(9) \qquad \frac{\sigma_\psi^2}{\tau_c^2} = 2\left(\frac{1}{Pe_m} + \frac{1}{Pe_t} + \frac{1}{n} + \frac{\theta}{3\tau_c} \right)$$

As each term of the variance becomes small, the contact time distribution more closely approaches that of a pure plug flow reactor. In this paper we are only interested in cases where σ_ψ^2/τ_c^2 is small because for good design we want to approach plug flow as closely as possible.

Since we are only interested in a reactor close to plug flow we should be able to make use of the fact that $\psi(t)$ is a simple peaked function, which for small values of σ_ψ^2/τ_c^2 is similar to the residence time distribution of a series of stirred tanks. If the number of tanks is large, this residence time distribution is close to a Guassian distribution and depends only on the variance.

This argument can be proven in a more rigorous way. In the Appendix the following approximate expression for $\psi(s)$ is derived which confirms the heuristic argument that $\psi(t)$ depends only on the normalized variance when it is small.

$$(10) \qquad \Psi(S) = \left[1 + \frac{(S\tau_c)^2}{2} \frac{\sigma_\psi^2}{\tau_c^2} \right] e^{-S\tau_c}$$

This approximation is good for values of $\sigma_\psi^2/\tau_c^2 < 1/10$.

Now let us discuss the effect on conversion of deviations from plug flow. The unconverted fraction is given directly from $\psi(s)$ by substituting for s the first order reaction rate constant, k. The unconverted fraction as a function of the nondimensional rate constant $k\tau_c$ is the following:

$$\Psi(k\tau_c) = \left[1 + \frac{(k\tau_c)^2}{2}\frac{\sigma_\psi^2}{\tau_c^2}\right] e^{-k\tau_c} \tag{11}$$

We must be careful in utilizing this result, however, because it is derived with the assumptions that $\sigma_\psi^2/\tau_c^2 \ll k\tau_c$ and $\sigma_\psi^2/\tau_c^2 \ll 1$. If these assumptions hold, then the percent deviation of the unconverted fraction, $\psi(k\tau_c)$, from the corresponding plug flow value is given by:

(12) % deviation from plug flow unconverted fraction =

$$100\left[\frac{(k\tau_c)^2}{2}\quad\frac{\sigma_\psi^2}{\tau_c^2}\right]$$

As $k\tau_c$ and the conversion increase, the percent deviation of $\psi(k\tau_c)$ from $e^{-k\tau_c}$ increases and the performance of the reactor moves further away from plug flow.

To determine the effect on selectivity of deviations from plug flow we can use eq. (11) in conjunction with a method outlined by Glasser, et.al. (1973).

SELECTIVITY

Glasser, et.al. suggest as a useful measure of the selectivity of an experimental reactor, the maximum amounts of material produced of each of the intermediates in the reaction scheme:

$$A_o \overset{k}{\rightarrow} A_1 \overset{k}{\rightarrow} A_2 \overset{k}{\rightarrow} \cdots A_i \overset{k}{\rightarrow} \cdots A_n$$

All the reaction rates are taken as equal. The maximum quantities of $A_1 \cdots A_{n-1}$ constitute an (n-1) dimensional vector. The maximum quantity of A_i can be obtained from:

$$S_i = \max_{k\tau_c} \left(\frac{a_i(k\tau_c)}{a_o^o} \right) = \max_{k\tau_c} \left[(-1)^i \frac{(k\tau_c)^i}{i!} \frac{d^i \psi(k\tau_c)}{d(k\tau_c)^i} \right] \tag{13}$$

where a_i is the concentration of species A_i and a_o^o is the initial concentration of A_o.

The vector for the ideal plug flow reactor is shown in Table I along with the values of $k\tau_c$ corresponding to the maximums. These vector components have the greatest magnitude possible for any reactor configuration. The differences between these and the respective components of the selectivity vector for any other reactor configuration gives a measure of the loss of selectivity, and hence a measure of the reactor's distance from plug flow.

In Table I we present the selectivity vector for various values of the variance as determined by using eq. (11). The following expression for the i^{th} selectivity vector component results from the development given in the Appendix:

$$(14) \qquad S_i = \frac{(i)^i}{i!} e^{-i} \left[1 - \frac{i\sigma_\psi^2}{2\tau_c^2}\right]$$

Since $\psi(k\tau_c)$ depends only on the variance, the selectivity vector, of course, also depends only on the variance of $\psi(t)$.

The percent deviation from the corresponding plug flow vector component is simply:

$$(15) \qquad \% \text{ deviation from plug flow} = 100i \frac{\sigma_\psi^2}{2\tau_c^2}$$

The coefficient i in this equation indicates why σ_ψ^2/τ_c^2 must be smaller for higher vector components to achieve the same closeness to plug flow as for lower components. For an approach to plug flow which is within 5% for S_1, a value of $\sigma_\psi^2/\tau_c^2 < 1/10$ is required, while to satisfy the same requirement for the fourth component a value of $\sigma_\psi^2/\tau_c^2 < 1/40$ is required. This sensitivity of higher vector components gives us a better indication of the value of the variance required to achieve a desired closeness to plug flow. It is noted that this sensitivity with increasing $k\tau_c$ occurs as well for the percent deviation of the unconverted fraction from the plug flow value.

We note that the locations of the vector components are the same as for the respective components for the plug flow vector. Strictly speaking this is not exactly true, but as shown in the Appendix, even if a less restrictive approximation for $\psi(k\tau_c)$ is used the location of the maximums are very nearly at the same values.

We now have an estimate on the upper limit of the normalized variance which insures a desired closeness to plug flow and can use this information together with eq. (9) to find values for the design parameters of the reactor. Before showing how this can be done, however, let us describe more completely each of the terms comprising the variance of $\psi(t)$ and discuss the qualitative effects of the reactor parameters on the selectivity.

The first two terms of the variance are well known and measure the extent of molecular and turbulent diffusion, respectively. McHenry and Wilhelm (1957) and Aris and Amundson (1957) found that for Re greater than 20, Pe_t can be approximated as:

$$Pe_t = 2\left(\frac{L}{d_p}\right)$$

Bischoff (1969) gives the following expression for 1/Pe based on work done by Edwards and Richardson (1968):

$$\frac{1}{Pe} = \frac{d_p}{L}\left[\frac{0.73}{ReSc} + \frac{0.45}{1 + \frac{7.3}{ReSc}}\right]$$

with the first term being $1/Pe_m$ and the second $1/Pe_t$. If this expression is rewritten in terms of the reactor parameters L, d_p, and τ_c the following is obtained:

$$\frac{1}{Pe} = \frac{0.73\varepsilon\tau_c D_m}{(1-\varepsilon)\,L^2} + \frac{0.45(1-\varepsilon)d_p^{\,2}}{(1-\varepsilon)Ld_p + 7.3\varepsilon\tau_c D_m} \tag{16}$$

where ε is the bed voidage and $\tau_c = L(1-\varepsilon)/u\varepsilon$.

The term $1/n = A_\alpha/\tau_\alpha hc$ is a measure of the extent of mass transfer to the catalyst particles. With the appropriate substitutions it can be rewritten as:

$$\frac{1}{n} = \frac{b}{\tau_c h}$$

and it is clear that it varies inversely with the mass transfer coefficient h and the external surface area to volume ratio of the catalyst, 1/b. Using the following expression for h offered by Carberry (1957) which is valid for $0.1 \leq Re \leq 1000$

$$h = 1.15 u Re^{-1/2} Sc^{-2/3}$$

one can express 1/n in terms of the reactor parameters L, d_p, and τ_c in the following way:

$$\frac{1}{n} = \frac{\mu^{\frac{1}{6}} \epsilon^{\frac{1}{2}} d_p^{\frac{3}{2}}}{6.9 (1-\epsilon)^{\frac{1}{2}} \rho^{\frac{1}{6}} D_m^{\frac{2}{3}} \tau_c^{\frac{1}{2}} L^{\frac{1}{2}}} \tag{17}$$

where μ is the viscosity.

The term $\theta/3\tau_c$ is a modified Thiele modulus describing the extent of intraparticle diffusion over the entire catalyst bed. It is proportional to the ratio of the Einstein diffusion time to the mean contact time of the reactor. In terms of reactor parameters it is written as:

$$\frac{\theta}{3\tau_c} = \frac{d_p^{\,2}}{108 \tau_c D_\beta} \tag{18}$$

EFFECTS OF REACTOR PARAMETERS ON THE VARIANCE

By substituting eq. (16),(17), and (18) into eq. (9), we can write the expression σ_ψ^2/τ_c^2 in terms of the reactor parameters as follows:

$$(19)\ \frac{\sigma_\psi^2}{\tau_c^2} = 2\left[\frac{0.73\varepsilon\tau_c D_m}{(1-\varepsilon)\,L^2} + \frac{0.45(1-\varepsilon)d_p^2}{(1-\varepsilon)Ld_p+7.3\varepsilon\tau_c D_m} + \frac{\mu^{1/6}\varepsilon^{1/2}d_p^{3/2}}{6.9(1-\varepsilon)^{1/2}\rho^{1/6}D_m^{2/3}\tau_c^{1/2}L^{1/2}} + \frac{d_p^2}{108\tau_c D_\beta}\right]$$

It is assumed for convenience that the particles are spherical. However, the methods outlined in this paper are by no means limited to a particular particle geometry.

It is noted that our equations say nothing about the diameter of the reactor; they are written with the implicit assumption that a uniform flow distribution exists through the catalyst bed. In reality, the choice for a proper reactor diameter is quite constrained. At low reactor length to diameter ratios it will be difficult to insure an even distribution unless special precautions are taken. In addition, the ratio of the reactor diameter to particle diameter must be reasonably large for the relations for Pe and h to hold.

Let us now turn to an examination of eq. (19). For reactors with small particles, molecular diffusion is the controlling effect and σ_ψ^2/τ_c^2 is essentially independent of the catalyst size and depends only on the length of the reactor. For reactors with large particles intraparticle diffusion is the controlling effect because it depends only on the catalyst size and is unaffected by the reactor length. Each of the other effects, however, can be decreased by sufficiently increasing the reactor length. If σ_ψ^2/τ_c^2 is too high and the particle size has to be

reduced accordingly, we can then determine the minimum L over the range of contact times in which the reactor can operate such that the contribution of intraparticle diffusion is negligible and the desired closeness to plug flow is achieved. If we are interested in scale-up of the reactor the first three terms have to be made small as compared to $\theta/3\tau_c$. Turbulent diffusion and mass transfer to the catalyst surface are dependent on both catalyt size and reactor length with their effects decreasing with increasing length or decreasing catalyst size.

We have no control over the parameters which are fixed by kinetic considerations; but we can always compensate somewhat for any ill effects of these parameters on plug flow by choosing a sufficiently long reactor. At fixed conditions, eq. (19) immediately gives the minimum L required to achieve the desired closeness to plug flow.

The only other design parameter we can sometimes choose is particle size. In most pilot plants, this size is chosen to be the same as in the actual plant. The smallest practical particle size in most industrial applications is about 1/16" with some limited use at 1/32". If we are mainly interested in achieving good kinetics and not in scale-up it is often advisable to use a smaller particle size. At constant reactor conditions, the minimum length decreases with decreasing particle size. However, the effect of molecular diffusion on selectivity is independent of particle size and gives an absolute lower bound for L.

It should be mentioned that eq. (19) does not include any rate parameters. These are, however, contained implicitly in τ_c. This is a considerable advantage of our design approach because its arguments are based directly on τ_c which is much easier to measure than kinetic

parameters. The mean contact time is often not known a priori, but due to economic and technical considerations the range of interest is predetermined in most cases.

THE EFFECT OF PRESSURE ON THE VARIANCE

A brief comment should be made about the effects of pressure on the variance as pilot plant data are normally obtained over a wide range of pressures. The effects of molecular diffusion and of longitudinal dispersion are independent of pressure because at a given feed rate $\tau_c D_m$ is independent of pressure. The same is true for mass transfer to the catalyst particles because $\rho^{1/6} D_m^{2/3} \tau_c^{1/2}$ is independent of pressure. Finally, the modified Thiele parameter is independent of pressure if D_β is merely an effective diffusion coefficient. However, when the catalyst pores are very small and Knudsen diffusion exists, then the Thiele parameter is inversely proportional to pressure. The total effect of pressure is in most cases quite small and for fixed inlet composition and constant reactor temperature the minimum length is a function only of the gravimetric feed rate and the particle size.

An additional word should be said about the dependence of reactor length on the product of mean contact time and molecular diffusivity. Although this product is independent of pressure it will be different for different gases. However, the variation for nonpolar hydrocarbons is apparently not all that wide. For example, using Lennard-Jones potentials it was found that at the chosen reactor temperature the products for butane, octane, and nonane were in the ratio of 1.85:1.18:1.

From eq. (19) it is observed that the molecular diffusion term is directly proportional to the product $\tau_c D_m$ and that L is proportional to the square root of $\tau_c D_m$ for small particle sizes. The dependence of reactor length on $\tau_c D_m$ in the turbulent diffusion term is a bit more complicated. For very large and very small values of $\tau_c D_m$, L is independent of $\tau_c D_m$. For intermediate values, the relationship is as given in eq. (19). The mass transfer term is inversely proportional to the 2/3 power of the product of the pressure and molecular diffusivity and the reactor length is inversely proportional to the 4/3 power. Finally the product $\tau_c D_\beta$ will be different for different gases if Knudsen diffusion exists. The modified Thiele parameter will then be directly proportional to the square root of the molecular weight of the gas. Large molecules will have low values of D_β and the effect of intraparticle diffusion will be increased.

EXAMPLE

We now offer an example to demonstrate our procedure for a hypothetical reactor. The parameters have been chosen to provide a reasonable idea of reactor lengths required for petroleum processes. It is important to realize there is a basic difference between the design of micro-reactors and industrial reactors. In micro-reactors we do not know a priori what the mean contact time should be and would want to evaluate the reactor over a range of values. Additionally, we often do not know the kinetics for the reactions involved and how sensitive they are to deviations from plug flow. Consequently, we would want values of the minimum reactor length as a function of space velocity and particle size.

The basic data for the gaseous catalytic reactor are the following:

Reactor Temperature = 925°F

Reactor Pressure = 8.0 psig

Space Velocity = $0.1 \leq \text{S.V.} \leq 10{,}000 \frac{\text{gms feed}}{\text{gms catalyst-hr}}$

Contact Time = $0.001715 \leq \tau_c \leq 171.5$ sec

The data for the feed is the following:

Gravity = 24.0° API

M Wt = $300 \frac{\text{gm}}{\text{mole}}$

Mean average boiling point = 675°F

$D_m = 0.0437 \frac{\text{cm}^2}{\text{sec}}$

$D_\beta = 0.0111 \frac{\text{cm}^2}{\text{sec}}$

Viscosity = 0.011 cp

Catalyst Properties

Aluminum-Silicate type catalyst

Size: $50 \leq d_p \leq 3\text{mm}$

External void fraction: $\varepsilon = 0.4$

Bulk dry density: $\rho_b = 0.875 \frac{\text{gm}}{\text{cm}^3}$

Dry particle density: $\rho_p = 1.46 \frac{\text{gm}}{\text{cm}^3}$

Note that in addition to mean contact time, data are provided in terms of the weight hourly space velocity (WHSV), the gravimetric feed rate divided by the weight of the catalyst bed. This parameter is widely used in the oil industry and is included in the example for this reason. For the convenience of the reader, both τ_c and WHSV appear as parameters in the figures.

In Figures 1, 2, and 3, L is plotted versus space velocity with particle size as a parameter and with normalized variances of 1/10, 1/50, and 1/100, respectively. In Table 2, with $\sigma_\psi^2/\tau_c^2 = 1/10$, values of $1/Pe_m$, $1/Pe_t$, $1/n$, and $\theta/3\tau_c$ are presented for various space velocities and for each of four particle sizes. This table is provided for reference in the following discussion of Figure 1.

For low space velocities the minimum length is merely determined by molecular diffusion. As the space velocity increases, each curve in Figure 1 passes through a minimum which corresponds to the absolute minimum length for a reactor with a given particle size. The effects of turbulent diffusion and mass transfer to the catalyst particles do not come into real prominence until just before the minimum, although molecular diffusion continues to dominate. Up to the minimum, mass

transfer effects are more important than the effects of turbulent diffusion, but are still somewhat less prominent than those of molecular diffusion. At the minimum, molecular diffusion is still the single largest contribution to the variance. Just beyond the minimum, the first three terms of eq. (19) are approximately equal with the intraparticle diffusion term being about half this value. Only relatively well past the minimum does the molecular diffusion term drop significantly in value, while the other three terms are about equal. Beyond this, $1/Pe_t$ finally becomes much smaller than $\theta/3\tau_c$ and $1/n$. With a further increase in space velocity, $\theta/3\tau_c$ becomes dominant and finally the case is reached where intraparticle diffusion is limiting and no increase in reactor length can compensate for its effects. Similar trends occur for the graphs of Figures 2 and 3.

As a result of the intraparticle diffusion contribution, there is a definite upper bound on space velocity for a given particle size. Stated in another way, for a given space velocity there is a maximum catalyst size which is permissible. With a larger catalyst, the variance condition cannot be met with a reactor of finite length. This catalyst size can be easily calculated from the following:

$$d_p = 7.35\left[\frac{\sigma_\psi^2}{\tau_c^2}\,\tau_c D_\beta\right]^{\frac{1}{2}}$$

The most difficult case to deal with in designing micro-reactors is that of a reactor with a low space velocity, because molecular diffusion is controlling and is independent of particle size. As a result, the contribution of molecular diffusion determines a lower bound on the minimum reactor length necessary to achieve a desired closeness to plug flow. The bound can be easily calculated from the following:

$$L = 1.21 \left[\frac{\epsilon \tau_c D_m}{(1-\epsilon) \frac{\sigma_\psi^2}{\tau_c^2}} \right]^{\frac{1}{2}}$$

If one is interested in scale-up, large catalyst particles may be required and as a result the effects of intraparticle diffusion can be large. In this case, it is necessary to design the pilot plant such that mixing processes in the interparticle phase are near plug flow. To assure this the first three terms of eq. (19) must be small. This will not give good kinetic results but will provide reliable scale-up. A graph of the minimum reactor length versus space velocity for this case is given in Figure 4 for $\sigma_\psi^2/\tau_c^2 = 1/50$ and particle diameters of 1mm and 3mm. Removing the intraparticle diffusion term has the effect of shifting the minimum in the curve downward and to the right. Beyond the minimum, the reactor length increases at a much slower rate with space velocity. The minimum reactor length asymptotically approaches a straight line whose slope is determined by the mass transfer term.

In comparing Figures 1, 2, and 3, it is observed that the minimum required reactor length, of course, increases with decreasing variance and that the maximum particle size decreases with decreasing variance. A value of 1/50 for σ_ψ^2/τ_c^2 should be sufficient for most cases, though for complex cases a value of 1/100 might be preferable. It is noted that the length of the reactor needed for good plug flow is in most cases considerably longer than those often used in micro-reactors. A reactor which is 10cm in length requires even at 1/4" reactor diameter several grams of catalyst.

It is noted again that this example does not lead to a specific a priori reactor design. We do not know τ_c a priori, nor do we know the required upper limit of the variance of the contact time distribution. In this sense, the design of micro-reactors is always an iterative procedure. In an effort to insure closeness to plug flow, a reactor can always be designed which is long and utilizes finely ground catalyst. However, this may entail a needless expense and alternatively the length chosen may not even be great enough. The former may be true at intermediate space velocities and the latter may be true at very low and very high space velocities or if the reaction kinetics are more complex and a high selectivity is required.

Depending on the product desired and the process envisioned we always begin the design of a micro-reactor with some knowledge of a range of space velocities which is reasonable. We can also estimate an upper bound on the molecular diffusivity and a lower bound on the average diffusivity inside the catalyst particle. Then, fixing the maximum permissible variance, say 0.1, and choosing a particle size, we can use eq. (19) to determine the minimum reactor length for various values of the space velocity over the range of interest and plot curves similar to those given in the accompanying figures. If L_{min} seems too large, then the particle size can be decreased provided we are not operating at very low space velocities where length is independent of d_p. An experiment can now be performed to determine the conversion and selectivity. It should be borne in mind, as shown in eq. (12), that the reactor is more sensitive to deviations from plug flow when conversion is high than when it is low. If selectivity might be a problem we

would want to redesign the reactor with a lower variance. Changing the variance by varying L or d_p would provide some clues as to the importance of closeness to plug flow for good selectivity.

SUMMARY AND DISCUSSION

An approach for the design of fixed bed catalytic micro-reactors has been described. The method is based on the assumption that a close approach to plug flow is necessary to assure good rate data and provide safe scale-up. It is shown that for a catalytic reactor near plug flow, the deviation from plug flow can be expressed in terms of the variance of the contact time distribution. An equation defining the variance in terms of design parameters is presented. For first order reactions we can estimate an upper limit on the variance by evaluating the complexity of the kinetics and calculating a selectivity vector based on a chosen reactor model. However, this procedure is only rigorous for first order or pseudo-first order systems with reaction rates of the following form:

$$\frac{da_i}{dt} = \frac{-k_i a_i}{1 + \sum_i k_i a_i}$$

where the denominator is approximately a function of total concentration and only weakly dependent on conversion. Reactions of this type are quite common in the petroleum industry. But since we are dealing with small deviations from plug flow the method is just as good for second order reactions. The only difference is that for purely first order systems we can get a quantitative estimate of the permissible limit of

the variance. For second order systems this is not true. However, since in most cases we really don't know the exact kinetics anyway, this distinction is more theoretical than it is practical. In most instances we rely on some reasonable estimate based on experience as to how closely we want to approach plug flow. This estimate will be based on the conversion desired and on the complexity of the reactions. The expressions for the variance and the selectivity vector are used to guide us in obtaining a better quantitative feeling for our estimates. In this sense, the method is not restricted to first order systems.

However, it is important to note that this method applies only to fixed bed reactors which are isothermal or have only small temperature rises. As will be shown in Section II, the effects of small deviations from isothermality on these reactors can be minimized by altering the reactor parameters of length, catalyst particle size, and space velocity in the same way as shown in this section to minimize deviations from plug flow.

Moderate temperature gradients can be diminished in size by diluting the catalyst with an inert material, such as sand, which has a high thermal conductivity. The diluent acts as a heat sink and also increases the reactor length and diameter which tends to decrease the radial and longitudinal temperature gradients. However, because the fluid velocity drops, so does the heat transfer coefficient.

If the temperature gradients are large, then another type of pilot reactor must be considered which will insure isothermality. Several isothermal reactors are used industrialiy; among these are the continuous stirred tank reactor, stirred batch reactor, the stirred-contained solids reactor, and the recirculating transport reactor. All of these reactors present other difficulties which are discussed in some detail by Weekman (1974).[1]

[1]Weekman, V.W., "Laboratory Reactors and Their Limitations, A.I.Ch.E.J., 20,833 (1974).

APPENDIX

The Variance of $\psi(t)$

Using expressions developed by Shinnar, et.al. (1972) relations for the first and second moments of $\psi(t)$ can be obtained. These expressions are the following:

(A1)
$$\eta_1 = \lambda K_1 \mu_1$$
$$\eta_2 = \lambda K_2 \mu_1 + \lambda^2 K_1^2 \mu_2$$

where η_i, μ_i, and K_i are the ith moments of $\psi(t)$, $f(t)$, and $\phi(t)$, respectively.

The distribution $\phi(t)$ is the sojourn time distribution for a single particle trip into the catalyst phase β. As shown by Shinnar, et.al., its Laplace transform, $\phi(s)$, is related to $\rho(s)$ in the following way:

(A2)
$$\rho(s) = \lambda(1-\phi(s))$$

Solving for $\phi(s)$ one finds:

(A3)
$$\phi(s) = \frac{1}{1 + \frac{b}{h} (s\theta)^{1/2} \tanh (s\theta)^{1/2}}$$

The first and second moments of $\phi(t)$ are found by evaluating

$$\left.\frac{-d\phi(s)}{ds}\right|_{s=o} \quad \text{and} \quad \left.\frac{d^2\phi(s)}{ds^2}\right|_{s=o}, \text{ respectively. These are:}$$

(A4)
$$K_1 = \tau_\beta$$

(A5)
$$K_2 = 2\tau_\beta^2 + \frac{2}{3}\tau_\beta\theta$$

Performing similar differentiation on f(s) gives:

(A6) $$\mu_1 = \tau_\alpha$$

(A7) $$\mu_2 = \frac{2\tau_\alpha^2}{Pe^2}\left(\frac{Pe^2}{2} + Pe + e^{-Pe} - 1\right)$$

The first and second moments of $\psi(t)$ are found to be:

(A8) $$\eta_1 = n\tau_\beta = \tau_c$$

(A9) $$\eta_2 = \tau_c^2\left(1 + \frac{2}{Pe} + \frac{2e^{-Pe}}{Pe^2} - \frac{2}{Pe^2} + \frac{2}{n} + \frac{2\theta}{3\tau_c}\right)$$

The normalized variance is:

(A10) $$\frac{\sigma_\psi^2}{\tau_c^2} = 2\left(\frac{1}{Pe} + \frac{e^{-Pe}}{Pe^2} - \frac{1}{Pe^2} + \frac{1}{n} + \frac{\theta}{3\tau_c}\right)$$

Approximation for $\psi(k\tau_c)$ and the Selectivity Vector

If Pe, n, and $3\tau_c/\theta$ are sufficiently large, it can be fairly easily demonstrated that for constant mean contact time, τ_c, the conversion of a fixed bed catalytic micro-reactor is proportional to the dimensionless variance σ_ψ^2/τ_c^2, of the contact time distribution.

The following is the expression for the moment generating function of f(t), the RTD in the interstitial phase:

(A11) $$f(s) = \frac{4q}{(1+q)^2\, e^{-Pe/2\,(1-q)} - (1-q)^2\, e^{-Pe/2\,(1+q)}}$$

where $q = (1 + 4\tau_\alpha S/Pe)^{1/2}$

If Pe >> 1 and is also large with respect to $S\tau_\alpha$, then q can be approximated as follows:

(A12) $$q \approx 1 + \frac{2S\tau_\alpha}{Pe}$$

With this approximation for q and the approximation that

$$\frac{4q}{(1+q)^2} \approx 1$$

the expression for f(s) becomes:

(A13) $$f(s) = e^{-S\tau_\alpha}\left(1 - \frac{S\tau_\alpha}{Pe}\right)$$

If the Taylor Series expansion of f(s) is made around $S\tau_\alpha/Pe = 0$, the expression for f(s) can be approximated as:

(A14) $$f(s) \approx e^{-S\tau_\alpha}\left[1 + \frac{(S\tau_\alpha)^2}{Pe}\right]$$

In the paper by Shinnar, et.al. (1972), the following expression for the moment generating function of $\psi(t)$ is presented:

(A15) $$\psi(s) = f\left[\frac{hc}{A_\alpha}(1 - \phi(s))\right]$$

The expression for $\frac{hc}{A_\alpha}(1-\phi(s))$ multiplied by τ_α is the following:

(A16) $$\frac{\tau_\alpha hc}{A_\alpha}(1-\phi(s)) = \frac{\frac{\tau_\alpha bc}{A_\alpha\theta}(s\theta)^{\frac{1}{2}}\tanh(s\theta)^{\frac{1}{2}}}{1 + \frac{b}{h\theta}(s\theta)^{\frac{1}{2}}\tanh(s\theta)^{\frac{1}{2}}}$$

An approximation for $(s\theta)^{1/2}$ tanh $(s\theta)^{1/2}$ for small $(s\theta)$ is the following:

$$(s\theta)^{1/2} \tanh (s\theta)^{1/2} \approx s\theta - \frac{(s\theta)^2}{3}$$

With the substitutions that $\tau_c = bc\tau_\alpha/A_\alpha$ and $b/h = \tau_c/n$, the approximation for (A16) becomes:

(A17) $$\frac{\tau_\alpha hc}{A_\alpha}(1-\phi(s)) \approx \frac{s\tau_c\left[1 - s\tau_c\left(\frac{\theta}{3\tau_c}\right)\right]}{1 + \frac{s\tau_c}{n}\left[1 - s\tau_c\left(\frac{\theta}{3\tau_c}\right)\right]}$$

The denominator can be approximated as $1 + s\tau_c/n$ since $(s\tau_c/n)(s\tau_c\theta/3\tau_c) << s\tau_c/n$. With this simplification and the approximation that:

$$\frac{1}{1 + \frac{s\tau_c}{n}} \approx 1 - \frac{s\tau_c}{n}$$

for $n >> 1$ and small $s\tau_c/n$, equation (A17) becomes:

(A18) $$\frac{\tau_\alpha hc}{A_\alpha}(1-\phi(s)) \approx s\tau_c\left[1 - s\tau_c\,\frac{\theta}{3\tau_c}\right]\left[1 - \frac{s\tau_c}{n}\right]$$

Upon substitution of (A18) into (A15), the following expression for $\psi(s)$ results:

(A19) $$\psi(s) \approx e^{-s\tau_c\left[1 - s\tau_c\frac{\theta}{3\tau_c}\right]\left[1 - \frac{s\tau_c}{n}\right]}\left[1 + \frac{(s\tau_c)^2\left(1 - \frac{s\tau_c}{n}\right)^2\left(1 - s\tau_c\left(\frac{\theta}{3\tau_c}\right)\right)^2}{Pe}\right]$$

The coefficient of the exponential can be approximated as:

$$1 + \frac{(s\tau_c)^2\left(1 - \frac{s\tau_c}{n}\right)^2\left(1 - s\tau_c\left(\frac{\theta}{3\tau_c}\right)\right)^2}{Pe} \approx 1 + \frac{(s\tau_c)^2}{Pe}$$

and the exponential itself can be approximated as:

$$e^{-s\tau_c\left[1 - s\tau_c\left(\frac{\Theta}{3\tau_c}\right)\right]\left[1 - \frac{s\tau_c}{n}\right]} \approx e^{-s\tau_c}\left[1 + (s\tau_c)^2\left(\frac{1}{n} + \frac{\Theta}{3\tau_c}\right)\right]$$

Substituting these expressions in (A19) and substituting k for s gives the following approximation for $\psi(k\tau_c)$:

$$\text{(A20)} \quad \psi(k\tau_c) \approx \left[1 + (k\tau_c)^2\left(\frac{1}{Pe} + \frac{1}{n} + \frac{\Theta}{3\tau_c}\right)\right]e^{-k\tau_c} = \left[1 + (k\tau_c)^2\,\frac{\sigma_\psi^2}{2\tau_c^2}\right]e^{-k\tau_c}$$

It is easy to see that in the limit as $\sigma_\psi^2/\tau_c^2 \to 0$, $\psi(k\tau_c) \to e^{-k\tau_c}$, the expression for the ideal plug flow reactor.

Selectivity Vector

The selectivity vector is determined as follows:

$$\text{(A21)} \qquad S_i = \max_{k\tau_c}\left[(-1)^i\,\frac{(k\tau_c)^i}{i!}\,\frac{d^i\psi(k\tau_c)}{d(k\tau_c)^i}\right]$$

By substitution of $\psi(k\tau_c)$ from (A20) and then by repeated differentiation with respect to $k\tau_c$, one can determine the values of $k\tau_c$ at which the maximum occur. It has been found that the location of the vector components occur exactly at the integer values $k\tau_c$ = 1, 2, 3...n for the 1st, 2nd, 3rd...nth vector component, respectively.

Upon substitution of these $k\tau_c$ into (A21), the following expression for the ith vector component results:

$$\text{(A22)} \qquad S_i = \frac{(i)^i}{i!}\,e^{-i}\left[1 - \frac{i\sigma_\psi^2}{2\tau_c^2}\right]$$

It is clear that the ith vector component depends only on the variance, if the variance is sufficiently small. The coefficient i in the term $i\sigma_\psi^2/2\tau_c^2$ explains why the variance must be smaller for higher vector components to achieve the same closeness to plug flow as for lower components.

It has been shown that for a less severe approximation of $\psi(k\tau_c)$ than (A20), say if:

$$\psi(kT_c) \approx e^{-kT_c\left[1 - (kT_c)\frac{\sigma_\psi^2}{2T_c^2}\right]}$$

then the location of the vector components are very nearly at $k\tau_c = 1$, 2, 3...n. For example, the derivative of the first vector component expression evaluated as $k\tau_c = 1$ is the following:

$$\left.\frac{dS_1}{dkT_c}\right|_{kT_c=1} = e^{-\left[1 - \frac{\sigma_\psi^2}{2T_c^2}\right]}\left[-\left(\frac{\sigma_\psi^2}{T_c^2}\right)^2\right]$$

It depends on the square of the variance and for sufficiently small σ_ψ^2/τ_c^2, the derivative is very nearly zero, indicating that the maximum occurs very near $k\tau_c = 1$. If $\sigma_\psi^2/\tau_c^2 = 1/10$, the derivative is only - 0.00386. Similar results can be found for higher order vector components.

NOMENCLATURE

A_i	reaction species
a_i	concentration of A_i
a_o^o	initial concentration of A_o
A_α	cross-sectional area of phase α
b	catalyst volume per unit interfacial surface area
c	interfacial surface area per unit length of reactor
D	overall diffusivity
D_m	molecular diffusivity
D_t	turbulent diffusivity
D_β	intraparticle diffusion coefficient
d_p	particle diameter
f(t)	residence time distribution in the interstitial phase
f(s)	Laplace transform of f(t)
g(t)	residence time distribution in the total system
g(s)	Laplace transform of g(t)
h	mass transfer coefficient
k	reaction rate constant
L	length of catalyst bed
	Laplace transform operator
n	hc/A_α
Pe_m,Pe_t,Pe	Peclet numbers for molecular, turbulent, and total diffusion, respectively
q	a dimensionless term defined in equation 5
q'	a dimensionless term defined in equation 7
Re	Reynolds number
s	Laplace transform variable
S_i	ith selectivity vector component

NOMENCLATURE (continued)

Sc	Schmidt number
t	time
u	interstitial fluid velocity
$X(t \mid \tau)$	conditional probability density defined in equation 2
$X(s \mid \tau)$	Laplace transform of $X(t)\,\tau)$

Greek Symbols

γ	tortuosity factor
ε	bed voidage
η_k	kth moment of contact time distribution $\psi(t)$
θ	b^2/D_β
K_k	kth moment of sojourn time distribution $\phi(t)$
λ	hc/A_α
μ	viscosity
μ_k	kth moment of soujourn time distribution f(t)
$\rho(s)$	a function of s
ρ_b	bulk dry particle density
ρ_p	dry particle density
σ_ψ^2	variance of contact time distribution $\psi(t)$
τ_c	mean contact time
τ_α	mean residence time in interstitial phase α
τ_β	b/h
$\phi(t)$	sojourn time distribution for a single particle trip into catalyst phase β from interstitial phase
$\phi(s)$	Laplace transform of $\phi(t)$
$\psi(t)$	contact time distribution
$\psi(s)$	Laplace transform of $\psi(t)$

REFERENCES

Aris, R., Amundson, N.R., A.I.Ch.E.J. 3, 280(1957).

Bischoff, K.B., Chem. Eng. Sci. 24, 607(1969).

Carberry, J.J., A.I.Ch.E.J. 3, 460(1960).

Edwards, M.F., Richardson, J.F., Chem. Eng. Sci. 23, 109(1968).

Glasser, D., Katz, S., Shinnar, R., I&EC Fund. 12, 165(1973).

Krambeck, F.J., Katz, S., Shinnar, R., Chem. Eng. Sci. 24, 1497(1969).

Kramers, H., Westerterp, K.R., "Elements of Chemical Reactor Design and Operation," Chapman and Hall Ltd., London, 1963.

Levenspiel, O., Kunii, D., "Fluidization Engineering," Wiley, New York, N.Y., 1969.

McHenry, K.W., Wilhelm, R.H., A.I.Ch.E.J. 3, 83(1957).

Mears, D.E., Chem. Eng. Sci. 26, 1361(1971).

Orcutt, J.C., Davidson, J.F., Pigford, R.L., Chem. Eng. Prog. Symp. Ser. 58(38), 1(1962).

Pigford, R.L., Chem. Eng. Prog. 68(9), 46(1972).

Shinnar, R., Naor, P., Katz, S., Chem. Eng. Sci. 27, 1627(1972).

Wehner, J.E., Wilhelm, R.H., Chem. Eng. Sci. 6, 89(1956).

Zahner, J.C., "Experimental Study of Laboratory Flow Reactions," Proceedings of the 1st International (5th European) Reaction Engineering Symposium, American Chemical Society, Washington, D.C., 1971.

Table I

Pure Plug Flow Reactor

Species (i)	$k\tau_c$	S_i
1	1	0.368
2	2	0.270
3	3	0.225
4	4	0.196

Vector for Model Discussed

Species (i)	$k\tau_c$	$\frac{\tau_c^2}{\sigma_\theta^2}$	S_i	% deviation from plug flow
1	1	10	0.350	5.00
2	2	10	0.243	10.00
3	3	10	0.191	15.00
4	4	10	0.157	20.00
1	1	20	0.358	2.50
2	2	20	0.256	5.00
3	3	20	0.208	7.50
4	4	20	0.176	10.00
1	1	50	0.364	1.00
2	2	50	0.264	2.00
3	3	50	0.218	3.00
4	4	50	0.188	4.00
2	2	100	0.267	1.00
3	3	100	0.222	1.50
4	4	100	0.192	2.00

Table 2

$$\frac{\sigma_{\psi}^2}{\tau_c^2} = \frac{1}{10}$$

d_p	WHSV	$\frac{1}{Pe_m}$	$\frac{1}{Pe_t}$	$\frac{1}{n}$	$\frac{\theta}{3\tau_c}$
100μ	0.10	.049987	.000001	.000011	0
	1.00	.049920	.000012	.000064	.000004
	5.12	.049700	.000062	.000217	.000021
	10.00	.049481	.000121	.000358	.000040
	41.00	.048326	.000482	.001026	.000166
	100.00	.046464	.001146	.001984	.000405
	325.00	.040483	.003521	.004669	.001327
	1000.00	.026863	.009351	.009730	.004050
	1300.00	.021857	.011514	.011321	.005308
	2600.00	.007978	.016607	.014799	.010616
	3900.00	.002730	.016185	.015266	.015819
	5250.00	.000946	.013219	.014600	.021232
	10,000.00	.000009	.002159	.007336	.040496
	10,500.00	.000004	.001433	.006100	.042463
150μ	0.10	.049975	.000003	.000021	.000001
	1.00	.049846	.000027	.000117	.000009
	5.12	.049416	.000139	.000398	.000047
	10.00	.048984	.000268	.000657	.000091
	41.00	.046698	.001060	.001869	.000373

d_p	WHSV	$\frac{1}{Pe_m}$	$\frac{1}{Pe_t}$	$\frac{1}{n}$	$\frac{\theta}{3\tau_c}$
	100.00	.043032	.002481	.003576	.000911
	325.00	.031680	.007267	.008068	.002986
	650.00	.019500	.012510	.012018	.005971
	1000.00	.010819	.015829	.014240	.009112
	1300.00	.006063	.016900	.015093	.011943
	5250.00	0	.000150	.002079	.047771
1mm	0.10	.049480	.000121	.000358	.000040
	0.25	.048891	.000297	.000711	.000101
	1.00	.046464	.001146	.001984	.000405
	5.12	.036295	.005282	.006350	.002073
	10.00	.026863	.009357	.009730	.004050
	20.00	.012703	.015189	.013814	.008294
	31.00	.005229	.016925	.015191	.012655
	41.00	.002340	.015853	.015220	.016587
	82.00	.000081	.005718	.011027	.033174
	100.00	.000009	.002159	.007336	.040496
3mm	0.10	.046763	.001036	.001837	.000364
	0.25	.043032	.002481	.003576	.000911
	0.64	.034933	.003864	.006870	.002333
	1.00	.028630	.008590	.009135	.003645
	1.25	.024763	.010266	.010415	.004556
	2.56	.010357	.015974	.014339	.009330
	5.12	.001554	.014777	.015009	.018661
	6.25	.000703	.012223	.014295	.022779
	10.00	.000034	.003981	.009539	.036446

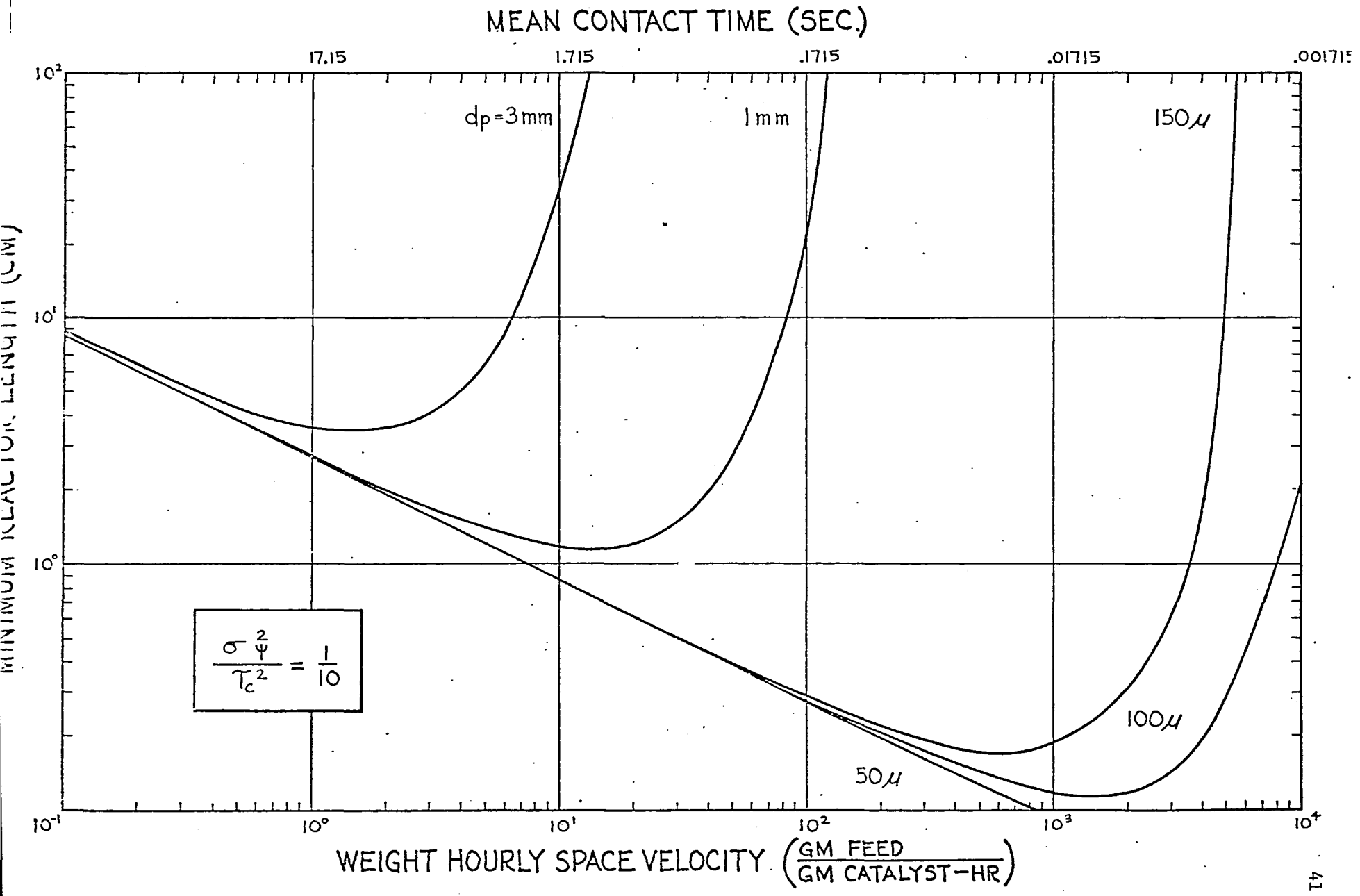

Fig. 1- Minimum reactor length vs space velocity.

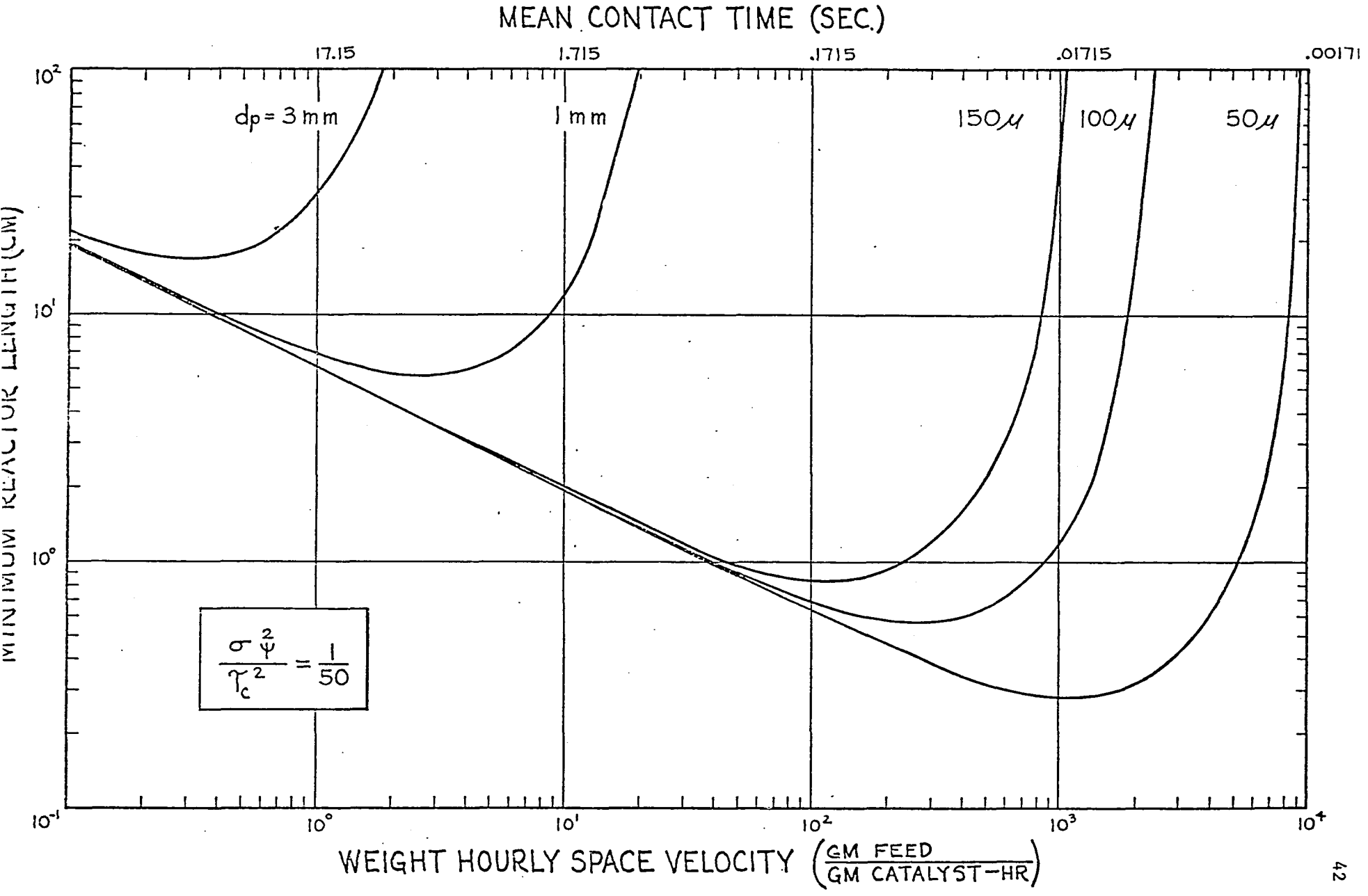

Fig. 2 – Minimum reactor length vs space velocity.

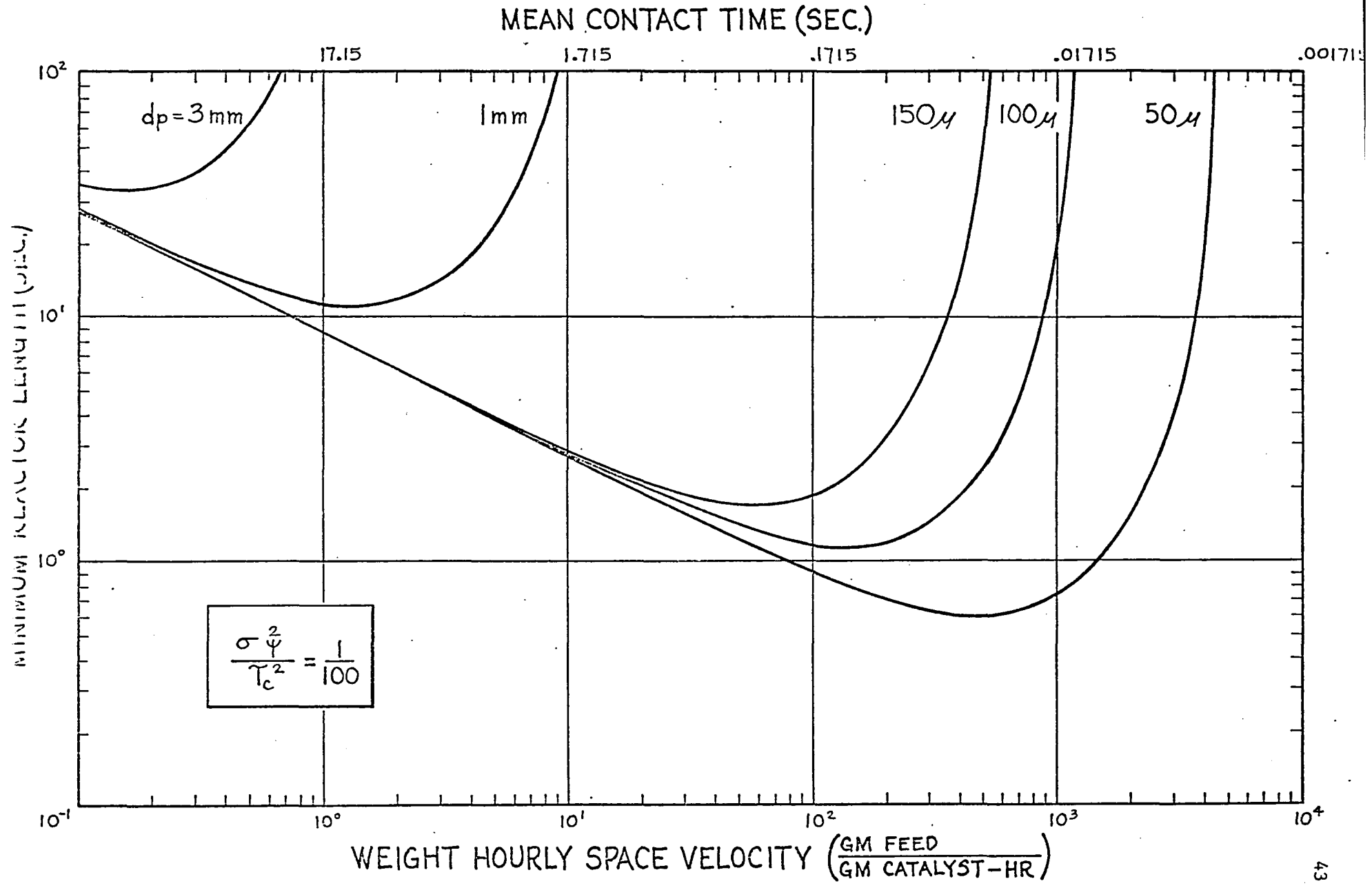

Fig. 3 — Minimum reactor length vs space velocity.

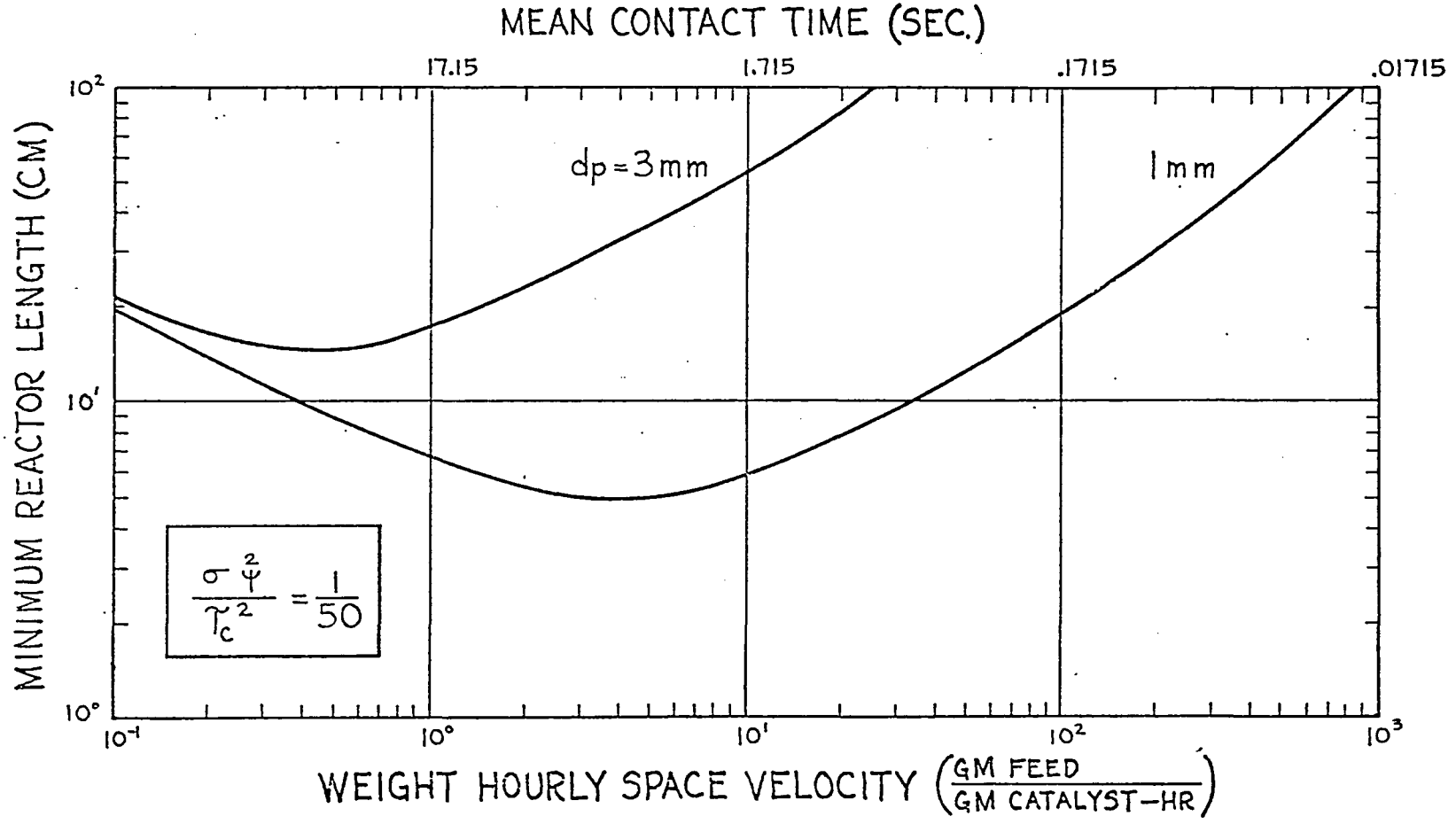

Fig. 4 – Minimum reactor length vs space velocity for scale up problem.

SECTION II - STABILIZATION OF REACTORS OPERATING AT UNSTABLE STEADY STATES. THE EFFECT OF DESIGN ON CONTROL

INTRODUCTION

In the aerospace industry, it is quite common to integrate the control considerations of a system with its basic design concepts. However, this is rare in the chemical industry, where in most cases, designs are based solely on projected steady state operating levels. Control of the plant is seriously considered only after the basic design is completed. Usually this procedure is justified since development work is carried out partly to facilitate conservative steady state designs which will not cause stability problems. So, in this sense, at least, control considerations do play a part in determining the design. However, it is still intriguing to consider how an integration of the control considerations into the basic design might pay off in easier control, better overall performance, or improved economy.

A suitable process for this study is one which is open loop unstable and is stabilized by a feedback control loop. Aris and Amundson have discussed one such process in a series of papers (1958a, 1958b, 1959) describing the stabilization of a stirred tank reactor involving an exothermic reaction. It is stabilized by adjusting the amount of heat removed by a coolant to maintain the desired reactor temperature. In this study we have chosen the somewhat more complex process shown schematically in Figure 1. Many exothermic industrial reactors, particularly those used in hydroprocessing and some oxidation reactions, utilize this configuration, with or without interstage cooling, where the adiabatic catalytic fixed bed reactor effluent is used to preheat the incoming fresh feed. The reactor inlet temperature might be further

adjusted by passing the feed through a furnace. Such reactors can exhibit potential instabilities in the following ways:

1. Multiple steady states can occur inside the catalyst phase as shown by several investigators (Liu and Amundson, 1962, 1963; Eigenberger, 1972a, 1972b). If this occurs, feedback control on the entire reactor is of no value. This behavior is usually avoided by determining stable operating levels during process development and pilot plant work.
2. The preheating of the fresh feed by the reactor effluent provides positive feedback of heat and allows the possible occurrence of multiple steady states. The steady state behavior can be described by the classical heat production curve--heat removal line diagram of Figure 2. We are interested in the intermediate steady state which is open loop unstable as shown by van Heerden (1953, 1958). Any small perturbation in inlet temperature, concentration or flow rate will cause the system to drift to one of the other two stable steady states.
3. In some cases even single steady states may be linearly unstable and show limit cycle behavior (Reilly and Schmitz, 1966, 1967; Parega and Reilly, 1969).

We will concentrate our discussion on the second case because of its applicability to industrial processes. However, we will touch on the third case as well, since the designer is often unaware of its potential existence.

DESCRIPTION OF PROBLEM

Typically packed bed reactors with positive feedback of heat consist of stages with quench zones between them. In hydroprocessing, H_2 would be added between stages to limit the temperature rise in the reactor. However, for simplicity we will first consider the system without quench and define for it a criterion for linear stability.

Linearized Stability Analysis

In addition to heat, in commercial processes unconverted feed is also fed back to the reactor after having been separated from the reactor effluent. This feedback of mass can also contribute to the occurrence of multiple steady states, as shown by several investigators (Luss and Amundson, 1967; Root and Schmitz, 1969, 1970). However, in this paper we are only interested in the effects of thermal feedback on reactor stability and will assume that the unreacted feed is first sent to a holding tank where its temperature and concentration are made to conform to those of the fresh feed.

Let us now write the overall transfer function for the process relating changes in reactor outlet temperature to fresh feed temperature, inlet concentration, and flow disturbances. All perturbations are defined as being around the steady state value. The linearized transfer functions for the reactor, heat exchanger, and furnace are respectively,

$$(1) \qquad \delta T_L = G_R^{T_L T_o}(s)\,\delta T_o(s) - G_R^{T_L \phi_R}(s)\,\delta \phi_R(s) + G_R^{T_L C_i}(s)\,\delta C_i(s)$$

$$(2)\quad \delta T_o'(s) = G_H^{T_o' T_L}(s)\,\delta T_L(s) + G_H^{T_o' T_F}(s)\,\delta T_F(s) - G_H^{T_o' \phi_H}(s)\,\delta \phi_H(s)$$

$$(3)\quad \delta T_o(s) = G_F^{T_o T_o'}(s)\,\delta T_o'(s) + G_F^{T_o \phi_g}(s)\,\delta \phi_g(s) - G_F^{T_o \phi_F}(s)\,\delta \phi_F(s)$$

We assume for the time being, that the furnace effluent temperature is uncontrolled, so that the fuel rate is fixed and $\delta\phi_g(S) = 0$. We will also assume that the flow rates through all three units are the same, that is $\phi_R = \phi_F = \phi_H$. In a later section it will be shown that this need not be true in all cases. If these transfer functions are now combined we obtain the overall transfer functions for the reactor outlet temperature as a function of disturbances in feed temperature, flow rate, and concentration:

$$(4)\quad \frac{\delta T_L(s)}{\delta T_F(s)} = \frac{G_R^{T_L T_o}(s)\, G_F^{T_o T_o'}(s)\, G_H^{T_o' T_F}(s)}{1 - G_R^{T_L T_o}(s)\, G_F^{T_o T_o'}(s)\, G_H^{T_o' T_L}(s)}$$

$$(5)\quad \frac{\delta T_L(s)}{\delta \phi(s)} = \frac{-\left[G_R^{T_L \phi}(s) + G_R^{T_L T_o}(s) G_F^{T_o T_o'}(s) G_H^{T_o' \phi}(s) + G_R^{T_L T_o}(s) G_F^{T_o \phi}(s)\right]}{1 - G_R^{T_L T_o}(s)\, G_F^{T_o T_o'}(s)\, G_H^{T_o' T_L}(s)}$$

$$(6)\quad \frac{\delta T_L(s)}{\delta C_i(s)} = \frac{G_R^{T_L C_i}(s)}{1 - G_R^{T_L T_o}(s)\, G_F^{T_o T_o'}(s)\, G_H^{T_o' T_L}(s)}$$

The characteristic equation for all three transfer functions is:

$$(7) \qquad 1 - G_R^{T_L T_o}(s)\, G_F^{T_o T_o'}(s)\, G_H^{T_o' T_L}(s) = 1 - G^*(s) = 0$$

For simplicity, we will drop the superscripts and use $G_R(S)$, $G_F(S)$, and $G_H(S)$.

It is noted that this is the characteristic equation for a positive feedback system. The positive feedback is in the form of heat and is due to the presence of the heat exchanger. The important crossover frequencies for such a system correspond to phase lags which are multiples of -360° and not -180°. For the system to be stable, eq. (7) must not have any positive roots. A necessary and sufficient condition for insuring this is that the largest value of the open loop frequency response, $|G^*(j\omega)|$, corresponding to a crossover frequency is less than unity.

$$(8) \qquad \max\left[|G^*(j\omega)|_{co}\right] < 1$$

A conservative stability criterion is one which forces $|G^*(j\omega)| < 1$ at <u>all</u> frequencies. This is a sufficient but not a necessary condition for stability. However, in practice, for this type of reactor it is really not very conservative as a simple argument will indicate.

Let us look at some typical forms of $|G_R(j\omega)|$, $|G_H(j\omega)|$ and $|G_F(j\omega)|$, the amplitude ratio curves. Shown in Figure 3 are several examples of linearized reactor frequency response curves corresponding to points on the heat production curve of Figure 2. The hash marks on

the curves indicate the frequencies at which the phase angle passes through a 360° rotation. We note that some of these curves have peaks. These occur because of the interaction between temperature and concentration waves which pass through the reactor as described by Foss and coworkers (1966, 1968, 1970, 1971). More will be said about this in a later section. We also note that by the nature of real systems these frequency response curves must always be damped at high frequencies due to backmixing and diffusional effects which occur. The frequency response and phase lag curves corresponding to typical open loop furnace and heat exchanger transfer functions are given in Figures 4(a) and 4(b) as curves B_1 and C_1. A typical frequency response curve for a reactor is also included in Figure 4(a) for the readers' convenience. The resulting open loop AR curve is given in Figure 4(a) as curve F. The hash marks on the curve indicate the crossover frequencies at which the phase response passes through a multiple of -360°. The largest AR corresponding to a crossover frequency determines the stability of the system. For the process considered, the largest open loop AR corresponds to a point on the peak of the reactor frequency response curve. The process is unstable. In practice, the normal delays in such a reactor, heat exchanger, and furnace system together with piping delays are such that a crossover frequency will also occur in the range where the natural dampening processes are still minimal. Thus, the stability condition $|G^*(j\omega)| < 1$ becomes the less conservative condition.

$$\max \left| G^*(j\omega) \right| < 1$$

In practice this should not be much more stringent than the condition of inequality (8).

This result is very important because it tells us the minimum amount of information necessary to insure good control and stability. It means that highly accurate information about the forms of $G_R(S)$, $G_H(S)$, and $G_F(S)$ and the values of the crossover frequencies are not required. This is fortuitous since in chemical processing this information is seldom available.

Using Figures 2-4, a more physical interpretation can be obtained of the stability of the system without control. In Figure 2, we show graphically the steady state heat balance for a packed bed reactor with a first order exothermic reactor A→B. Curve A is the heat production curve and gives the temperature rise in the reactor as a function of reactor inlet temperature. Line B is the heat removal line which determines how much heat is removed from the reactor effluent to preheat the fresh feed. Strictly speaking, this line is nonlinear because the steady state equations describing the furnace are nonlinear. However, it can be written in the following form if it is linearized around a point of intersection with the heat production curve.

$$\delta T_L - \delta T_o = \left(\frac{1}{G_F(0)\, G_H(0)} - 1 \right) \delta T_o - \frac{G_H^{T_o' T_F}(0)}{G_H^{T_o' T_L}(0)} \delta T_F$$

This relation applies only for a small neighborhood of the intersection point. The corresponding linearized equation for the heat production curve is:

$$\delta T_L - \delta T_o = \left[G_R(0) - 1 \right] \delta T_o$$

With no controls on the heat exchanger, furnace, or reactor, the condition that $G^*(0) < 1$ is simply the slope condition, namely, that the slope of the heat removal line is larger than the slope of the heat production curve at the steady state.

If $|G_R(j\omega)|$ has no peak and decreases monotonically, then the stability condition of ineq. (8) becomes the slope condition. This is also the stability condition for a pure plug flow reactor operated adiabatically, since its frequency response is flat. If $|G_R(j\omega)|$ has a maximum, which can occur under a variety of conditions, then satisfaction of the slope condition is not sufficient to insure stability. For cases given in Figure 3, steady states below the inflection point of the heat production curve of Figure 2 will be stable if the slope condition is satisfied. However, for cases with higher conversion where a peak exists, this is not sufficient. As a result, if three steady states can occur, then it is possible that the stability sequence will be S-N-N, where S = stable and N = not stable. It is also possible to have a single unstable steady state which will move to a stable limit cycle with any perturbation.

Let us now discuss how a reactor with a maximum in its frequency response can be stabilized. One approach is to modify $G_H(S)$ or $G_F(S)$ so that the gain of the heat feedback loop is lowered such that $|G^*(j\omega)|$ is reduced below unity. This can be achieved by increasing the heat duty of the furnace. This reduces the required size of the heat exchanger and decreases the amount of heat feedback to the reactor. The effect on the respective frequency responses are given as curves B(1-3) and C(1-3) in Figure 4(a). The effect is to increase the slope of the heat removal line.

In practice, however, an open loop furnace will almost never be used. Rather a control scheme will be provided to maintain the furnace exit temperature by adjusting the fuel rate to the furnace. The open loop furnace transfer function can simply be replaced by the closed loop transfer function $G_F^*(S)$ in eq. 7 and the preceding arguments remain valid. A typical form of $|G_F^*(j\omega)|$ is given as curve D in Figure 4(a). The AR is very low at low frequencies, reaches a maximum with increasing frequency then decreases. The occurrence of a peak is typical of systems with feedback control. Near the resonance frequency the furnace will have little dampening effect. For this reason, the size and location of the reactor peak is important for controller design. The control system should dampen the reactor AR where the peak occurs; at the same time it must be designed so its own peak occurs at a sufficiently high frequency where the reactor response is highly attenuated.

Large industrial furnaces are normally sluggish and the peak of $|G_F^*(j\omega)|$ occurs at relatively low frequencies. Consequently, it is important to provide a temperature control loop in the system which responds quickly and whose resonance region occurs at high frequencies. In one possible control scheme, fresh feed is bypassed around the heat exchanger and the bypass flow is adjusted according to fluctuations in the furnace inlet temperature. A typical response of a closed loop heat exchanger with bypass control is given in Figure 4 and the resulting overall response $|G^*(j\omega)|$ is also given in Figure 5 along with the curve for the case using only furnace fuel control. Bypass control improves stability considerably, but proper utilization of such a scheme requires consideration in the original design.

An important result of this study is that the three elements of $G^*(S)$ can be investigated separately and then combined later to give $|G^*(j\omega)|$. The effect of the design on the frequency response of each element and on the control of the system can be determined systematically.

Nonlinear Stability Analysis

The reactor frequency responses considered thus far were found for small perturbations about a steady state. However, such reactors can be highly nonlinear due to the exponential dependence of the reaction rate constant on temperature. Unless the nonlinearities are considered, linear stability analysis is only of limited value. There are two types of nonlinearities which will be discussed here qualitatively. The figures used for illustration were developed from examples which will be discussed in more detail in a later section.

The first type of nonlinear behavior is in response to large perturbations in reactor inlet temperature. In Figure 6, we present a typical outlet temperature response of a reactor to inlet temperature disturbances varying sinusoidally with time. The reactor is the same one for which the heat production curve of Figure 2 was generated. The linear frequency response corresponding to the same nominal inlet temperature is given in Figure 3.

The nonlinear responses are not symmetrical about the nominal outlet temperature. The distortions are caused by the higher harmonics which occur due to the reaction rate nonlinearity. However, the responses lack strong secondary peaks and have the same frequencies as the input disturbances. These results make it tempting to plot nonlinear frequency response curves, and substitute these responses for $|G_R(j\omega)|$

in the stability criterion. Sets of two nonlinear curves are plotted in Figure 7. One is simply the average value of the maximum and minimum of the output response divided by the input amplitude. The second is the difference between the larger of the two output amplitudes and the old steady state value divided by the input amplitude. Such curves for several nominal inlet temperatures are given in Figure 7 for the range of frequencies corresponding to $|G_R(j\omega)|_{max}$. Also shown are the corresponding linear responses. For nominal inlet temperatures below the inflection point, the nonlinear response has a larger amplitude ratio than does the corresponding linear response. At inlet temperatures above the inflection point the situation is reversed and the linearized frequency response can be confidently used in designing the process.

A second type of nonlinearity is illustrated by curve A in Figure 8. This is the heat production curve for a reactor with three consecutive first order reactions A→B→C→D. For the heat removal line given, five steady states are possible, with the middle three being very close together. If the desired steady state is at point S, then the system is linearly stable. However, a nonlinear perturbation in inlet temperature may cause it to become unstable. If the open loop reactor is perturbed with a sinusoidal input of large amplitude the apparent $|G_R(j\omega)|$ can have much larger values than the linearized response.

There have been many approaches to nonlinear stability analysis described in the literature (Ritter and Douglas, 1970; Denn 1975). Most of them, apart from direct simultation, are not applicable to the system discussed here, since they depend on more reliable information than would normally be available. We propose a "poor man's" nonlinear

stability analysis which is quite simple and by simulation can be demonstrated to be adequate. The problem can be approached in two ways.

If it is desired that the system be globally stable, then it is necessary to determine the worst reactor frequency response, be it linear or nonlinear. This can be done by examining all of the possible steady states of the system and finding the one which produces the largest $|G_R(j\omega)|_{max}$ and the worst dampening characteristics. This should be done first for the linearized frequency responses and then the nonlinear response corresponding to the worst case should be examined. If we can stabilize the reactor having the worst frequency response, then the system will be globally stable. This requires that $|G^*(j\omega)| < 1$, but also that the control system provides sufficient gain margin to account for any uncertainties.

Alternatively, we can estimate the maximum perturbation we expect and generate the corresponding nonlinear frequency response curve. This $|G_R(j\omega)|$ would then be used to determine the necessary control elements which would include a reasonable safety factor to allow for our lack of knowledge. The amount of compensation that can be provided is limited by the saturation level of the controller. For example, in the standard furnace control scheme, the fuel flow has an upper limit, so for large drops in feed temperature the desired outlet temperature may not be physically obtainable. If temperature rises occur which exceed the fluid steady state temperature change, even closing the valve will not maintain the desired outlet temperature.

If the nonlinear reactor behavior is a problem, the designer has several options. He can redesign the reactor to obtain a different

frequency response curve with a smaller peak. This can be done by lowering the conversion in the reactor and recycling more unreacted feed. Alternatively, the design can be changed to limit the temperature rise in the reactor while maintaining the desired conversion. From the design engineer's point of view, any substantial changes in the reactor design are worthwhile only if the selectivity and yield are improved or if the catalyst life can be enhanced. These gains would have to be weighed against any increased capital and operating costs which might be incurred. Changes in the reactor design suggested by the control engineer which might improve the process stability may be at odds with these constraints. Consequently, to have a process which is efficient, economical, and easily controlled requires compromises between the design and control considerations.

Another option is to introduce a control element into the reactor configuration. The reactor can be divided up into a number of catalyst beds with controlled quench streams introduced between them to limit the temperature rise. This changes $G_R(S)$ in the preceding equations to some $G_R^*(S)$. The designer can also increase the heat load of the furnace to reduce the heat feedback in the system. However, this approach poses the problem of heat disposal from the reactor effluent and significantly increases the operating costs for fuel.

Any design involves proper balancing of steady state, control, and economic requirements. This analysis shows that we can decouple these considerations for each unit by looking at the effects of steady state design and control on $G_R(S)$, $G_H^*(S)$, and $G_F^*(S)$ individually and then match them to obtain the desired properties for $G^*(S)$.

EFFECT OF DESIGN ON $G_R(S)$

Since a catalytic fixed bed reactor involves complex interactions between the heat and mass transfer mechanisms and the reaction mechanism, it is very difficult to measure or compute accurately the transfer function $G_R(S)$. For purposes of controller design, estimates are required of $|G_R(0)|$, $|G_R(j\omega)|_{max}$ and ω_c, the cutoff frequency. We arbitrarily define the cutoff frequency as being that corresponding to $|G_R(j\omega)| = 0.35$. If both $|G_R(0)|$ and $|G_R(j\omega)|_{max}$ are low, then determining ω_c is less important since the process is either stable or easy to stabilize.

Data from Laboratory Experiments

The main non-kinetic parameters affecting the reactor behavior such as fluid and catalyst physical properties, heat and mass transfer coefficients and bed voidage can be obtained in fairly routine laboratory experiments on bench scale or pilot plant equipment. From work which may be more involved, a reaction mechanism and rate expressions can be obtained. The heat production curve of reactor temperature rise vs. inlet temperature can be obtained experimentally. The slope of this curve at any point is related to $G_R(0)$ by

$$\text{slope} = G_R(0) - 1$$

From experiments of this type we can get a good feeling for the steady state behavior of the reactor. However, to understand its dynamic behavior and obtain estimates for $|G_R(j\omega)|_{max}$ and ω_c, the use of dynamic models in conjunction with pilot plant studies is helpful.

Reactor Modeling

As shown by Crider and Foss (1966, 1968) and Sinai and Foss (1970), an important feature of catalytic fixed bed reactor behavior is that there are two independent waves, a concentration wave and a temperature wave, which travel through the reactor at different velocities. The concentration wave travels at approximately the fluid velocity while the temperature wave travels at a slower velocity which is dependent on the thermal properties of the fluid and the catalyst. These waves of differing velocities are produced primarily because of the large thermal holdup in the solid phase. These phenomena have also been studied in non-reactive systems by Amundson (1956) and Aris (1957).

Two simple models for adiabatic fixed bed reactors which describe the wave phenomenon have been proposed in the literature, that of Liu and Amundson (1962) and that of Crider and Foss (1968). These are described in Table 1 where the concentrations and reaction rates are given in vector notation.

In the former model the reaction occurs in the catalyst phase and both convective heat and mass transfer effects are included. Liu and Amundson show that for a single irreversible first order reaction the equations are relatively easy to solve numerically using the method of characteristics (Acrivos, 1956). All of the nonlinear responses in this work were found using this model.

In the latter model the packing is assumed to be inert and the first order reaction occurs in the interstitial phase. If these equations are linearized, and a single irreversible first order reaction occurs, they can be solved analytically for the linearized reactor

transfer functions. One of these is given in Table 1. The mathematical development is given in the Appendix. More complex models are also available (Liu and Amundson 1963; Eigenberger 1972a,b).

The results of the two models are similar. In Tables 2 and 3, details are given for two examples used throughout this work. Case 1 given in Table 2 is a simple exothermic reaction A→B; Case 2 is a simplified version of a hydrocracker with a more complex consecutive reaction.

Gas Oil → Jet Fuel → Gasoline → Light Gases

In Figures 9 and 10, we present for case 1 typical responses to a step change in inlet temperature and linearized frequency responses computed from both models. Both models give very similar step responses and for purposes of rough estimation are equivalent. Due to the wave interaction, the reactor outlet temperature first decreases before it increases to a new steady state. This occurs because the step increase in feed temperature heats the catalyst near the reactor inlet which increases the reaction rate and reduces the concentration of the fluid. Since the thermal wave velocity is less than the fluid velocity, the reactor outlet first experiences a decrease in reaction rate due to the depletion of reactant upstream. Only when the thermal wave reaches the outlet do the reaction rate and temperature start to increase. This "wrong way" response has been verified experimentally by Foss and coworkers (1970, 1971) and Van Doesberg and de Jung (1976a,b).

As shown by Crider and Foss (1968) and Aris (1957), the ratio of the thermal wave residence time, τ_{th}, to that of the fluid residence time, τ_f, depends on the densities and heat capacities of the fluid and catalyst. The approximate relationship is

$$\frac{\tau_{th}}{\tau_f} = \frac{\rho_p c_p (1-\epsilon) + \rho_f c_f \epsilon}{\rho_f c_f \epsilon} = \left(1 + \frac{1}{\beta}\right)$$

This ratio can vary from about 2 for a pure liquid reacting fluid to about 1000 for a gaseous reacting fluid. It is the delay time of the thermal wave, τ_{th}, which affects the phase response of the reactor. The first -360° crossover point will occur at approximately $\omega = \frac{2\Pi}{\tau_{th}}$. This should be a good estimate for the frequency at which $|G_R(j\omega)|_{max}$ occurs.

Both models give similar estimates for the size of the peak of the frequency response and the range of frequencies over which it occurs. These peaks are caused by the interaction of the temperature and concentration waves traveling at differing velocities through the reactor. The size of the peak is related to the extent of the initial "wrong way" response to a step input. Its existence has been verified experimentally by Sinai and Foss (1970).

When a complex system is modeled for purposes of control we always face the same difficulties. The actual process is complex physically and mathematically. It is difficult to define an exact model and measure its important parameters. What is required is a simple model which describes the essential features of the process. It must be conservative in the sense that a controller which can handle a process described by this model should be able to handle the same process

described by a whole set of potential models. All that is required are similar estimates for $|G_R(j\omega)|_{max}$ and the frequency at which it occurs. We also need an estimate for the cutoff frequency, ω_c.

Dispersion Effects

Although both models discussed give similar estimates for the peak, they suffer from the fact that they do not include the dispersion effects of backmixing and intraparticle diffusion. Dispersion effects have filtering properties and should tend to reduce the size of the reactor peak and the cutoff frequency; neglecting them gives conservative results for controller design.

To estimate how the filtering capacity of the mixing processes affect the reactor response, we develop a nonreactive model for a packed bed which includes the effects of turbulent diffusion, convective heat transfer, and intraparticle thermal diffusion. The model is described in the Appendix. Using techniques analagous to those used in earlier studies (Silverstein and Shinnar, 1975; Shinnar, et.al. 1972), the transfer function relating the outlet temperature to disturbances in inlet temperature is developed. Treating this as a moment generating function, the variance of the residence time distribution of the thermal wave can be calculated. This is then a measure of the dispersion of the wave due to mixing processes.

The normalized variance is

(9a) $$\frac{\sigma_g^2}{T_{th}^2} = 2\left[\frac{1}{Pe_{th}} - \frac{1-e^{-Pe_{th}}}{Pe_{th}^2} + \frac{1}{\eta_{th}(1+B)^2} + \frac{\Theta_{th}}{3T_{th}(1+B)}\right]$$

where Pe_{th} is the Peclet Number for thermal dispersion, $n_{th}(1+B)^2$ is a dimensionless number measuring the extent of convective heat transfer to the solids and $\frac{\theta_{th}}{3\,\tau_{th}(1+B)}$ describes the extent of intraparticle thermal diffusion over the entire solid bed. The normalized variance can be rewritten in terms of reactor parameters as

$$(9b) \qquad \frac{\sigma_g^2}{T_{th}^2} = 2\left[\frac{k_{eff}\,T_\alpha}{\rho c_v L^2} + \frac{1}{H_\rho T_{th} B(1+B)} + \frac{d_p^2 \rho_p c_p}{108\, k_p T_{th}(1+B)}\right]$$

where k_{eff} is the effective thermal conductivity of the bed defined by Yagi and Kunii (1957). The thermal dispersion term, $\frac{1}{Pe_{th}}$ is proportional to $\frac{d_p}{L}$ and for most industrial reactors will be small. For this reason, the second term of eq. (9a) has been omitted in eq. (9b).

Utilizing an expression developed by McHenry and Wilhelm (1957), the following simplified transfer function can be written for the bed:

$$(10) \qquad \frac{T_L}{T_o} = e^{-\omega^2 \frac{\sigma_g^2}{2}}$$

An estimate for ω_c can be made by the relation

$$(11) \qquad \omega_c \approx \frac{1.449}{\sigma_g}$$

This value can be compared to the cutoff frequency calculated using only the convective heat transfer term in eq. 9. Normally, the convective heat transfer term will dominate and the difference will be small. However, if there <u>is</u> a significant difference between these two values, because the effects of intraparticle diffusion are large, then inclusion

of these effects in the reactor model might be advisable. Exclusion of these effects would give a conservative estimate of ω_C for control purposes.

Properties of Frequency Response for Reactor Case 1

In Figure 3, $|G_R(j\omega)|$ is presented for a number of different reactor conditions for case 1 described in Table 2. They correspond to points on the heat production curve of Figure 2. The ratio of $|G_R(j\omega)|_{max}$ to $G_R(0)$ increases with reactor inlet temperature and with temperature rise through the reactor. In the high conversion region of the heat production curve, where the slope approaches zero and $G_R(0)$ approaches unity, there is a possibility of $|G_R(j\omega)|_{max}$ being much larger than unity. Without proper controls this can lead to instabilities with the system shifting to the low conversion steady state if three operating points are possible. If the system is designed for only one high conversion steady state, then a stable limit cycle can result.

If the maximum adiabatic temperature rise through the reactor increases, then the heat production curve becomes steeper and $|G_R(j\omega)|_{max}$ will also increase. This is shown by curves A and C in Figure 11. Such cases may be difficult to stabilize with conventional control schemes and modification of the reactor design may be necessary to reduce the temperature rise in the reactor. This can be done by reducing the conversion or by reducing ΔT_{ad} through the reactor by diluting the feed with a large recycle stream or with an inert diluent. The effect of the latter on the frequency response is shown by curves B and D in Figure 11. Both of these approaches carry some penalties. Reducing conversion

of these effects in the reactor model might be advisable. Exclusion of these effects would give a conservative estimate of ω_C for control purposes.

Properties of Frequency Response for Reactor Case 1

In Figure 3, $|G_R(j\omega)|$ is presented for a number of different reactor conditions for case 1 described in Table 2. They correspond to points on the heat production curve of Figure 2. The ratio of $|G_R(j\omega)|_{max}$ to $G_R(0)$ increases with reactor inlet temperature and with temperature rise through the reactor. In the high conversion region of the heat production curve, where the slope approaches zero and $G_R(0)$ approaches unity, there is a possibility of $|G_R(j\omega)|_{max}$ being much larger than unity. Without proper controls this can lead to instabilities with the system shifting to the low conversion steady state if three operating points are possible. If the system is designed for only one high conversion steady state, then a stable limit cycle can result.

If the maximum adiabatic temperature rise through the reactor increases, then the heat production curve becomes steeper and $|G_R(j\omega)|_{max}$ will also increase. This is shown by curves A and C in Figure 11. Such cases may be difficult to stabilize with conventional control schemes and modification of the reactor design may be necessary to reduce the temperature rise in the reactor. This can be done by reducing the conversion or by reducing ΔT_{ad} through the reactor by diluting the feed with a large recycle stream or with an inert diluent. The effect of the latter on the frequency response is shown by curves B and D in Figure 11. Both of these approaches carry some penalties. Reducing conversion

reduces the amount of heat feedback but increases pumping and separation costs because of the larger recycle stream that is required. With dilution the reactor inlet temperature will increase to attain the desired conversion, and the reactor outlet temperature will decrease. Since the reactor outlet temperature sets the temperature levels in the heat exchanger, these effects will mean a smaller ΔT for heat exchange. These, together with the increased mass flow, will require a larger combined heat duty for the furnace and heat exchanger. The increase in furnace and heat exchanger sizes will increase the capital costs and the fuel costs. Depending on what the diluent is, its cost may also be high. Additionally, greater capital costs will be incurred due to the need for larger separation units and larger compressors to handle the larger recycle stream.

The linearized Crider and Foss Model gives a reasonable estimate of what to expect for first order reactions but is useless for more complex kinetics because an analytical solution is no longer possible. If a pilot plant reactor exists, then an estimate for $|G_R(j\omega)|$ can be obtained by fitting an empirical expression to the open loop step response. The size of the step input can be made large so that the effects of non-linearities can also be estimated. The fitting function, however, must be chosen to describe the "wrong way" response as shown in Figures 9 and 10, otherwise an estimate for $|G_R(j\omega)|_{max}$ will not be obtained.

This approach suffers from a scale-up problem. It is important that scalable conditions be chosen for the pilot plant and for the industrial reactor which do not produce multiple steady states in the catalyst phase. Under such conditions, the effect of scale-up is to

increase the heat and mass transfer coefficients to the catalyst surface and to reduce the effects of backmixing. From a kinetic standpoint, the reactor tends to approach plug flow more closely with scale-up. As discussed in the Appendix for heat transfer effects and in Section I for mass transfer effects, the effects of thermal and mass diffusion and convective transfer rates on the kinetic behavior of the pilot plant reactor can be minimized so that it is similar to that of the industrial reactor. This is possible because the kinetic behavior is relatively insensitive to changes in the variances of the respective residence time distributions. If the coefficients of variation can be made reasonably small, then the pilot plant will kinetically approach plug flow reasonably closely.

The reactor frequency response, however, as shown in eq. 10 depends on frequency as well as the variance of the thermal residence time distribution. Thus even small relative differences in the variances of the RTD of the pilot plant reactor and the RTD of the industrial reactor can be magnified at moderate frequencies to cause significant differences in the amplitude ratios of the two reactors. This is shown in Figure 12 where Hp is varied in the Crider and Foss model. Increasing Hp is equivalent to reducing the variance. Thus, the industrial reactor will be harder to control than the pilot plant reactor. Actually, for very large Hp, the variance will reach some limiting value since thermal diffusion effects in the solid phase are independent of fluid flow and reactor length. Consequently, there will be some upper limit on the cutoff frequency, ω_c.

It is observed from the figure that the cutoff frequencies are uniformly spaced. This follows from eq. 11. Using this equation, the

cutoff frequency can be estimated for the industrial reactor from pilot plant data by:

$$(12) \qquad \frac{(\omega_c)_{indust}}{(\omega_c)_{pilot}} = \frac{(\sigma_g)_{pilot}}{(\sigma_g)_{indust}}$$

For a reactor where only convective heat transfer effects are important, this becomes

$$(13) \qquad \frac{(\omega_c)_{indust}}{(\omega_c)_{pilot}} = \sqrt{\frac{(H_\rho)_{indust}}{(H_\rho)_{pilot}}} = \left(\frac{L_{indust}}{L_{pilot}}\right)^{\frac{1}{4}}$$

Since the peak approaches an asymptotic value, its size for the industrial case can be estimated graphically from the size of the peaks of several pilot plant responses with successively longer reactors and from the estimate for (ω_C) indust.

Criterion for Global Stability

By applying the "poor man's" nonlinear analysis to the example of case 1, a criterion for global stability can be determined. It can be seen from Figures 2 and 3 that although operation at the inflection point gives the largest $G_R(0)$, the frequency response for the reactor with $T_0 = 590°F$ represents an upper bound on both the size of the reactor peak and on ω_C. This is the "most difficult" operating point to stabilize on the heat production curve. It remains now to determine by simulation the nonlinear frequency response for this operating point. Sine waves should be used having amplitudes equal to the largest inlet temperature disturbance anticipated. As shown earlier in Figure 7, the nonlinear response has a lower $|G_R(j\omega)|_{max}$ and ω_C than the linear response. Hence, the "most difficult" linear case to stabilize is also more difficult to stabilize than any nonlinear case. If a control system is

designed to stabilize this linear case, then it will stabilize all possible nonlinear cases as well. The process will operate within a large "practical region of stability" (Perlmutter, 1972) limited only by the heat duties and control action of the furnace and heat exchanger. If the kinetics are complex the simple model is inadequate and pilot plant data are needed to empirically determine the required frequency responses.

It should be noted that operating at an intermediate steady state normally implies that complex kinetics are involved. At the flat upper part of the heat production curve undesirable side reactions may occur, while at lower operating temperatures they are suppressed. Thus, the simple first order model applies as long as the reactor inlet temperature is maintained below some upper limit. However, since many industrial processes involve complex reactions it is important that such cases be considered.

Complex Kinetics

Case 2 given in Table 3 is a simplified example of a hydrocracker. An actual hydrocracker is a trickle bed reactor, while the model presented here is for a single fluid phase having physical properties whose values are averaged between those of typical gaseous and liquid phases. The model, however, should illustrate some of the behavior of a hydrocracker. In actual development work it is important that pilot plant studies be carried out to compensate for our ignorance about the kinetics and hydrodynamics.

The kinetic rate constants for the first two reactions, k_1 and k_2, are taken from the work of Stangeland and Kittrell (1972) and are listed

in Table 3. The third reaction has been added in this example to account for the large temperature rises which may occur in a hydrocracker if cracking is allowed to produce significant amounts of gaseous products. It is assumed for the purposes of this example that the activation energy for the third reaction is the same as that for the second, but its pre-exponential factor is $\frac{1}{10}$ that of the second. The values of the heats of reaction were determined by assigning empirical formulas to species A, B, C, and D and then applying the method outlined by Jaffe (1974). The heats of reaction together with other pertinent reactor parameters are listed in Table 3.

Some heat production curves for this reactor are presented in Figure 8 and the linearized frequency responses for typical operating points are given in Figure 13. With consecutive reactions the heat production curve can have more than one inflection point and, if ΔT_{ad} is high, can have very large slopes. The form of the frequency response curve is similar to that for case 1, but it reflects the steepness of the heat production curve and can have potentially large values of $G_R(0)$ and $|G_R(j\omega)|_{max}$. This can be seen from curve A in Figure 8 and from the frequency response curve for point 1 in Figure 13. For this case, equal amounts of make-up H_2 plus recycle enter the reactor to total 2,000 SCFD/BPD. A mixture of jet fuel and gasoline is the desired product and production of light gases has to be minimized. Consequently, operation at an inherently unstable steady state such as point 1 may be necessary.

There are three ways in which we can modify the frequency response of the reactor. The first is by diluting the feed. In partial oxidation, some reactors are run with a large excess of air as a heat sink.

In hydroprocessing, large excesses of H_2 are used for the same purposes. If, in our example, the recycle flow is tripled, the amount of gas entering the reactor is 4,000 SCFD/BPD. The resulting heat production curve is given as B in Figure 8. Just as in the A→B case, the effect is to reduce ΔT_{ad} and the steady state gains at intermediate conversions. The steep part of the curve is shifted toward higher temperatures. The chosen operating point corresponding to the more diluted case is marked by the numeral 1. The frequency response is given as curve B in Figure 13.

Because in both the single reaction and consecutive reaction examples of Figures 11 and 13 respectively, dilution decreases ΔT_{ad}, the effect is to significantly decrease $|G_R(j\omega)|_{max}$ which makes the control problem easier. However, the cutoff frequency is a little higher and the rate of dampening beyond the peak is lower. This makes control a bit harder. This occurs because the thermal time constant must decrease with dilution. The effect is similar to what occurs for two first order systems with different time constants. The one with the higher time constant will be more highly damped at a given ω.

An alternate approach the designer can take to limit the temperature rise in the reactor is to operate it at a lower temperature and accept a lower conversion. In the A→B example, depending on what reactor inlet temperature is chosen, this approach can greatly ease the control problem. As shown in Figure 3, a reactor operating below the inflection point of the heat production curve will have a low $G_R(0)$, will exhibit no peak and will dampen at a relatively low ω_C.

To determine the effect of inlet temperature and extent of reaction on the frequency response of the hydrocracker three points 1, 2, and 3 were chosen on curve B of Figure 8. The frequency response curves are given in Figure 13 as curves B, C, and D. The reactor peak and ω_c decrease with decreasing temperature. If the reactor is operated at a temperature higher than 760°F, corresponding to point 1 on the heat production curve, $G_R(0)$ and the peak will be extremely high. The reactor will be unduly sensitive to small changes in temperature because of rapid cracking to light products.

In both examples, the amount of heat feedback is lower when the reactor inlet temperature is decreased, but the heat exchanger may be larger anyway because of a lower ΔT for heat transfer. The potential control gains will also have to be weighed against the increased pumping and separation costs which will be incurred.

Another approach which is often used with hydrotreaters to maintain desired temperature levels and improve selectivity is to add cold H_2 quench streams tapped off from the gas recycle stream. The quench gas is added at several points along the length of the reactor which is usually in 4 or 5 sections. Each section after the first then behaves as a reactor with a diluted feed stream. The amount of quench gas necessary to reduce the maximum temperature rise in the reactor to a desired level is less than the amount of diluent required in the case discussed previously. This is due to the large temperature difference between the quench gas and the reacting fluid. Similar penalties are incurred by using quench as are incurred by diluting the feed. The reactor inlet temperature is higher and the outlet temperature is lower than in the base case. Consequently, a larger combined heat duty for

the heat exchanger and furnace will be required. Separation and compressor costs may also increase. The mathematical development leading to an expression for the reactor transfer function is given in the Appendix.

In this example the reactor consists of 5 sections. The aim is to achieve a given conversion and to limit the temperature rise in the reactor to a given value. This is accomplished by adjusting the length of each bed and the temperature drops between them, so that the temperature rises in the individual beds are as nearly uniform as possible. No attempt at optimization is made here. It is assumed that quench gas is available at 150°F. Quench reactors were designed to correspond to each of the three indicated points on the heat production curve B in Figure 8. The inlet and outlet temperatures for a typical case are given in Table 3. The heat production curves for the quench cases are given in Figure 8 as curves 1, 2, and 3. They were generated by maintaining the bed lengths and quench flows constant in each case and varying the inlet temperature. The effect of quench is to move the heat production curve to the right and to lower the steady state gain of the reactor compared to the nonquench case. Additionally, in each case, the new operating point is somewhat further away from the very steep part of the heat production curve. This is an advantage in preventing or minimizing temperature runaways in response to large inlet temperature disturbances. The frequency responses corresponding to points 1 and 2 on the heat production curves 1 and 2 are given as curves E and F, respectively in Figure 13. In these cases where the peak has already

been lowered by dilution, it is lowered still further by quench. Indeed, the usual industrial procedure is to utilize both dilution and quench to keep the temperature rise in the reactor at a low level.

The improvement, however, is limited to small perturbations. If the nonlinear frequency responses are generated as was described earlier for the first order reaction case, the curves of Figure 14 are generated. Curves A and B correspond to the nominal inlet temperatures indicated by numbers 2 on curves B and 2, respectively in Figure 8. The sine wave input has an amplitude of 20°F. From the heat production curve it is observed that in the nonquench case inlet temperatures will periodically occur which correspond to very large temperature rises in the reactor. In the quench case, the potential rises are smaller. Despite this difference, the nonlinear frequency responses are rather close together near the peak. It is at lower frequencies where the AR of the nonquench case is much larger than that of the quench case. The lower AR at low ω for the quench case is not beneficial for control. As noted earlier, the important region for control is at and beyond the reactor peak. Similar relationships occur between curves C and D which correspond to the nominal inlet temperatures indicated by numbers 1 in curves B and 1 in Figure 8. The sine wave input has an amplitude of 10°F. The results remain similar when the maximum nonlinear responses are used as shown in Curves E, F, G, and H. It is clear from the frequency responses that if large temperature perturbations occur, adding uncontrolled quench streams does little to aid in stabilizing the reactor.

Reducing the temperature rise in the reactor by either dilution or intermediate quench is not just required for stability and control. In many cases, it is required, from steady state design considerations to prevent undesirable side reactions, such as cracking to light products, or to slow catalyst deactivation. From a control standpoint dilution is more desirable because of its more marked effect on the reactor frequency response. However, the design engineer would probably prefer the quench technique, because the streams can be introduced at a considerably lower temperature than the diluent. This reduces the total mass flow and the required compressor, heat exchanger, and furnace loads.

In either case, however, with large perturbations, $|G_R(j\omega)|_{max}$ can still be extremely large. The improvement in the frequency response with dilution and quench comes primarily for smaller perturbations, which do not extend into the very steep region of the heat production curve where the effects of temperature on high cracking rates are manifested. Once the high cracking rates are allowed to occur, a runaway situation ensues and little improvement in the frequency response can be made by dilution or quench. This points to the need for some improved control methods to limit the temperature perturbations into the reactor. Fuel control of the furnace will not stabilize the system by itself. In such cases the need for heat exchanger bypass control is evident. An alternate approach is to control the reactor temperature by adjusting the quench flows. This scheme is discussed in the next section.

QUENCH CONTROL

One common method for improving the reactor performance is to adjust the flow of the quench gas by some feedback or feedforward control scheme based on temperature measurements. Let us first consider feedback control.

In the usual scheme, the temperature is measured at the outlet of a reactor section and changes are made in the quench rate to the inlet of that bed. The mathematical development for the pertinent transfer functions are given in the Appendix.

For comparison purposes, curve E, the frequency response with steady state quench for case 1, corresponding to curve A of Figure 11, is presented. The peak and ω_c are somewhat diminished compared to curve A but not to the same extent as for the dilution case of curve B. Curve F shows the effect of feedback control applied to one of the intermediate quench streams. By loop tuning, PI control settings were found for the loop. Adding control lowers the AR at low frequencies, but has little effect on the size of the peak. The delay through the reactor is long so that the resonant region of the feedback control loop occurs near the resonant peak of the uncontrolled reactor. Similar responses were found when the control point was changed.

A more promising control scheme involves measuring the temperature at the inlet to the reactor bed after the quench stream has been thoroughly mixed with the hot reaction product of the preceding bed. The quench flow is then adjusted according to fluctuations of this temperature. To implement this scheme a small mixing device must be placed between the beds. The pertinent transfer functions are given in the Appendix.

The effect on $|G_R(j\omega)|$ is shown for two cases. In Figure 15, this scheme is applied to the same case given in Figure 11 for comparison purposes. The effect on the frequency response of the reactor depends on the location of the controlled mixing tank. In no case is $G_R(0)$ reduced below unity. At first glance this seems strange since at low frequencies a PI controller should reduce the gain to low values. The reason for this is that the controller dampens the temperature disturbance to the next bed, but not the concentration disturbance which will continue to cause upsets through the rest of the reactor. As a result, the reactor can be viewed as being in two parts. The first part consists of those beds upstream from the controlled tank and the second part consists of those downstream from the tank. The controlled tank converts the temperature disturbance to the first section to a concentration disturbance into the succeeding section. This change eliminates the peak in the reactor response, but increases the steady state gain. The effect on the steady state gain depends on the location of the mixing tank which determines $G^{TT}(0)$ before the tank and $G^{TC}(0)$ after it. If additional controlled tanks are added between the other beds, the reactor frequency response is damped even more.

From the curves, it seems that the best place to add the controlled mixing tank is at an early point of the reaction. In fact, introducing it in front of the reactor would give the best control and the most reduction in the steady state gain. With reference to the Appendix, the steady state gain for an inlet temperature disturbance is $G^{TT}(0) = r_S(X_L)[1 + I(0,X_L)]$ while for an inlet concentration disturbance it is reduced to $G^{TC}(0) = r_S(X_L)\ I(0,X_L)$. Unfortunately, introducing quench

control at the inlet carries a penalty. The feed would have to be overheated which increases fuel costs and the size of the furnace. Additional overheat is required to expand the nonlinear operating range of the controller. If more overheat is added, then the quench flow can be reduced to a larger degree to compensate for drops in inlet temperature. Compensation for increases in inlet temperature is limited by the size of the compressors. An alternate approach is to place the controlled mixing tank after the first section which is reduced in size. However, if it is made too small, then as the catalyst ages, the temperature rise in this section will be low and again the nominal quench rate may be too low to allow for compensation of large negative disturbances in temperature. Simulation of various alternatives should suggest a reasonable design.

The example just discussed was for a steady state operating point with high conversion located close to the asymptotic upper bound on the heat production curve. To determine the effect of this control scheme on a reactor operating in the intermediate region a simple two stage reactor was designed. Each stage is 12 feet long and there is enough quench added to drop the temperature between stages by 20°F during uncontrolled operation. All other parameters for the reactor are the same as in the previous case. The results are shown in Figure 16. In this case the steady state gain, $G_R(0)$, is reduced below that of the uncontrolled case.

Use of a controlled mixing tank significantly dampens the reactor frequency response and its use in conjunction with furnace control and heat exchanger bypass control represents a powerful yet simple way of controlling the process. Dilution of the feed and use of quench streams are limited by economic considerations in their effect on the reactor frequency response. However, since these will usually be part of the basic reactor design, use of a controlled mixing tank should be a relatively inexpensive addition. The reactor must be constructed as two distinct sections with a mixing tank of the required size between them. In current practice a space is provided between reactor beds where mixing is supposed to take place. However, the residence time is usually so small that the mixing is incomplete and accurate temperatures are hard to measure.

In such cases, an alternative scheme is to measure the temperature disturbance before the quench section and use feedforward control. Fluctuations in the outlet temperature of the next bed are used to make slow set point adjustments in the feedforward loop. Most of the advanced control schemes for hydrocrackers are based on this approach in some form or another (Sayles, et.al. 1973; Stormont, 1969). Theoretically feedforward control provides perfect control. However, its effectiveness is limited by our lack of knowledge of the system. It is because of this lack of knowledge that the feedback loop for set point adjustment is required.

MODIFYING HEAT FEEDBACK LOOP

Steady State Considerations

As mentioned earlier, one approach to stabilize the reactor is to reduce the gain of the uncontrolled heat feedback loop, $G_F(0)G_H(0)$, to offset $|G_R(j\omega)|_{max}$. To reduce the heat feedback in this way a larger furnace must be utilized. Actually, if the heat exchanger could be eliminated from the loop altogether and the furnace designed to supply all the necessary preheat, then the system would be unconditionally stable. However, such approaches carry heavy penalties. Fuel costs would be very large and the problem of heat disposal from the reactor effluent is posed. This increases the interaction of the system with the rest of the plant creating potential stability problems elsewhere. In most cases the stability problem can be solved by proper feedback control. Two approaches for modifying the heat feedback loop by control will be discussed here:

1. Control of fuel supply to the furnace.
2. Bypass control of the heat exchanger.

These control loops are noninteractive and can be used together. It is noted that the models used in this work to generate the frequency response curves for the heat exchanger (Cohen and Johnson, 1956) and furnace (Roffel and Rijnsdorp, 1974) are described in detail in the Appendix. The transfer functions for the controlled units are also developed in the Appendix.

Control of Fuel Supply to the Furnace

Large industrial furnaces are quite sluggish, exhibiting considerable time lag in their response because of their capacity to store heat in the walls and tubes. As explained earlier, it is desirable to have a furnace frequency response which dampens the peak of the reactor frequency response and whose own peak is relatively low and occurs at a high enough frequency to be dampened by the reactor. Unfortunately this may be difficult to achieve in a furnace, particularly if $|G_R(j\omega)|_{max}$ is large. As an example, curve D in Figure 4 is presented, the response of a typical large industrial furnace of the size needed for a hydrocracker. The design parameters are given in Table 4 for the furnace and heat exchanger.

In the example given, furnace fuel control stabilizes all of the steady states of the heat production curve of Figure 2. However, the gain margin of the worst case is only 1.1. This does not provide enough margin for the inaccuracies of the models used. The controlled furnace will probably be inadequate for stabilizing a reactor with a frequency response similar to those given in Figure 14.

It is important that the steady state design of the furnace be integrated with the control system design. Sufficient control latitude must be designed into the system to deal with large temperature changes. On the one hand, the steady state heat duty must be sufficiently large to control these; on the other hand it must not be so large that fuel costs are too high. The control action is limited by the amount of fuel that can be supplied and by the steady state heat duty. In the example given, the steady state heat duty is 8.1 MMBTU/hr with a 33°F temperature

rise through the furnace. If half of the maximum fuel rate is nominally supplied, then step changes in temperature approximately as large as $\pm 33^{\circ}F$ can theoretically be damped even if the control valve is saturated. However, while the valve is saturated in either direction, the controller is ineffective. It can only call for changes in fuel flow which are within the linear range of the control valve. Even if disturbances are never this large, the speed with which large perturbations are damped out will be limited by these same saturation effects.

The effectiveness of furnace control in stabilizing a given reactor must be examined on a case by case basis. The designer might want to augment the furnace control with a modification of the reactor design, use of a controlled mixing tank between reactor stages, or by introducing bypass control of the heat exchanger.

Bypass Control of Heat Exchanger

In this control scheme the amount of bypass is varied by measuring the temperature of the mixed stream leaving a mixing section where the bypass stream and exchanger effluent are combined. The goal is to attenuate the temperature perturbations before they reach the furnace so that the control problem for the furnace is easier. The only limitation on a fast response is the speed of the thermocouple and valve dynamics.

As shown by curve E in Figure 4, the effect of bypass control of the heat exchanger is to dampen the heat exchanger response over the range of frequencies of the reactor peak. This, together with the attenuated response of the standard controlled furnace (curve D), should significantly enhance the stability of the process. As shown in

curve B of Figure 5, the peak of the open loop response of the complete system is sharply lowered. Again, the control loop introduces a peak in the heat exchanger response which must occur over a range of frequencies where the reactor is damped if stability is to be insured.

The amount of fresh feed bypassing the heat exchanger does not have a strong effect on the linear frequency response. However, it significantly affects the nonlinear range of control. The nominal bypass fraction must be sufficiently large so that large changes in inlet temperature can be dampened and the heat exchanger must be designed so that it can handle wide swings in throughput. This reduces ΔT at the outlet and requires design of units larger than those required for the unbypassed case. In the example given, the temperature rise of the fresh feed through the heat exchanger is 178°F. A positive step change as large as 178°F can be dealt with by bypassing all the feed around the exchanger. The maximum size of the negative step that can be handled can be much larger due to the larger ΔT driving forces at both ends of the exchanger. The size of the negative step change that can be dealt with increases with the bypass fraction. However, it is noted that the size of the bypass fraction is limited by the reactor effluent temperature. The bypass fraction must be small enough to provide a reasonable ΔT driving force at this end of the exchanger. Consequently, control is more limited when large drops in reactor outlet temperature occur due to concentration changes.

The effect of bypass control on the furnace frequency response was also examined. It was found that there is no substantial improvement in the stability of the process. The reason heat exchanger bypass control

works well and furnace bypass does not is that the driving force for heat transfer can be significantly altered by bypass in the heat exchanger, but not in the furnace. In the former case the mode of heat transfer is by convection, while in the latter it is by radiation.

Effect of Uncontrolled Mixing Tank in Series

The main problem of control is offsetting the gain of the resonant peak of the reactor frequency response. One way of doing this is by introducing a filter that acts in the region of the peak. A stirred storage tank of sufficient size for the heated feed to the reactor could achieve this. In Figure 17 we present the open loop frequency responses for several such cases utilizing different sized mixing tanks for the reactor of case 1 and a heat feedback loop utilizing furnace fuel control.

For liquid feeds a conventional mixing tank can be used. Holdup times of 5 to 10 minutes are probably feasible. Mixing energy must be provided in the form of a conventional agitator or by a high capacity recirculation pump. In spite of this energy cost, if the reactor frequency response has a high gain and there are advantages in operating at this particular steady state, this may be a reasonable approach for improving control.

For gaseous feeds, this approach is less feasible with a conventional mixing tank because its size would have to be very large to provide a reasonable holdup time. However, the ideas outlined earlier regarding dispersion in a fixed bed catalytic reactor can be applied to design a column with inert packing which would serve the same purpose as

a stirred vessel. The first three terms of eq. 9 decrease with the length of the bed. However, the fourth term, describing the extent of intraparticle thermal diffusion, is independent of bed length. It can be written in terms of dimensional bed parameters as:

$$\frac{\Theta_{th} T_{th}^2}{3T_c(1+B)^2} = \frac{d_p^2 \rho_p c_p T_{th}}{108 k_p (1+B)}$$

To make this large, so that temperature disturbances are damped, the bed must be designed so that the fluid residence time is high and the particles are large. A packing material should be chosen which has a low thermal conductivity. It should also have a relatively high specific heat so that B is small and τ_{th} is high. Actually with such a design, the other terms of eq. 9 should also contribute significantly to the size of the variance, σ_g^2. If the particle size is suitably chosen, $\frac{1}{Pe_{th}} \propto \frac{d_p}{L}$ should also be relatively large. As shown previously, the heat transfer term normally has the largest effect on the variance with conventionally sized particles. Since it is directly proportional to d_p^{1+a} (where $0 < a < 1$), the contribution should be substantial with larger particles.

This approach has the advantages of a lower energy cost and of requiring a smaller vessel size than would the conventional stirred tank approach. It is not as directly applicable to liquid feeds because $\frac{\tau_{th}}{\tau_f}$ is much smaller than for a gaseous or mixed phase feed. However, the size and agitation costs for a conventional mixing tank might be reduced if a packed bed thermal dispersion unit were used in series.

SUMMARY

This work shows how a complex positive feedback system can be analyzed by dealing with its component units spearately. Frequency response curves can be estimated for each unit either from mathematical models or by generating empirical transfer functions from curve fits of pilot plant step responses. It was shown how the frequency response of the scaled-up plant reactor can be estimated from the pilot plant response. By dealing with each unit separately, the design engineer can easily determine how the frequency response has to be modified to obtain a desired stability margin.

A conservative stability criterion was first set down for the system; for stability to be insured the amplitude ratio of the open loop frequency response for the entire system must be <1 at all frequencies. It was shown for the positive feedback system consisting of a fixed bed reactor, heat exchanger and furnace that the open loop frequency response contains a peak. Thus, the conservative stability criterion is replaced by the condition that $\max|G^*(j\omega)|<1$. Because of the differences in the fluid velocity and the velocity at which temperature disturbances are propagated through the reactor, its frequency response may contain a peak. The frequency at which the peak occurs can be estimated by knowing the thermal time constant $\tau_{th} = \tau_f(1+B)$. The frequencies corresponding to these peaks will in many cases be close to the frequency at which $\max|G^*(j\omega)|$ occurs, because the reactor will dampen peaks that may occur if controls are applied to the other two units. In other cases, the control problem is complicated by the sluggish response of the furnace.

Two approaches are taken to stabilize the system. The first involves modifying the reactor response so that its peak is lower and occurs at low frequencies where it is damped by a controlled unit. The second involves modifying the frequency responses of the furnace and heat exchanger by suitably chosen control schemes so that the gain of their frequency responses are low when the reactor gain is high and vice versa. By dealing with each unit separately the design engineer can easily determine how the frequency responses have to be modified to obtain a desired stability margin.

The steady state design, if considered with control in mind, can tremendously ease many potential stability problems. This bears directly on the two approaches for stabilizing the system. The effect on the respective frequency responses of several modifications in the system design were discussed. Some of these are:

1. Limiting the temperature rise in the reactor by
   (a) reducing conversion,
   (b) diluting the feedstream with an inert diluent or with large excesses of a reactant,
   (c) diluting the reaction mixture with intermediate quench streams.
2. Use of quench control applied to the reactor.
3. Bypass control of the heat exchanger and furnace.
4. Introducing a mixing tank of sufficient size at the reactor inlet to dampen temperature disturbances.

All of these approaches carry some processing and economic penalties which are briefly outlined. The choice of how to proceed involves compromises between steady state performance, control, and economic considerations.

One promising approach is to apply bypass control to the heat exchanger. It was found that this control scheme was able to stabilize even the most difficult case presented by a model for a hydrocracker involving complex kinetics. This approach necessitates some additional capital expense by requiring an oversized heat exchanger to allow it to compensate for large temperature disturbances.

The operating region of any controller is physically limited. In the bypass case, the bypass fraction can only lie between 0 and 1. The controller can not call for flows outside of this region. As a result, the linear behavior of the controller is limiting. In some equipment, this limitation on the control action may make stabilization impossible for large disturbances. However, by choosing a suitably large nominal bypass fraction the control action of the heat exchanger can be made sufficiently wide to handle any reasonable disturbance. Bypass control of the furnace was similarly investigated. However, it offered no substantial improvement over the standard controlled furnace.

The nonlinear behavior of the reactor was examined and two approaches for stability were discussed. In the first, the frequency response is determined for the largest anticipated temperature disturbance about the design inlet temperature. A control scheme is then designed to insure that within the limits of these disturbances the system is stable. It was demonstrated for the single first order reaction case that, depending on the position on the heat production curve of the reactor, the linear case may be more difficult to stabilize than the nonlinear. In the second approach, the linear and nonlinear frequency responses are generated for all the operating points on the heat production curve.

The control system is then designed to stabilize the single most difficult case. This approach establishes global stability for the system.

Using a complex kinetic model for hydrocracking, it was determined that this reactor is rather difficult to stabilize. This is due to the potentially large temperature rises in the reactor which can occur if significant cracking to light products occurs. This causes the heat production curve to be extremely steep at temperatures where this cracking occurs. As a result, if nonlinear perturbations in inlet temperature extend into this region, the frequency response will have very large gains and accompanying large peaks. The only scheme which stabilized these cases was bypass control of the heat exchanger in conjunction with the standard controlled furnace. Introducing quench streams reduced the reactor gain but seemed to do little to lower the reactor peak. Diluting the feed with a larger H_2 recycle stream alleviates the problem, but this approach carries economic penalties due to high energy costs for compression.

In addition to heat exchanger bypass control, a modified quench control scheme was suggested which eliminates the reactor peak. In this approach, the reactor is divided into two parts with a small mixing tank between them to which the quench stream is added. The flow of this stream is adjusted according to fluctuations in the tank outlet temperature. It was found that the standard quench control scheme of measuring the temperature at the outlet of the reactor bed immediately downstream of the mixing section was unsatisfactory due to the large thermal delay of the bed. The modified scheme significantly dampens the reactor freqency response and its use in conjunction with furnace fuel control

and heat exchanger bypass control represents a powerful yet simple way of controlling the process.

Introduction of a holding tank at the reactor inlet to dampen temperature disturbances represents a way of increasing stability without use of control loops. However, the overall response time of the system for desired set point changes will increase. Here again, as with all of the approaches discussed, the designer must make compromises between steady state performance, control, and economic considerations.

Concept of Nonlinear Analysis

The "poor man's" nonlinear analysis is not intended to rigorously establish stability criteria or to establish if stability exists. Its purpose is to help the designer obtain an idea of how the reactor will behave in response to large perturbations. This behavior is established in two ways in this thesis. The first approach is to vary the reactor inlet temperature with sine waves of varying frequency and large amplitude. From a reactor model, the designer can determine the steady state output response. This response is a nonsymmetric periodic function which has no secondary peaks and has the same frequency as the input function. A nonlinear frequency response for the reactor is plotted based on the maximum amplitude of this response.

Alternatively, a large step change in inlet temperature is introduced, and from a reactor model the output response is determined. The response can also be determined in pilot plant tests. Using the sum of linear functions as shown in the thesis, this output can be curve fitted by linear regression. From this function the linearized-nonlinear

transfer function for the reactor can be determined and the nonlinear frequency response can be established.

From the magnitude of the steady state gain, resonance peak, and dampening characteristics of this pseudo-nonlinear frequency response, the designer can determine what type of control schemes might be useful to stabilize the system. If these parameters are small, then standard furnace fuel control might be all that is necessary to control the process. If they are large, then the designer must think in terms of modifying either the steady state reactor design or adding controls to the reactor in the form of quench control of an intermediate mixing section or by further modifying the heat feedback loop of the process by introducing heat exchanger bypass control.

Once a possible control scheme is chosen, the designer can then dynamically simulate the behavior of the process using mathematical models. He can now determine the response of the system to various types of upsets and determine if the controls are adequate. If they are not, he might have to think in terms of further modifying the basic steady state design to obtain a process which is controllable over a region in which he feels his system will operate. If he must operate within a small practical region of stability, then using the computer simulations, he can determine under what conditions he can safely shutdown the process without experiencing intolerable temperature excursions.

This approach is applicable to other similar distributed parameter processes where the control problem arises not because the individual units can be unstable, but because the process as a whole can have

stability problems due to external feedback of heat or mass. However, it must be noted that to implement this approach successfully, the designer must have a good understanding of the physical and chemical processes occurring in the system so that, for control purposes, mathematical models can be established which simulate the real process in a reasonably faithful way.

For example, the primary unit in the process analyzed in this work, is a fixed bed catalytic reactor. In recent years it has become known that its main dynamic features are due to the interaction of concentration and temperature waves which pass through the reactor at different speeds. Simple models can be written to adequately simulate these interactions provided a decent kinetic model is available.

This work represents, to the author's knowledge, the first published attempt at analyzing and offering solutions to the stability problems of complex distributed parameter reaction systems of this kind, where feedback control loops are used to stabilize the process. Heretofore, only the open loop stability characteristics of reactors were analyzed. No attention was paid to other units which may be part of a typical industrial process. No attempt was made to stabilize the reactor with any type of feedback or feedforward control.

APPENDIX

Derivation of Reactor Transfer Functions

The fluid mass and heat balances are respectively:

$$\text{(A1)} \qquad \frac{\partial C_f}{\partial t} + \frac{\partial C_f}{\partial x} = -r(C_f, T_f) = -e^{\frac{AT_f}{T_o+T_f}} C_f$$

$$\text{(A2)} \qquad \frac{\partial T_f}{\partial t} + \frac{\partial T_f}{\partial x} = r(C_f, T_f) + H_p (T_p - T_f)$$

where the parameters are defined in Table 1. The particle heat balance is:

$$\text{(A3)} \qquad \frac{dT_p}{dt} = H_p B (T_f - T_p)$$

These equations are linearized and the Laplace transforms are taken to give:

$$\text{(A4)} \qquad \frac{\partial \delta C_f}{\partial x} + (s + r_{C_f}) \delta C_f = -r_{T_f} \delta T_f$$

$$\text{(A5)} \qquad \frac{\partial \delta T_f}{\delta x} + (s + H_p - r_{T_f}) \delta T_f = H_p \delta T_p + r_{C_f} \delta C_f$$

$$\text{(A6)} \qquad \delta T_p = \frac{H_p B \delta T_f}{S + H_p B}$$

where δ indicates deviation from a steady state value, s is the Laplace transform variable, and r_{C_f} and r_{T_f} are partial derivatives with respect to concentration and temperature respectively. These equations can be combined to eliminate δT_p and δC_f to give a second order homogeneous differential equation for δT_f.

$$\text{(A7)} \qquad \frac{\partial^2 \delta T_f}{\partial x^2} + a_1(x)\frac{\partial \delta T_f}{\partial x} + a_2(x)\delta T_f = 0$$

where:

$$a_1(x) = 2S + r_{C_f} - r_{T_f} - \frac{1}{r_{C_f}}\frac{dr_{C_f}}{dx} + \frac{H_p S}{S + H_p B}$$

$$a_2(x) = Sr_{C_r} - \frac{dr_{T_f}}{dx} + S^2 - Sr_{T_f} - \frac{dr_{C_f}}{dx}\left(\frac{S}{r_{C_f}} + \frac{H_p}{r_{C_f}} - \frac{r_{T_f}}{r_{C_f}} - \frac{H_p^2 B}{r_{C_f}(S+H_p B)}\right) + r_{C_f} H_p + \frac{H_p(S^2 - r_{C_f} H_p B)}{S+H_p B}$$

To solve eq. (A7), it is necessary to know a solution a priori. Such a solution is $\delta T_f = r_s e^{-sx}$ where subscript s refers to the steady state. Solving the set of eqs. (A4-A6) gives four transfer functions relating the temperature and concentration at any point in the reactor to perturbations in either variable at the reactor inlet. The transfer functions are:

$$\text{(A8)} \qquad G^{cc}(s,x) = \exp\left[-sx - \frac{H_p sx}{s+H_p B}\right] - \left[1 - \frac{H_p s\, C_s(x)}{r_s(s+H_p B)}\right] e^{-sx}\, r_s(x)\bar{I}(s,x)$$

$$\text{(A9)} \qquad G^{cT}(s,x) = \left[1 - \frac{H_p S}{S + H_p B}\right] \exp\left[-sx - \frac{H_p S x}{S + H_p B}\right] - \left[1 - \frac{H_p S\, C_s(x)}{r_s(x)(S + H_p B)}\right] e^{-sx} r_s(x) - \left[1 - \frac{H_p S}{S + H_p B}\right]\left[1 - \frac{H_p S\, C_s(x)}{r_s(x)(S + H_p B)}\right] e^{-sx} r_s(x)\bar{I}(s,x)$$

$$\text{(A10)} \qquad G^{TC}(s,x) = e^{-sx} r_s(x)\, \bar{I}(s,x)$$

(A11) $$G^{TT}(s,x) = e^{-sx} r_s(x) \left[1 + \left(1 - \frac{H_p S}{S + H_p B}\right)\right] \bar{I}(s,x)$$

where $\bar{I}(s,x) = \int_0^x \frac{-H_p S\, y}{e^{S + H_p B}} \frac{d\,y}{C_s(y)}$

Crider and Foss provide an approximate relation for $\frac{1}{C_s(x)}$, which allows $\bar{I}(s,x)$ to be evaluated analytically. They approximate the reaction rate by:

$$\frac{AT}{e^{T_o+T}} \approx e^{kT}$$

where K is a coupling parameter defined as

$$K = \frac{A - 0.5972}{T_o + 0.2701}$$

The approximation for $\frac{1}{C_s(x)}$ is

$$\frac{1}{C_s(x)} \approx \frac{e^{Kx} - 1}{C_{sa}} + 1 + b\,(e^{qx} - 1)$$

The parameters b and q depend on K and can be determined from graphs provided by Crider and Foss (1968). The parameter C_{sa} is defined as:

$$C_{sa} = \exp\,(E_1(K) - \gamma - \ln K)$$

where γ is Euler's constant.

Derivation of Heat Exchanger Transfer Function

The appropriate heat balances are:

(A12) tube side fluid: $\rho_f A_i C_f \frac{\partial T_o}{\partial t} + \rho_f A_i C_f u_H \frac{\partial T_o}{\partial x} = \pi D_i h_i (T_w - T_o)$

(A13) tube balance: $\rho_w A_w C_w \frac{\partial T_w}{\partial t} = \pi D_o h_o (T_R - T_w) - \pi D_i h_i (T_w - T_o)$

(A14) shell side fluid: $\rho_R V_R C_R \frac{\partial T_R}{\partial t} = \phi_R C_R (T_L - T_R) - \pi D_o h_o L (T_R - T_w)$

where T_L is the reactor effluent temperature and ϕ_R is the mass flow rate in the shell side of the exchanger. If we assume that there is no bypass control around the heat exchanger, then these equations are linear and u_H and h_i are constant. However, with bypass, the flow rate in the tubes varies; the equations are now nonlinear and a linearized solution is necessary. The development for this more general case is presented here.

If we assume that the tube side heat transfer coefficient is proportional to the 8/10 power of the mass flow rate, ϕ_H, we obtain the following linearized and Laplace transformed equations:

(A15) $\tau_1 u_s \frac{\partial \delta T_o(s,x)}{\partial x} + \delta T_o(s,x)[1+\tau_1 s] = \delta T_w + \delta u \left[0.8 \frac{(T_{w_s} - T_{o_s}(x))}{u_s} - \tau_1 \frac{dT_{o_s}}{dx}\right]$

(A16) $(\tau_2 s + 1)\, \delta T_w(s) = a_1 \delta T_R(s) + a_2 \delta T_o(s,x) - a_3 \frac{\delta u(s)}{u_s}$

(A17) $(\tau_3 s + 1)\, \delta T_R(s) = b_1 \delta T_L(s) + b_2 \delta T_w(s)$

where the constants are defined in Table A1.

If the δT_W and δT_R are eliminated, a single differential equation for $\delta T_0(s,x)$ results

$$\text{(A18)} \qquad \frac{\partial \delta T_o(s,x)}{\partial x} + \frac{\delta T_o(s,x)}{u_s \tau_1} a_H(s) = \frac{b_H(s)}{u_s \tau_1} \delta T_L(s) - \left[\frac{c_H(s)}{u_s \tau_1} + \frac{dT_{o_s}}{dx}\right] \frac{\delta \phi_H(s)}{\phi_{H_s}}$$

This is easily solved to give:

$$\text{(A19)} \quad \delta T_o(s,x) = \frac{b_H(s)}{a_H(s)} \left(1 - e^{-\frac{a_H(s)}{\tau_1}\frac{x}{u_s}}\right) \delta T_L(s) + e^{-\frac{a_H(s)}{\tau_1}\frac{x}{u_s}} \delta T_o(s,0)$$

$$- \left[\frac{c_H(s)}{a_H(s)} \left(1 - e^{-\frac{a_H(s)}{\tau_1}\frac{x}{u_s}}\right) + e^{-\frac{a_H(s)}{\tau_1}\frac{x}{u_s}} \int_o^x e^{\frac{a_H(s)\,y}{\tau_1 u_s}} dT_{o_s}(y)\right] \frac{\delta \phi_H(s)}{\phi_{H_s}}$$

The integral term in eq. (A19) can be evaluated analytically. The steady state temperature profile is:

$$T_{o_s}(x) = \frac{b_H(o)}{a_H(o)} \left(1 - e^{-\frac{a_H(o)}{\tau_1}\frac{x}{u_s}}\right) T_{L_s} + T_{o_s}(o)\, e^{-\frac{a_H(o)}{\tau_1}\frac{x}{u_s}}$$

and the integral is

$$\text{(A20)} \quad e^{\frac{-a_H(s)}{\tau_1}\frac{x}{u_s}} \int_o^x e^{\frac{a_H(s)y}{\tau_1 u_s}} dT_{o_s}(y) = \frac{a_H(o)(T_{L_s} - T_{o_s}(o))}{a_H(s) - a_H(o)} \left[e^{\frac{-a_H(o)x}{u_s \tau_1}} - e^{\frac{-a_H(s)x}{u_s \tau_1}}\right]$$

If there is no variation in mass flow through the tubes, then the heat exchanger transfer function reduces to the first two terms of eq. (A19):

$$\text{(A21)} \qquad \delta T_o(s,x) = \frac{b_H(s)}{a_H(s)} \left(1 - e^{-\frac{a_H(s)}{\tau_1}\frac{x}{u_s}}\right) \delta T_L(s) + e^{-\frac{a_H(s)}{\tau_1}\frac{x}{u_s}} \delta T_o(s,o)$$

Derivation of Furnace Transfer Function

This derivation is similar to that for the heat exchanger. The appropriate heat balances are:

(A22) tube side fluid: $$M_o c_f \frac{\partial T_o}{\partial t} + u_s M_o c_f \frac{\partial T_o}{\partial x} = \alpha_o A_t (T_t - T_o)$$

(A23) tube balance: $$M_t c_{pt} \frac{dT_t}{dt} = Q_{\substack{to \\ tube}} - \alpha_o A_t (T_t - T_o)$$

(A24) hot gases: $$M_g c_{pg} \frac{dT_g}{dt} = \phi_g (-\Delta H) - Q_{gw} - Q_{gt} - Q_{out}$$

(A25) wall balance: $$M_w c_{pw} \frac{dT_w}{dt} = Q_{gw} - Q_{wt} - Q_{loss}$$

where the heat transferred via radiation and convection from the gas to the walls and tubes, respectively are:

(A26) $$Q_{gw} = A_w \epsilon_w f_1 \sigma \left[\left(\frac{T_g}{100}\right)^{3.4} - \left(\frac{T_w}{100}\right)^{3.4} \right] + A_w \epsilon_w f_2 \sigma (T_g^4 - T_w^4) + A_w \alpha_c (T_g - T_w)$$

(A27) $$Q_{gt} = A_t \epsilon_t f_1 \sigma \left[\left(\frac{T_g}{100}\right)^{3.4} - \left(\frac{T_t}{100}\right)^{3.4} \right] + A_t \epsilon_t f_2 \sigma (T_g^4 - T_t^4) + A_t \alpha_c (T_g - T_t)$$

The heat transferred from the walls to the tubes via radiation is:

(A28) $$Q_{wt} = A_t \epsilon_{wt} \sigma (T_w^4 - T_t^4) - A_t \epsilon_w f_1 \sigma \left[\left(\frac{T_w}{100}\right)^{3.4} - \left(\frac{T_t}{100}\right)^{3.4} \right] - A_t \epsilon_w f_2 \sigma (T_w^4 - T_t^4)$$

The heat loss through the furnace stack is:

(A29) $$Q_{out} = \phi_g c_{pg} (T_g - T_{ref})$$

The heat loss through the furnace walls is estimated by:

$$Q_{loss} = 0.56 (W_L)^{0.75} W (T_w - T_{amb})^{1.25} \quad \text{(A30)}$$

where W_L is the length of the wall and W is the width. The heat supplied to the tubes, $Q_{to\ tube} = Q_{gt} + Q_{wt}$.

If these equations are linearized and the Laplace transform taken, a single differential equation for T_o is obtained:

$$\frac{\partial T_o(s,x)}{\partial x} + \frac{a_F(s)}{u_s} \delta T_o(s,x) = \frac{b_F(s)}{u_s} \delta \phi_g(s) - \frac{c_F(s)}{u_s} \delta \phi_f(s) - \frac{dT_{o_s}}{dx} \frac{\delta \phi_f(s)}{\phi_{f_s}} \quad \text{(A31)}$$

where ϕ_f is the fluid flow through the tubes. This is easily solved to give:

$$\delta T_o(s,x) = \delta T_o(s,0) e^{-\frac{a_F(s)x}{u_s}} + \frac{b_F(s)}{a_F(s)} \left(1 - e^{-\frac{a_F(s)x}{u_s}}\right) \delta \phi_g(s) \quad \text{(A32)}$$

$$- \frac{c_F(s)}{a_F(s)} \left(1 - e^{-\frac{a_F(s)x}{u_s}}\right) \delta \phi_f(s) - e^{-\frac{a_F(s)x}{u_s}} \int_o^x e^{\frac{a_F(s)y}{u_s}} dT_{o_s}(y) \frac{\delta \phi_f(s)}{\phi_{f_s}}$$

Since the steady state fluid temperature profile is the result of solving four nonlinear equations, the integral must either be estimated by approximating $T_{o_s}(x)$ by an empirical expression so an analytical solution is possible or by a numerical integration. Definitions of all terms are presented in Table A2. Equation (A32) can be rewritten as:

$$\delta T_o(s,x) = \delta T_o(s,0) e^{-\frac{a_F(s)x}{u_s}} + G_F^{T_o \phi_g}(s) \delta \phi_g(s) - G_F^{T_o \phi_F}(s) \delta \phi_F(s) \quad \text{(A33)}$$

If there is no change in mass flow through the tubes and feedback control is applied by measuring the outlet temperature $T_o(L)$ and adjusting the fuel flow, ϕ_g, the closed loop transfer function is:

$$\text{(A34)} \qquad \frac{\delta T_o(s,L)}{\delta T_o(s,0)} = \frac{e^{-\tau_F a_F(s)}}{1 + \frac{K_c G_F^{T_o} \phi_g(s)\, e^{-\tau_d s}}{(1+\tau_m s)(1+\tau_v s)}}$$

As $S \to \infty$, $\frac{\delta T_o(\infty,L)}{\delta T_o(\infty,0)}$ approaches a finite value greater than zero. This is a failing of the model used, which does not account for thermal diffusion in the furnace tubes. To compensate for this a first order response is added in series to provide reasonable attenuation at high frequencies.

Quench Control of Reactor

A. Standard Scheme

In this approach the reactor is divided into several beds. The temperature of the reaction mixture leaving a stage is measured and the flow of quench gas is adjusted to the mixing chamber immediately preceding it. Control loops can be designed for any one or all of the mixing sections. In the development that follows it is assumed that controls exist for all of the mixing sections. To determine the effect of controls on fewer sections, it is only required to set the proportional control constants on the uncontrolled sections equal to zero. If they are all set equal to zero, the transfer function for the uncontrolled quench case results.

The transfer functions relating the outlet of bed 1 to the inputs are:

(A35) $$\delta T_1 = (G^{TT})_1 \delta T_o + (G^{TC})_1 \delta C_o$$

(A36) $$\delta C_1 = (G^{CT})_1 \delta T_o + (G^{CC})_1 \delta C_o$$

The balance around the first mixing section is:

$$W_{f_1} c_f (T_1 - T_{20}) + W_C c_C (T_C - T_{20}) = M\bar{c} \frac{d T_{20}}{dt}$$

where W_{f_1} is the fluid flow through bed 1, and W_C is the coolant flow rate. If this is linearized and the Laplace transform taken we obtain:

(A37) $$\delta T_{20} = \frac{\delta T_1}{1+\tau s} - \frac{K_{g_2} \delta W_c}{1+\tau s}$$

where $\tau = M\bar{c}/(W_f c_f + W_C c_C)$. It is assumed that for convenience that $\frac{W_C c_C}{W_f c_f} << 1$. The relationship for the concentration into and out of the mixing tank is simply

(A38) $$\delta C_{20} = \frac{\delta C_1}{1+\tau' s} \quad ; \quad \tau' = \frac{V}{q}$$

The relationships for the second bed are:

(A39) $$\delta T_2 = (G^{TT})_2 \delta T_{20} + (G^{TC})_2 \delta C_{20}$$

(A40) $$\delta C_2 = (G^{CC})_2 \delta C_{20} + (G^{CT})_2 \delta T_{20}$$

Substituting eqs. (A37) and (A38) and using the following control law

(A41) $$\delta W_c(s) = \frac{K_v K_c (1 + \frac{1}{\tau_I s})}{(1 + \tau_v s)(1 + \tau_m s)} \delta T_2(s)$$

we obtain:

(A42) $$\delta T_2(s) = \frac{\frac{(G^{TT})_2}{1+\tau s} \delta T_1(s) + \frac{(G^{TC})_2}{1+\tau' s} \delta C_1(s)}{1 + \frac{(G^{TT})_2 K_{g2} K_v K_c (1 + \frac{1}{\tau_I s})}{(1+\tau_v s)(1+\tau_m s)(1+\tau s)}}$$

(A43) $$\delta C_2(s) = \frac{(G^{CT})_2}{1+\tau s} \delta T_1(s) + \frac{(G^{CC})_2}{1+\tau' s} \delta C_1(s) - \frac{(G^{CT})_2 K_{g2} K_v K_c (1 + \frac{1}{\tau_I s}) \delta T_2(s)}{(1+\tau_v s)(1+\tau_m s)(1+\tau s)}$$

In general, for the i^{th} reactor bed, where $i > 1$:

(A44) $$\delta T_i(s) = \frac{\frac{(G^{TT})_i}{1+\tau s} \delta T_{i-1}(s) + \frac{(G^{TC})_i}{1+\tau' s} \delta C_{i-1}(s)}{1 + \frac{(G^{TT})_i K_{gi} K_v K_c (1 + \frac{1}{\tau_I s})}{(1+\tau_v s)(1+\tau_m s)(1+\tau s)}}$$

(A45) $$\delta C_i(s) = \frac{(G^{CT})_i}{1+\tau s} \delta T_{i-1}(s) + \frac{(G^{CC})_i}{1+\tau' s} \delta C_{i-1}(s) - \frac{(G^{CT})_i K_{gi} K_v K_c (1 + \frac{1}{\tau_I s}) \delta T_i(s)}{(1+\tau_v s)(1+\tau_m s)(1+\tau s)}$$

By using these recursive equations, the input-output relationship for the entire controlled reactor can be determined.

B. Temperature Control of Intermediate Mixing Section

The development for the transfer functions is similar to the previous one. The recursive formulae are:

$$\text{(A46)} \qquad \delta T_i(s) = \frac{\frac{(G^{TT})_i}{1+TS}\,\delta T_{i-1}(s)}{1 + \frac{K_v K_{gi} K_c \left(1+\frac{1}{T_I S}\right) e^{-T_d S}}{(1+\tau_v S)(1+\tau_m S)(1+TS)}} + \frac{(G^{TC})_i\,\delta C_{i-1}(s)}{1+TS}$$

$$\text{(A47)} \qquad \delta C_i(s) = \frac{\frac{(G^{CT})_i}{1+TS}\,\delta T_{i-1}(s)}{1 + \frac{K_v K_{gi} K_c \left(1+\frac{1}{T_I S}\right) e^{-T_d S}}{(1+\tau_v S)(1+\tau_m S)(1+TS)}} + \frac{(G^{CC})_i\,\delta C_{i-1}(s)}{1+TS}$$

Bypass Control of Fired Heater

A heat balance around the mixing tank gives:

$$\text{(A48)} \qquad \rho c_p V \frac{dT_o}{dt} = \phi_f c_p (T_{L_F} - T_o) + W_B c_p (T_o' - T_o)$$

If this equation is linearized, rewritten utilizing the bypass relations $W_B = fW_s$ and $\phi_f = (1-f)W_s$, and the Laplace transform taken, the following is obtained;

$$\text{(A49)} \qquad \delta T_o(s) = \frac{(1-f_s)\,\delta T_{L_F}(s) + f_s\,\delta T_o'(s)}{1+\tau_t S} - \frac{(T_{L_{Fs}} - T_{o_s}')\,\delta f(s)}{1+\tau_t S}$$

where T_{L_F} is the furnace outlet temperature, f is the bypass fraction, τ_t is the mean residence time in the tank, and subscript s denotes the steady state value.

Equation (A32) can be rewritten if we recognize that $\delta\phi_f(S) = -W_S\,\delta f(S)$, and utilizing eq. (A48) we obtain

$$\delta T_o(S) = \left[\frac{(1-f_s)\,e^{-\tau_F a_F(s)}}{1+G_F^{\tau\phi_g}(s)\,K_c\left(1+\frac{1}{\tau_I S}+\tau_D S\right)} + f_s\right]\frac{\delta T_o'(S)}{1+\tau_t S}$$

(A50)

$$+\left[\frac{W_s(1-f_s)\,G_F^{\tau\phi_g}(s)}{1+G_F^{\tau\phi_g}(s)\,K_c\left(1+\frac{1}{\tau_I S}+\tau_D S\right)} - \left(T_{L_{F_s}} - T_{o_s}'\right)\right]\frac{\delta f(S)}{1+\tau_t S}$$

The control law for the bypass loop including a finite time delay and valve and thermocouple dynamics is:

$$\delta f(S) = \frac{e^{-\tau_{B_F} S}\,K_{B_F}\left(1+\frac{1}{\tau_{I_B} S}\right)}{(1+\tau_m S)(1+\tau_v S)}\,\delta T_o(S) \tag{A51}$$

Substituting (A51) into (A50) gives:

$$\delta T_o(S) = \frac{\left[\frac{(1-f_s)\,e^{-\tau_F a_F(s)}}{1+G_F^{\tau\phi_g}(s)\,K_c\left(1+\frac{1}{\tau_I S}+\tau_D S\right)} + f_s\right]\frac{\delta T_o'(S)}{1+\tau_t S}}{1+\left[\left(T_{L_{F_s}} - T_{o_s}'\right) - \frac{W_s(1-f_s)\,G_F^{\tau\phi_s}(s)}{1+G_F^{\tau\phi_g}(s)\,K_c\left(1+\frac{1}{\tau_I S}+\tau_D S\right)}\right]\frac{K_{B_F}\left(1+\frac{1}{\tau_{I_B} S}\right)e^{-\tau_{B_F} S}}{1+\tau_t S}} \tag{A52}$$

Bypass Control of Heat Exchanger

The transfer function for the mixing tank is

$$\delta T_o'(S) = \frac{(1-f_s)\,\delta T_{L_H}(S) + f_s\,\delta T_F(S)}{1+\tau_t S} - \frac{\left(T_{LH_s} - T_{F_s}\right)\delta f(S)}{1+\tau_t S} \tag{A53}$$

where T_{LH} is the heat exchanger outlet temperature.

Utilizing eq. (A19) for $\delta T_{LH}(S)$ and recognizing that $\delta\phi_H(S) = -W_S\ \delta f(S)$ we obtain

$$(A54)\quad \delta T_o'(s) = \frac{(1-f_s)\,G_H^{T_o'T_F}(s) + f_s}{1+\tau_t s}\,\delta T_F(s) + \frac{(1-f_s)\,G_H^{T_o'T_L}(s)}{1+\tau_t s}\,\delta T_L(s) + \left[\frac{W_s(1-f_s)\,G_H^{T_o'\phi_H}(s)}{1+\tau_t s} - \frac{T_{LH_S} - T_{F_S}}{1+\tau_t s}\right]\delta f(s)$$

Utilizing a control law similar to that given in eq. (A51) we obtain

$$(A55)\quad \delta T_o'(s) = \frac{\dfrac{f_s + (1-f_s)\,G_H^{T_o'T_F}(s)}{1+\tau_t s}\,\delta T_F(s) + \dfrac{(1-f_s)\,G_H^{T_o'T_L}(s)}{1+\tau_t s}\,\delta T_L(s)}{1 + \dfrac{K_{B_H}\left(1+\frac{1}{\tau_I s}\right)}{(1+\tau_t s)(1+\tau_m s)(1+\tau_v s)}\left[\dfrac{(T_{LH_S} - T_{F_S}) - G_H^{T_o'\phi_H}(s)}{(T_{LH_S} - T_{F_S}) - G_H^{T_o'\phi_H}(0)}\right]}$$

Model for Thermal Dispersion In A Nonreactive Packed Bed

In this model, the bed is composed of two phases. Phase α is the interstitial phase and Phase β is the intraparticle phase. Heat transfer occurs between them via convection. Initially it is assumed that the bed has some steady state temperature profile. At time = 0, the inlet temperature is perturbed with an impulse function. The following development describes how the variance of the RTD of the resulting thermal wave can be determined if transfer functions for each phase are established. The development is exactly analogous to that given for fluid residence time distributions in Section I.

Phase α

Phase α is modeled as a tubular column with backmixing of heat. All of the transport processes due to molecular and turbulent diffusion are described by a single effective thermal conductivity, k_{eff}, for which an empirical correlation has been developed by Yagi and Kunii (1957). The thermal transport phenomena in phase α are described by:

$$\rho_f c_f \frac{\partial T_\alpha}{\partial t} = k_{eff} \frac{\partial^2 T_\alpha}{\partial z^2} - \rho_f c_f u \frac{\partial T_\alpha}{\partial z} \tag{A56}$$

where T_α is a deviation variable with respect to the steady state. This equation can be written in the following normalized form:

$$\tau_\alpha \frac{\partial T_\alpha}{\partial t} = \frac{1}{Pe_{th}} \frac{\partial^2 T_\alpha}{\partial x^2} - \frac{\partial T_\alpha}{\partial x} \tag{A57}$$

The dimensionless terms are defined as:

$$Pe_{th} = \frac{\rho_f c_f u L}{k_{eff}} \; ; \; \tau_\alpha = \frac{L}{u} \; ; \; x = \frac{z}{L}$$

where u is the velocity, which is assumed constant across the catalyst bed, L is the length of the bed, τ_α is the mean residence time in phase α, ρ_f is the fluid density, c_f is its specific heat, and Pe_{th} is the Peclet number for thermal dispersion.

If the Laplace transform of eq. (A57) is taken, we obtain the following expression for the Laplace transform of the thermal RTD in phase α:

$$f_T(s) = \frac{4q}{(1+q)^2 e^{\left(\frac{Pe_{th}}{2}\right)(q-1)} - (q-1)^2 e^{-\left(\frac{Pe_{th}}{2}\right)(1+q)}} \tag{A58}$$

where the normalized boundary conditions are:

$$@ \quad x = 0: \quad T_{\alpha_o} - T_\alpha = -\frac{1}{Pe_{th}} \frac{dT_\alpha(s,x)}{dx}$$

$$@ \quad x = 1: \quad \frac{dT_\alpha}{dx} = 0$$

and q is defined as:

$$q = \left(1 + \frac{4\tau_\alpha}{Pe_{th}} s\right)^{1/2}$$

where s is the Laplace transform variable.

If eq. (A58) is viewed as a moment generating function, then the first and second moments of $f_T(t)$ can be found to be

(A59) $$\mu_1 = \tau_\alpha$$

(A60) $$\mu_2 = 2(\tau_\alpha^2/Pe_{th}^2)\left(Pe_{th} + e^{-Pe_{th}} - 1 + \frac{Pe_{th}^2}{2}\right)$$

Phase β

The shape of the particles is neglected and it is assumed that they can be described as thin plates of thickness 2b. The transport of heat to the particle surface is described by a heat transfer coefficient, h. The internal conduction processes are described by a one dimensional diffusion model with thermal conductivity k_β and with diffusing length b, the catalyst volume per unit interfacial surface area. Mathematically this is written as:

(A61) $$\rho_\beta c_\beta \frac{\partial T_\beta}{\partial t} = k_\beta \frac{\partial^2 T_\beta}{\partial z^2}$$

where T_β is a deviation variable with respect to the steady state value. Normalized with respect to the characteristic dimension, b, this becomes

(A62) $$\Theta_{th} \frac{\partial T_\beta}{\partial t} = \frac{\partial^2 T_\beta}{\partial x^2}$$

where $X = \frac{z}{b}$ and $\theta_{th} = \frac{b^2 \rho_\beta c_\beta}{k_\beta}$

The pertinent normalized boundary conditions are:

(A63) @ x = 0: $$-\frac{dT_\beta}{dx} = \frac{h\theta_{th}}{\rho_\beta c_\beta b}(T_\alpha - T_\beta) = \frac{h'\theta_{th}}{b}(T_\alpha - T_\beta)$$

(A64) @ x = 1: $$\frac{dT_\beta}{dx} = 0$$

where x = 0 is the surface of the particle and x = 1 is the center line.

If the Laplace transforms are taken of eqs. (A62)-(A64), an expression can be found for the Laplace transform of the RTD $\phi(t)$, which is defined in Section I. This is:

(A65) $$\phi(s) = \left.\frac{T_\beta}{T_\alpha}\right|_{x=0} = \frac{1}{1 + \frac{b\sqrt{\theta_{th}s}}{h'\theta_{th}} \tanh\sqrt{\theta_{th}s}}$$

The first and second moments of $\phi(t)$ are

(A66) $$K_1 = \frac{b}{h'} = \tau_\beta$$

(A67) $$K_2 = 2\tau_\beta^2 + \frac{2}{3}\tau_\beta\,\theta_{th}$$

The RTD for the thermal wave in the entire system is $g_T(t)$. Its moments can be found from the moments of $f_T(t)$ and $\phi_T(t)$ as shown in the following relations

(A68) $$\nu_1 = (1+\lambda K_1)\mu_1$$

(A69) $$\nu_2 = \lambda K_2 \mu_1 + (1+\lambda K_1)^2 \mu_2$$

where $\lambda = \frac{h'}{Bb}$ and $B = \frac{\rho_f c_f \epsilon}{\rho_\beta c_\beta (1-\epsilon)}$

Our goal is to determine the variance of $g_T(t)$ and to evaluate its effect and the effects of its terms on the dampening of the reactor frequency response $|G^{TT}(j\omega)|$. In particular, we are interested in assessing how scaling up of the reactor will affect the frequency response and the control scheme developed from pilot plant studies. Making the proper substitutes into eqs. (A68) and (A69) we obtain:

(A70) $$\nu_1 = \left(1 + \frac{1}{B}\right)\tau_\alpha = \tau_{th}$$

(A71) $$\nu_2 = 2(\tau_{th}-\tau_\alpha)^2\left(\frac{1}{n} + \frac{\theta_{th}}{\tau_{c_{th}}}\right) + 2\tau_{th}^2\left(\frac{1}{Pe_{th}} + \frac{e^{-Pe_{th}}}{Pe_{th}^2} - \frac{1}{Pe_{th}^2} + \frac{1}{2}\right)$$

where $n = \lambda\tau_\alpha$ and $\tau_{c_{th}} = n\tau_\beta$. The variance of $g_T(t)$ can be found from $\sigma_g^2 = \nu_2 - \nu_1^2$ and is calculated to be:

$$(A72) \qquad \frac{\sigma_g^2}{\tau_{th}^2} = 2\left[\frac{1}{Pe_{th}} - \frac{1-e^{-Pe_{th}}}{Pe_{th}^2} + \frac{1}{n(1+B)^2} + \frac{\Theta_{th}}{3\tau_{c_{th}}(1+B)^2}\right]$$

In terms of reactor parameters, it can be written as:

$$(A73) \qquad \frac{\sigma_g^2}{\tau_{th}^2} = 2\left[\frac{k_{ess}\tau_\alpha}{\rho c_f L^2} + \frac{1}{H_p \tau_{th} B(1+B)} + \frac{d_p^2 \rho_p c_p}{108 k_p \tau_{th}(1+B)}\right]$$

The effects of space velocity, particle size, reactor length and diffusivities on $\frac{\sigma_g^2}{\tau_{th}^2}$ are exactly analagous to their effects on $\frac{\sigma_\psi^2}{\tau_c^2}$ as described in Section I. Consequently, for purposes of achieving a close approach to plug flow in kinetic terms between the pilot plant and industrial reactor, the coefficient of variation $\frac{\sigma_g^2}{\tau_{th}^2}$ can be made small. This close approach is possible because the kinetic behavior is relatively insensitive to small changes in the variance.

However, the situation is different with regard to the frequency response of the reactor $|G_R(j\omega)|$. It depends directly on the product $\omega^2\sigma_g^2$ as demonstrated by McHenry and Wilhelm (1957) who offer the following simplified transfer function:

$$(A74) \qquad \frac{T_L}{T_o} = e^{-\frac{\omega^2\sigma_g^2}{2}}$$

Because of the dependence on ω, even small relative differences in σ_g^2 between the pilot plant reactor and the industrial reactor can be magnified at moderate frequencies to cause significant differences in the amplitude ratios of the two reactors. The industrial reactor will have a smaller variance and as a result its frequency response will not dampen as quickly as the pilot plant response. Thus, the industrial reactor will be harder to control than the pilot plant reactor.

NOMENCLATURE

a_p	catalyst surface area per unit volume of reactor
$a_F(s)$, $b_F(s)$, $C_F(s)$	polynomials in furnace transfer functions
$a_H(s)$, $b_H(s)$, $C_H(s)$	polynomials in heat exchanger transfer functions
A	$\frac{E}{RT_o}$
A_i	cross sectional area of heat exchanger tubes
A_w	heat transfer area in heat exchanger
A_t	tube heat transfer area in furnace
AR_{co}	amplitude ratio at crossover frequency
AR_p	amplitude ratio at peak in reactor frequency response
B	dimensionless heat transfer coefficient $\frac{\rho_f c_f \varepsilon}{\rho_p C_p (1-\varepsilon)}$
c_c	specific heat of quench gas
c_f	specific heat of fluid
c_p	particle specific heat
c_{pt}	tube specific heat in furnace
c_{pw}	specific heat of furnace wall
c_R	specific heat of reaction fluid
C_f	fluid phase concentration
C_i	inlet concentration to the reactor
C_p	acid phase concentration
d_p	particle diameter
D	diameter
E	activation energy
f_s	bypass fraction

NOMENCLATURE (continued)

$G_{FOL}(s)$	furnace transfer function relating outlet to inlet temperature
$G_{HF}(s)$	heat exchanger transfer function relating outlet to fresh feed temperature
$G_{HL}(s)$	heat exchanger transfer function relating outlet to reactor effluent temperature
$G_{OL}(s)$	open loop transfer function for process
$G_R^{ij}(s)$	reactor transfer function relating effect of input disturbance j on output i
$G_F^{ij}(s)$	furnace transfer function relating effect of input disturbance j on output i
$G_H^{ij}(s)$	heat exchanger transfer function relating effect of input disturbance j on output i
$g(s)$	reactor transfer function relating outlet to inlet concentration for tracer
H_p	normalized heat transfer coefficient defined in Table I
h_p	interphase heat transfer coefficient
K_B	proportional setting in bypass control loop
K_C	proportional control setting
k	reaction rate constant
k_p	particle thermal conductivity
k_∞	reaction rate constant pre-exponential
L	reactor length, total length of tubes in heat exchanger
M	mass hold up
M_g	mass hold up of fuel in furnace
M_o	mass hold up of oil in furnace
M_t	tube mass in furnace
M_w	wall mass of furnace

NOMENCLATURE (continued)

n_{th}	convective heat transfer parameter
Pe_{th}	Peclet number for thermal dispersion
$Q_{to\ tube}$	heat to tubes in furnace
Q_{gw}	heat in furnace from gas to walls
Q_{gt}	heat from gas to tubes
Q_{wt}	heat from walls to tubes
Q_{out}	heat leaving from stack
Q_{loss}	heat loss through walls
R	gas constant
r	reaction rate
s	Laplace transform variable
$S_g\rho_p$	specific inner surface of catalyst
T_C	temperature of quench gas
T_F	fresh feed temperature
T_f	fluid temperature
T_g	fuel temperature in furnace
T_L	reactor exit temperature
T_o	reactor inlet temperature or furnace outlet temperature, dimensionless parameter in eq. (13)
T_o'	heat exchanger outlet or furnace inlet temperature
T_P	catalyst temperature
T_R	temperature of reacted fluid downstream of heat exchanger, reference temperature
T_t	tube temperature in furnace
T_w	wall temperature
t	time

NOMENCLATURE (continued)

U	overall heat transfer coefficient
u	velocity
V_R	shell side volume
W_B	flow rate of bypass stream
W_C	mass flow rate of quench gas
W_S	flow rate of fresh feed
X_L	normalized reactor length defined in Table I
Z	distance

Greek Symbols

α_o	tube side heat transfer coefficient in furnace
α_c	heat transfer coefficient on gas side
β	mass transfer coefficient
γ	voidage of particle
$(-\Delta H)$	heat of reaction
ϵ	voidage of bed
ρ_f	fluid density
ρ_p	particle density
σ_g^2	variance of residence time distribution of thermal wave
τ_D	derivative time
τ_d	delay time
τ_F	furnace residence time
τ_f	fluid residence time
τ_H	heat exchanger residence time
τ_I	integral time
τ_m	thermocouple time constant

NOMENCLATURE (continued)

τ_t	tank time constant
τ_{th}	thermal wave residence time
τ_v	valve time constant
ϕ_f	feed rate to furnace
ϕ_g	fuel flow rate in furnace
ϕ_m	mass flow of reaction fluid in furnace
ϕ_R	flow rate of reaction fluid
ω	frequency

REFERENCES

Acrivos, A., "Method of Characteristics Technique - Application to Heat and Mass Transfer Problems," Ind. Eng. Chem., 48, 703(1956).

Amundson, N.R., "Solid-Fluid Interactions in Fixed and Moving Beds. Fixed Beds With Small Particles," Ind. Eng. Chem. 48, 26(1956).

Aris, R., "On Shape Factors For Irregular Particles - II. The Transient Problem. Heat Transfer to a Packed Bed," Chem. Eng. Sci., 7, 8,(1957).

Aris, R., and Amundson, N.R., "An Analysis of Chemical Reactor Stability And Control - I. The Possibility of Local Control, With Perfect or Imperfect Control Mechanisms," Chem. Eng. Sci., 7, 121(1958).

Aris, R., and Amundson, N.R., "An Analysis of Chemical Reactor Stability And Control - II. The Evolution of Proportional Control," Chem. Eng. Sci., 7, 132(1958).

Aris, R., et.al., "An Analysis of Chemical Reactor Stability And Control - IV. Mixed Derivative and Proportional Control," Chem. Eng. Sci., 11, 199 (1959).

Cohen, W.C., and Johnson, E.F., "Dynamic Characteristics of Double-Pipe Heat Exchangers," Ind. Eng. Chem., 48, 1031(1956).

Crider, J.E., and Foss, A.S., "An Analytical Solution for the Dynamics of a Packed Adiabatic Chemical Reactor," A.I.Ch.E.J., 14, 77(1968).

Crider, J.E., and Foss, A.S., "Computational Studies of Transients in Packed Tubular Chemical Reactors," A.I.Ch.E.J., 12, 514(1966).

Denn, M.M., Stability of Reaction and Transport Processes, Prentice-Hall, Inc., Englewood Cliffs, New Jersey (1975).

Eigenberger, G., "On the Dynamic Behavior of the Catalytic Fixed Bed Reactor In the Region of Multiple Steady States - I. The Influence of Heat Conduction In Two-Phase Models," Chem. Eng. Sci. 27, 1909 (1972a).

Eigenberger, G., "On the Dynamic Behavior of the Catalytic Fixed Bed Reactor In the Region of Multiple Steady States - II. The Influence of the Boundary Conditions in the Catalyst Phase," Chem. Eng. Sci., 27, 1917(1972b).

Hoiberg, J.A., Lyche, B.C., and Foss, A.S., "Experimental Evaluation of Dynamic Models for a Fixed-Bed Catalytic Reactor," A.I.Ch.E.J., 17, 1434(1971).

REFERENCES (continued)

Jaffe, S.B., "Kinetics of Heat Release in Petroleum Hydrogenation," Ind. Eng. Chem., Process Des. Develop., 13, 34(1974).

Liu, S.-L., and Amundson, N.R., "Stability of Adiabatic Packed-Bed Reactors. An Elementary Treatment," Ind. Eng. Chem., Fundamentals, 1, 200(1962).

Liu, S.-L., and Amundson, N.R., "Stability of Adiabatic Packed-Bed Reactors. Effect of Axial Mixing," Ind. Eng. Chem., Fundamentals, 2, 183(1963).

Luss, D., and Amundson, N.R., "Stability of Loop Reactors," A.I.Ch.E.J., 13, 279(1967).

McHenry, K.W., and Wilhelm, R.H., "Axial Mixing of Binary Gas Mixtures Flowing in a Random Bed of Spheres," A.I.Ch.E.J., 3, 83(1957).

Parega, G., and Reilly, M.J., "Dynamic Effects of Recycle Elements In Tubular Reactor Systems," Ind. Eng. Chem., Fundamentals, 8, 442(1969).

Perlmutter, D., Stability of Chemical Reactors, Prentice-Hall, Inc., Englewood Cliffs, New Jersey (1972).

Ritter, A.B., and Douglas, J.M., "Frequency Response of Nonlinear Systems," Ind. Eng. Chem. Fundamentals, 9, 21(1970).

Reilly, M.J., and Schmitz, R.A., "Dynamics of a Tubular Reactor with Recycle: Part I. Stability of the Steady State," A.I.Ch.E.J., 12, 153(1966).

Reilly, M.J., and Schmitz, R.A., "Dynamics of a Tubular Reactor with Recycle: Part II. Nature of the Transient State", A.I.Ch.E.J., 13, 519(1967).

Roffel, B., and Rijnsdorp, J.E., "Dynamics and Control of a Gas-Fired Furnace," Chem. Eng. Sci., 29, 2083(1974).

Root, R.B., and Schmitz, R.A., "An Experimental Study of Steady State Multiplicity in a Loop Reactor," A.I.Ch.E.J., 15, 670(1969).

Root, R.B., and Schmitz, R.A., "An Experimental Study of Unstable States in a Loop Reactor," A.I.Ch.E.J., 16, 356(1970).

Sayles, J.H., et.al., "Computer Control Maximizes Hydrocracker Throughput", Instrument. Tech., 44, May (1973).

Shinnar, R., et.al., "Interpretation and Evaluation of Multiple Tracer Experiments," Chem. Eng. Sci., 27, 1627 (1972).

REFERENCES (continued)

Silverstein, J., and Shinnar, R., "Design of Fixed Bed Catalytic Microreactors," Ind. Eng. Chem., Process Des. Dev., 14, 127(1975).

Sinai, J., and Foss, A.S., "Experimental and Computational Studies of the Dynamics of a Fixed Bed Chemical Reactor," A.I.Ch.E.J., 16, 659(1970).

Stangeland, B.E., and Kittrell, J.R., "Jet Fuel Selectivity in Hydrocracking," Ind. Eng. Chem. Process Des. Dev., 11, 15(1972).

Stormont, D.H., "New Analog Computer Controls Hydrocracker Conversion Level," Oil and Gas J., 100, Sept. (1969).

van Doesburg, H., and de Jong, W.A., "Transient Behavior of an Adiabatic Fixed-Bed Methanator - I," Chem. Eng. Sci., 31, 45(1976a).

van Doesburg, H., and de Jong, W.A., "Transient Behavior of an Adiabatic Fixed-Bed Methanator - II," Chem. Eng. Sci., 31, 53 (1976b).

van Heerden, C., "The Character of the Stationary State of Exothermic Processes," Chem. Eng. Sci., 8, 133(1958).

van Heerden, C., "Autothermic Processes," Ind. Eng. Chem., 45, 1242(1953).

Yagi, S. and Kunii, D., "Studies on Effective Thermal Conductivities in Packed Beds," A.I.Ch.E.J., 3, 373(1957).

TABLE 1

REACTOR MODELS

Liu and Amundson Model

Fluid phase mass and heat balances:

$$\frac{\partial \bar{C}_f}{\partial t} + u \frac{\partial \bar{C}_f}{\partial z} = \frac{\beta a_p}{\epsilon} (\bar{C}_p - \bar{C}_f)$$

$$\rho_f c_f \frac{\partial T_f}{\partial t} + \rho_f c_f u \frac{\partial T_f}{\partial z} = \frac{h_p a_p (1-\epsilon)}{\epsilon} (T_p - T_f)$$

Catalyst phase mass and heat balances:

$$\frac{\partial \bar{C}_p}{\partial t} = \frac{6\beta}{d_p \gamma} (\bar{C}_f - \bar{C}_p) - \frac{S_g \rho_p}{\gamma} \bar{r}$$

$$\rho_p c_p \frac{\partial T_p}{\partial t} = \frac{6h_p}{d_p} (T_f - T_p) + S_g \rho_p \sum_i (-\Delta H)_i r_i$$

Crider and Foss Model

Dimensionless mass and heat balances:

$$\frac{\partial \bar{C}_f}{\partial t} + \frac{\partial \bar{C}_f}{\partial x} = -\bar{r}$$

$$\frac{\partial T_f}{\partial t} + \frac{\partial T_f}{\partial x} = \bar{r} + H_p (T_p - T_f)$$

$$\frac{\partial T_p}{\partial t} = H_p B (T_f - T_p)$$

For single first order irreversible reaction A→B, these become:

$$\frac{\partial C_f}{\partial t} + \frac{\partial C_f}{\partial x} = - r\,(C_f, T_f) = -e^{AT_f/(T_o+T_f)} C_f$$

$$\frac{\partial T_f}{\partial t} + \frac{\partial T_f}{\partial x} = r\,(C_f, T_f) + H_p\,(T_p - T_f)$$

$$\frac{\partial T_p}{\partial t} = H_p B\,(T_f - T_p)$$

These equations can be linearized and solved analytically to give the transfer function relating the outlet temperature of the reactor to inlet changes in temperature:

$$G_R(s) = r_s(X_L)\, e^{-SX_L} \left[1 + \left(1 - \frac{H_p S}{S+H_p B}\right) \bar{I}\,(S, X_L) \right]$$

where $\bar{I}\,(S,X_L) = \int_o^{X_L} e^{\frac{-H_p S y}{S+H_p B}} \frac{dy}{C_{f_s}(y)}$

The dimensionless parameters are defined as follows:

$$A = \frac{E}{RT_R} \qquad C_f = \frac{a_f}{a_o}$$

$$B = \frac{\rho_f c_f \varepsilon}{\rho_p c_p (1-\varepsilon)} \qquad T_f = \frac{T_f^* - T_R}{\Delta T_{ad}}$$

$$H_p = \frac{h_p a_p (1-\varepsilon)}{\rho_f c_f \varepsilon\, k_\infty\, e^{-A}} \qquad T_o = \frac{T_R}{\Delta T_{ad}}$$

$$t = t^*\, k_\infty\, e^{-A} \qquad T_p = \frac{T_p^* - T_R}{\Delta T_{ad}}$$

$$x = \frac{x^*}{u}\, k_\infty\, e^{-A}$$

where T_R = reference temperature

starred values are dimensional

TABLE 2

REACTOR PARAMETERS

Case 1. Reactor With Single First Order Reaction A→B

$h = 30 \frac{BTU}{hr\ ft^2\ °F}$ $\quad S_g\rho_c = 6.08 \times 10^7\ ft^{-1}$

$\Delta T_{ad} = 130°F$ $\quad \gamma_i = 0.4$

$(-\Delta H) = 15 \frac{Kcal}{g\text{-}mole}$ $\quad \gamma = 0.35$

$u = 0.4 \frac{ft.}{sec}$ $\quad \rho C_{pc} = 30.333 \frac{BTU}{ft^3\ °F}$

$\beta = 1.915 \frac{ft.}{sec}$ $\quad \rho_f c_f = 4.58 \frac{BTU}{ft^3\ °F}$

$d_p = 3\ mm$ $\quad k_\infty = 7.5 \times 10^7\ min^{-1}$

$a_p = 375\ ft^{-1}$ $\quad E = 40 \frac{Kcal}{g\text{-}mole}$

$L = 60\ ft$

Typical Temperature Profile in Reactor with Quench

Bed	Temperature In (°F)	Temperature Out (°F)	Length (ft)
1	642	676	6
2	648	679	7
3	653	683	10.5
4	666	686	16.5
5	679	686	24

TABLE 3

REACTOR PARAMETERS

Case 2. Hydrocracker with Reactions:

$$\text{Gas Oil} \xrightarrow{k_1} 2.099\ \text{Jet Fuel} \xrightarrow{k_2} 3.79\ \text{Gasoline} \xrightarrow{k_3} \text{Light Products}$$

$k_{1\infty} = 4.75 \times 10^9$ $\quad E_1 = 50 \frac{\text{Kcal}}{\text{g-mole}}$ $\quad (-\Delta H)_1 = -34.8 \frac{\text{Kcal}}{\text{g-mole G.O.}}$

$k_{2\infty} = 5.065 \times 10^9$ $\quad E_2 = 55 \frac{\text{Kcal}}{\text{g-mole}}$ $\quad (-\Delta H)_2 = -13.4 \frac{\text{Kcal}}{\text{g-mole Jet}}$

$k_{3\infty} = 5.065 \times 10^8$ $\quad E_3 = 55 \frac{\text{Kcal}}{\text{g-mole}}$ $\quad (-\Delta H)_3 = -31.8 \frac{\text{Kcal}}{\text{g-mole Gasoline}}$

Other parameters are the same as for the reactor with single first order reaction.

Typical Temperature Profile in Reactor with Quench-Corresponds to Point 3 of Curve 3 in Figure 8.

Bed	Temperature In (°F)	Temperature Out (°F)	Length (ft)
1	760	783	9
2	766	785	10
3	772.5	789	12
4	779	791.5	16
5	785	792	18

TABLE 4

PARAMETERS FOR UNITS IN HEAT FEEDBACK LOOP

Heat Exchanger Parameters

The following parameters were used in the unbypassed exchanger.

$T_F = 365°F$

$T_o' = 543°F$

$Q = 44 \frac{MMBTU}{hr}$

$T_{R_{in}} = 645°F$

$T_{R_{out}} = 515°F$

$\pi D_o LN = 4231 \text{ ft}^2$

$U_o = 87.81 \frac{BTU}{ft^2\text{-hr-}°F}$

$L = 121 \text{ ft}$

$u_H = 20 \text{ ft/sec}$

Tube Diameter = 1 in.

$\tau_1 = 2.25 \text{ sec}$

$\tau_2 = 2.72 \text{ sec}$

$\tau_3 = 0.728 \text{ sec}$

$a_1 = 0.7876$

$a_2 = 0.2124$

$b_1 = 0.0524$

$b_2 = 0.9476$

Furnace Parameters

$Q = 8.1 \frac{MMBTU}{hr}$

tube OD = 6.625 in.

tube ID = 6.065 in.

$\rho_f = 4.56 \frac{lb}{ft^3}$

$u_f = 66.7 \frac{ft}{sec}$

$A_t = 405 \text{ ft}^2$

$L = 234 \text{ ft}$

$\alpha_o = 100 \frac{BTU}{hr \text{ ft}^2 °F}$

$\alpha_c = 2.47 \frac{BTU}{ft^2 \text{ hr } °F}$

wall surface = 1300 ft^2

heat flux = $20{,}000 \frac{BTU}{hr \text{ ft}^2}$

flame temperature = 3432°F

Avg. skin temperature is 200°F above outlet temperature of fluid.

Table A1

Dimensionless Heat Exchanger Parameters

$$a_1 = \frac{D_o h_{os}}{D_o h_{o_s} + D_i h_{i_s}} \qquad b_2 = \frac{\pi D_o h_o L}{\phi_{R_s} C_R + \pi D_o h_o L}$$

$$a_2 = \frac{D_i h_{i_s}}{D_o h_{o_s} + D_i h_{i_s}} \qquad \tau_1 = \frac{\pi D_i h_{i_s}}{\rho A_i C}$$

$$a_3 = \frac{-0.8 D_i h_i (T_{w_s} - T_{o_s})}{D_o h_{o_s} + D_i h_{is}} \qquad \tau_2 = \frac{\rho_w A_w C_w}{\pi (D_o h_{o_s} + D_i h_{i_s})}$$

$$b_1 = \frac{\phi_{R_s} C_R}{\phi_{R_s} C_R + \pi D_o h_o L} \qquad \tau_3 = \frac{\rho_R V C_R}{\phi_R C_R + \pi D_o h_o L}$$

$$a_H(s) = 1 + \tau_1 s - \frac{a_2(1+\tau_3 s)}{(1+\tau_2 s)(1+\tau_3 s) - a_1 b_2}$$

$$b_H(s) = \frac{a_1 b_1}{(1+\tau_2 s)(1+\tau_3 s) - a_1 b_2}$$

$$C_H(s) = \frac{a_3(1+\tau_3 s)}{(1+\tau_2 s)(1+\tau_3 s) - a_1 b_2} - 0.8(T_{w_s} - T_{os})$$

Table A2

Dimensionless Furnace Parameters

$$Q_{gw} = A_w \varepsilon_w f_1 \sigma \left[\left(\frac{T_g}{100}\right)^{3.4} - \left(\frac{T_w}{100}\right)^{3.4} \right] + A_w \varepsilon_w f_2 \sigma (T_g^4 - T_w^4) + A_w \alpha_c (T_g - T_w)$$

$$Q_{gt} = A_t \varepsilon_t f_1 \sigma \left[\left(\frac{T_g}{100}\right)^{3.4} - \left(\frac{T_t}{100}\right)^{3.4} \right] + A_t \varepsilon_t f_2 \sigma (T_g^4 - T_t^4) + A_t \alpha_c (T_g - T_t)$$

$$Q_{wt} = A_t \varepsilon_{wt} \sigma (T_w^4 - T_t^4) - A_t \varepsilon_w f_1 \sigma \left[\left(\frac{T_w}{100}\right)^{3.4} - \left(\frac{T_t}{100}\right)^{3.4} \right] - A_t \varepsilon_w f_2 \sigma (T_w^4 - T_t^4)$$

$$Q_{out} = \phi_{gas} C_{pg} (T_g - T_{ref}) \; ; \quad Q_{loss} = 0.56 (w_L)^{.75} w (T_w - T_{amb})^{1.25}$$

$$K_1 = 4T_{w_s}^3 (\varepsilon_{w_t} \sigma - \varepsilon_w f_2 \sigma) - 3.4 T_{w_s}^{2.4} \frac{\varepsilon_w f_1 \sigma}{(100)^{3.4}}$$

$$K_2 = 4T_{t_s}^3 (\varepsilon_{w_t} \sigma - \varepsilon_w f_2 \sigma) - 3.4 T_{t_s}^{2.4} \frac{\varepsilon_w f_1 \sigma}{(100)^{3.4}}$$

$$K_3 = 4T_{g_s}^3 \varepsilon_t f_2 \sigma + \alpha_c + \frac{3.4 T_{g_s}^{2.4}}{(100)^{3.4}} \varepsilon_t f_1 \sigma \; ;$$

$$K_4 = 4T_{t_s}^3 \varepsilon_t f_2 \sigma + \alpha_c + \frac{3.4 T_{t_s}^{3.4} \varepsilon_t f_1 \sigma}{(100)^{3.4}}$$

$$K_5 = \frac{3.4 \varepsilon_w f_1 \sigma}{(100)^{3.4}} T_{g_s}^{2.4} + 4\varepsilon_w f_2 \sigma T_{g_s}^3 + \alpha_c \; ; \; K_6 = \frac{3.4 \varepsilon_w f_1 \sigma T_{w_s}^{2.4}}{(100)^{3.4}} + 4\varepsilon_w f_2 \sigma T_{w_s}^3 + \alpha_c$$

Table A2 (cont.)

$$T_1 = \frac{M_o C_{po}}{\alpha_{o_s} A_t}$$

$$T_3 = \frac{M_g C_{pg}}{\phi_{gs} C_{pg} + K_5 A_w + K_3 A_t}$$

$$T_2 = \frac{M_t C_{pt}}{(K_2+K_4) A_t}$$

$$\alpha' = \frac{(-\Delta H') - C_{pg}(T_{g_s} - T_{ref}) - \frac{3}{4}\frac{\alpha_{c_s}}{\phi_{g_s}}[A_w(T_{g_s} - T_{w_s}) + A_t(T_{g_s} - T_{t_s})]}{\phi_{g_s} C_{p_g} + K_5 A_w + K_3 A_t}$$

$$\phi = \frac{K_1}{K_2+K_4}$$

$$w = \frac{K_6 A_w}{\phi_{gs} C_{pg} + K_5 A_w + K_3 A_t}$$

$$\gamma = \frac{K_3}{K_2+K_4}$$

$$\beta = \frac{K_4 A_t}{\phi_{gs} C_{pg} + K_5 A_w + K_3 A_t}$$

$$\frac{T_2}{T_{12}} = \frac{\alpha'_{o_s}}{K_2+K_4}$$

$$T_4 = \frac{M_w C_{pw}}{K_6 A_w + K_1 A_t + K_7}$$

$$C_{gt} = \frac{\frac{3}{4}(T_{g_s} - T_{t_6})\frac{\alpha_{cs}}{\phi_{gs}}}{K_2+K_4}$$

$$\eta = \frac{K_5 A_w}{K_6 A_w + K_1 A_t + K_7}$$

Table A2 (cont.)

$$C_{ft} = \frac{\frac{3}{4}\alpha'_{os}(T_{t_s} - T_{o_s})}{K_2 + K_4} \qquad \mu = \frac{K_2 A_t}{K_6 A_w + K_1 A_t + K_7}$$

$$C_{wg} = \frac{A_w (T_{g_s} - T_{w_s})\frac{3}{4}\ \frac{\alpha_{c_s}}{\phi_{gs}}}{K_6 A_w + K_1 A_t + K_7}$$

$$A(s) = \frac{1}{T_1}\left\{ sT_1 + 1 - \frac{\frac{T_2}{T_{12}}\left[(1+T_3 s)(1+T_4 s) - w\eta\right]}{\left(T_2 s + 1 + \frac{T_2}{T_{12}}\right)\left[(1+T_3 s)(1+T_4 s) - w\eta\right] - \phi\eta\beta - \gamma\beta(1+T_4 s) - \gamma\mu w - \phi\mu(1+T_3 w)} \right\}$$

$$b(s) = \frac{1}{T_1}\left\{ \frac{\phi\eta\alpha' + \gamma\alpha'(1+T_4 s) + \gamma w C_{wg} + C_{gt}(1+T_3 s)(1+T_4 s) - C_{gt} w\eta + \phi C_{wg}(1+T_3 s)}{\left(T_2 s + 1 + \frac{T_2}{T_{12}}\right)\left[(1+T_3 s)(1+T_4 s) - w\eta\right] - \phi\mu\beta - \gamma\beta(1+T_4 s) - \gamma\mu w - \phi\mu(1+T_3 s)} \right\}$$

$$C(s) = \frac{1}{T_1}\left[\frac{C_{ft}\left[(1+T_3 s)(1+T_4 s) - w\eta\right]}{\left(T_2 s + 1 + \frac{T_2}{T_{12}}\right)\left[(1+T_3 s)(1+T_4 s) - w\eta\right] - \phi\eta\beta - \gamma\mu w - \gamma\beta\mu(1+T_4 s) + \phi\mu(1+T_3 s)} \right]$$

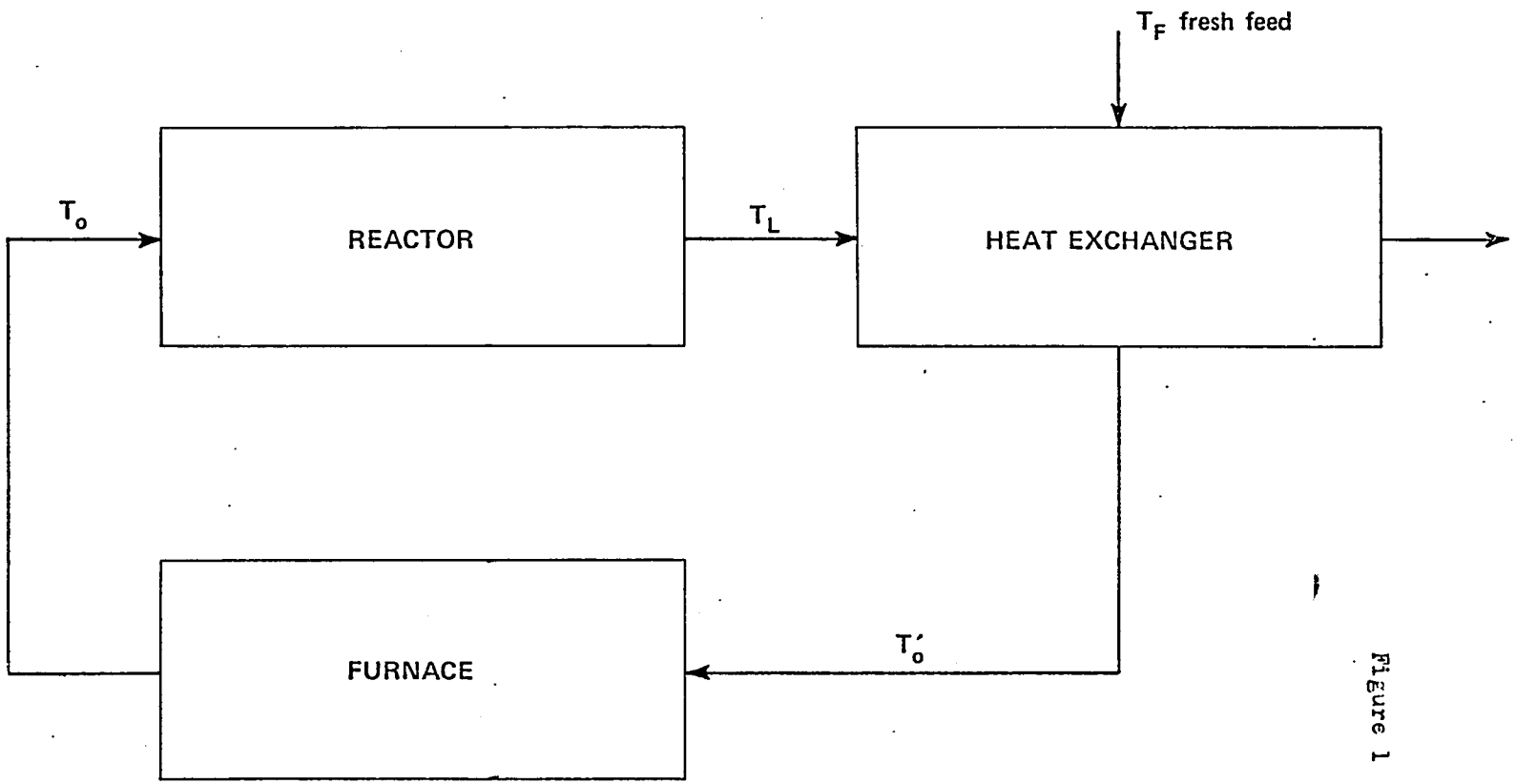

Figure 1

Schematic of Reactor with External Heat Feedback

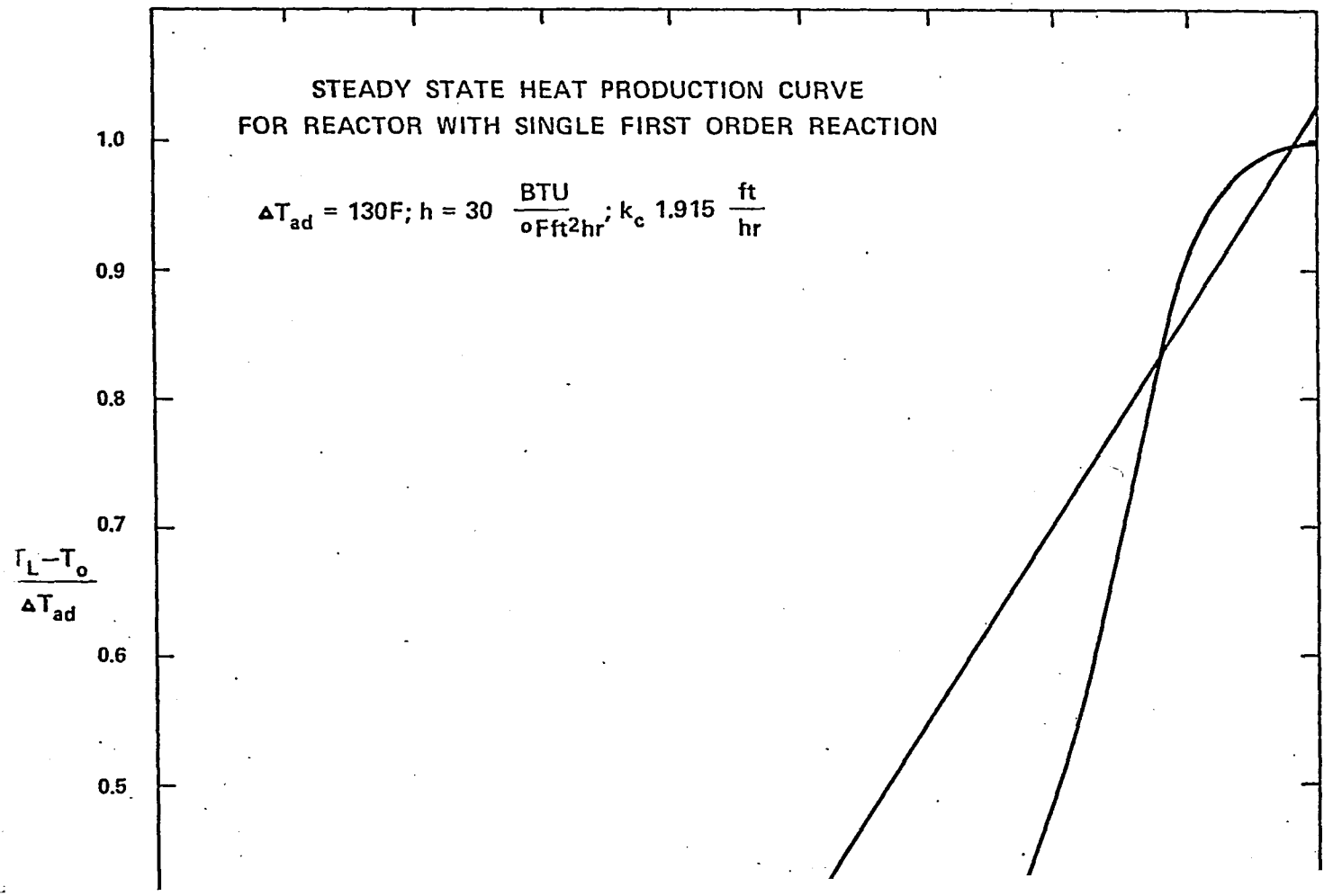
STEADY STATE HEAT PRODUCTION CURVE
FOR REACTOR WITH SINGLE FIRST ORDER REACTION
ΔT_{ad} = 130F; h = 30 $\frac{BTU}{^oFft^2hr}$; k_c 1.915 $\frac{ft}{hr}$
1.0
0.9
0.8
0.7
0.6
0.5
$\frac{T_L - T_o}{\Delta T_{ad}}$

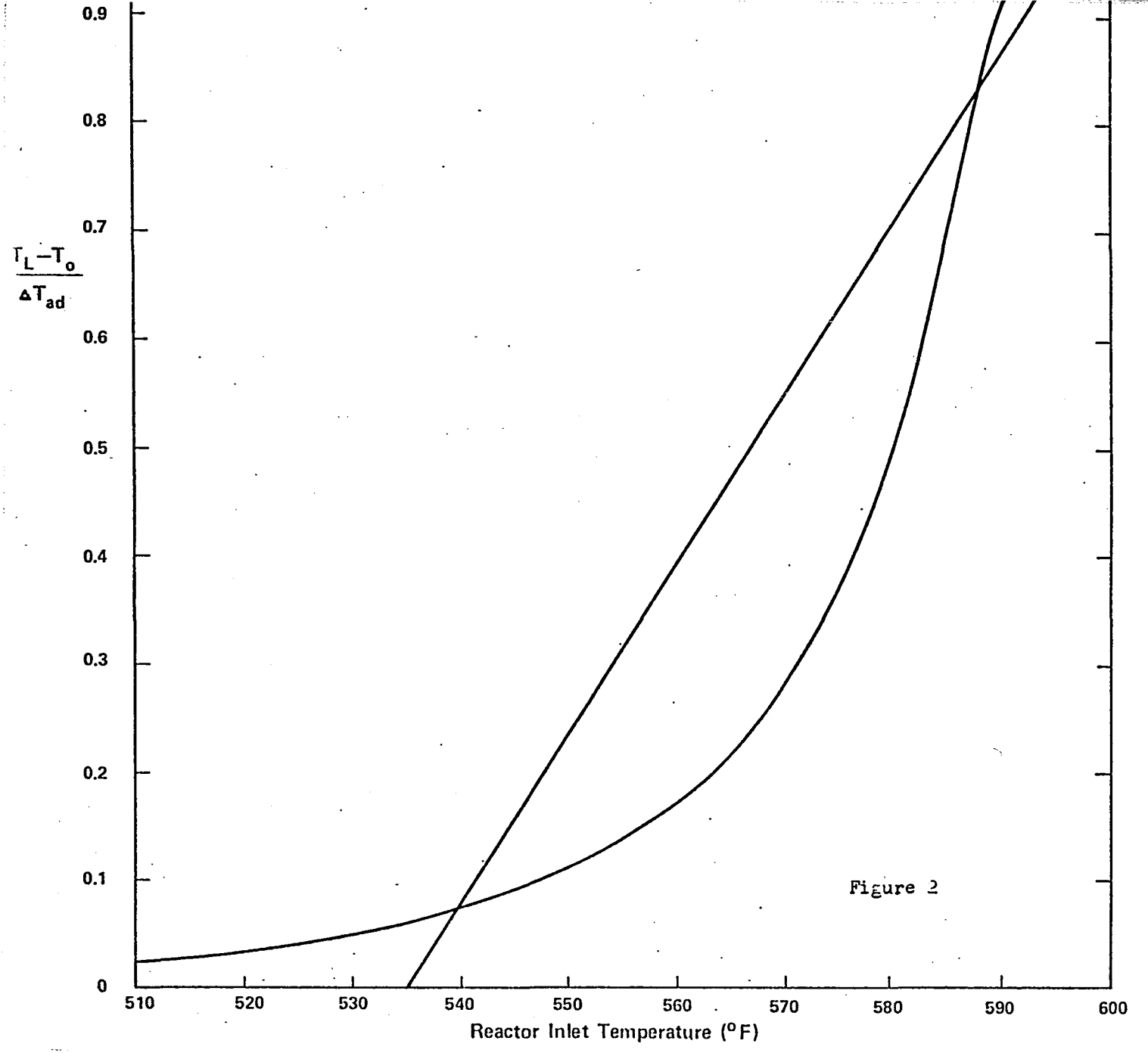
0.9
0.8
0.7
0.6
0.5
0.4
0.3
0.2
0.1
0
$\frac{T_L - T_o}{\Delta T_{ad}}$
510
520
530
540
550
560
570
580
590
600
Reactor Inlet Temperature (°F)

Figure 2

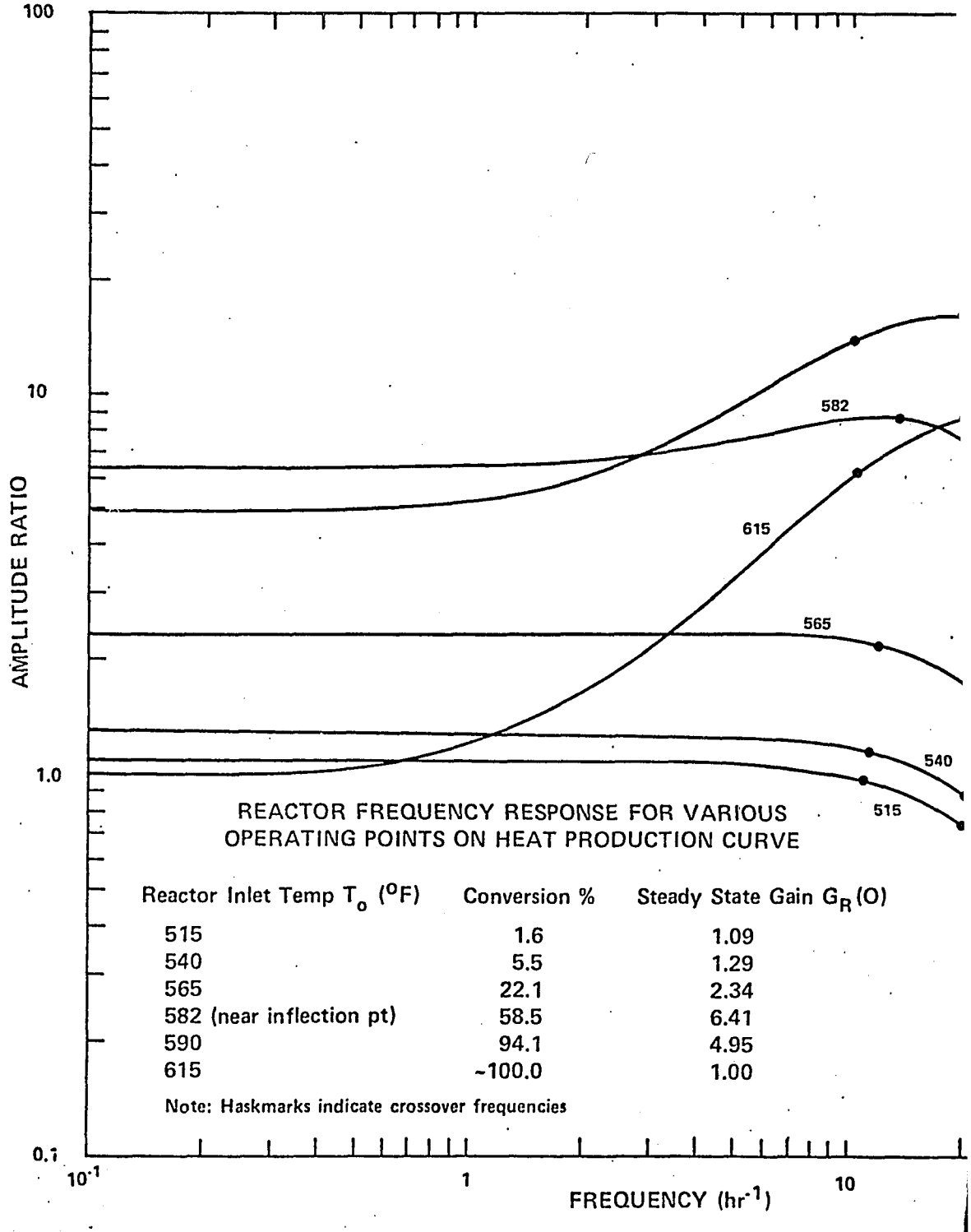

REACTOR FREQUENCY RESPONSE FOR VARIOUS OPERATING POINTS ON HEAT PRODUCTION CURVE

Reactor Inlet Temp T_o (^oF)	Conversion %	Steady State Gain $G_R(O)$
515	1.6	1.09
540	5.5	1.29
565	22.1	2.34
582 (near inflection pt)	58.5	6.41
590	94.1	4.95
615	~100.0	1.00

Note: Haskmarks indicate crossover frequencies

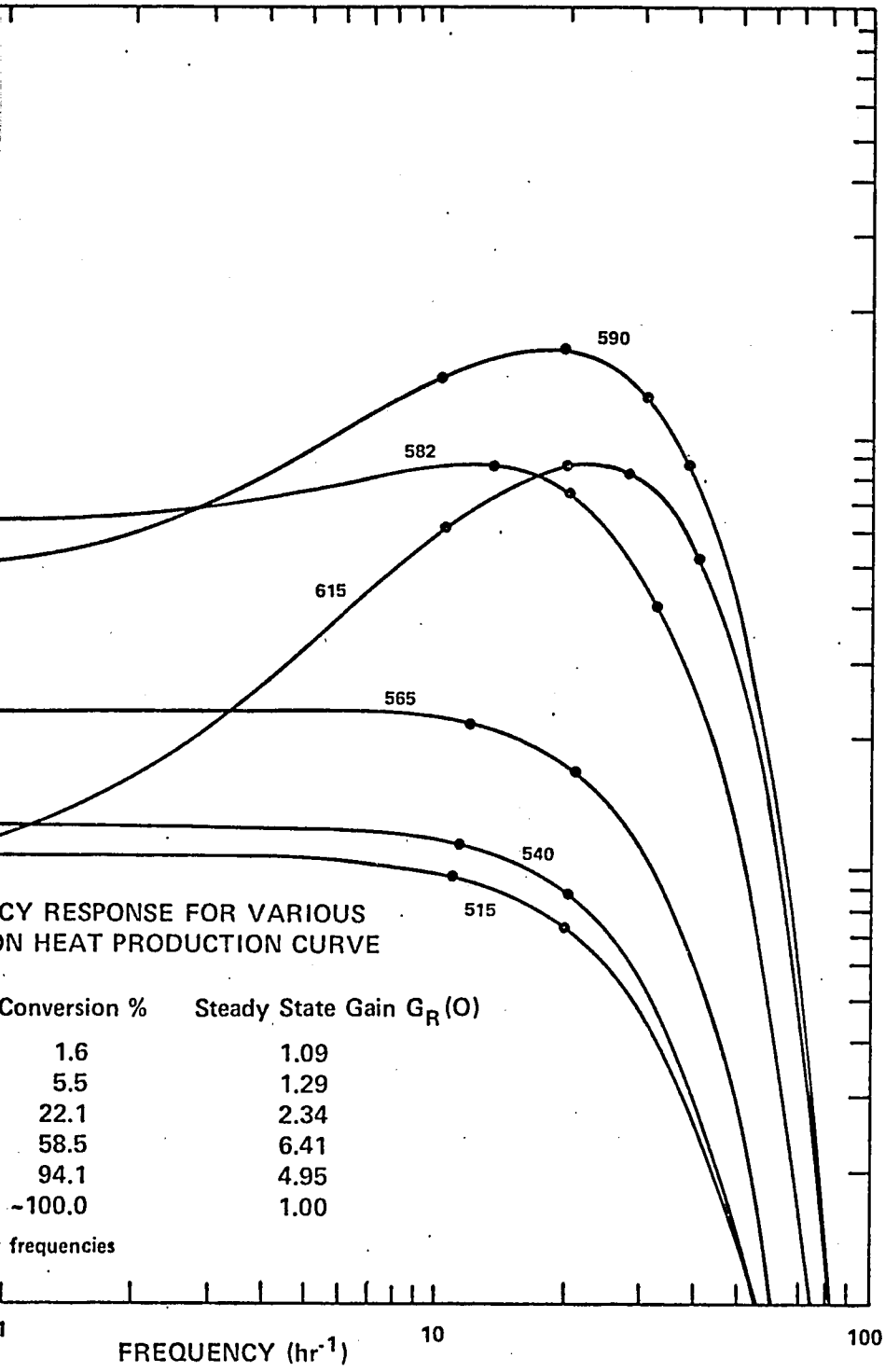
590
582
615
565
540
515
CY RESPONSE FOR VARIOUS
ON HEAT PRODUCTION CURVE
Conversion %
Steady State Gain $G_R(O)$
1.6
1.09
5.5
1.29
22.1
2.34
58.5
6.41
94.1
4.95
~100.0
1.00
frequencies
1
10
100
FREQUENCY (hr^{-1})

Figure 3

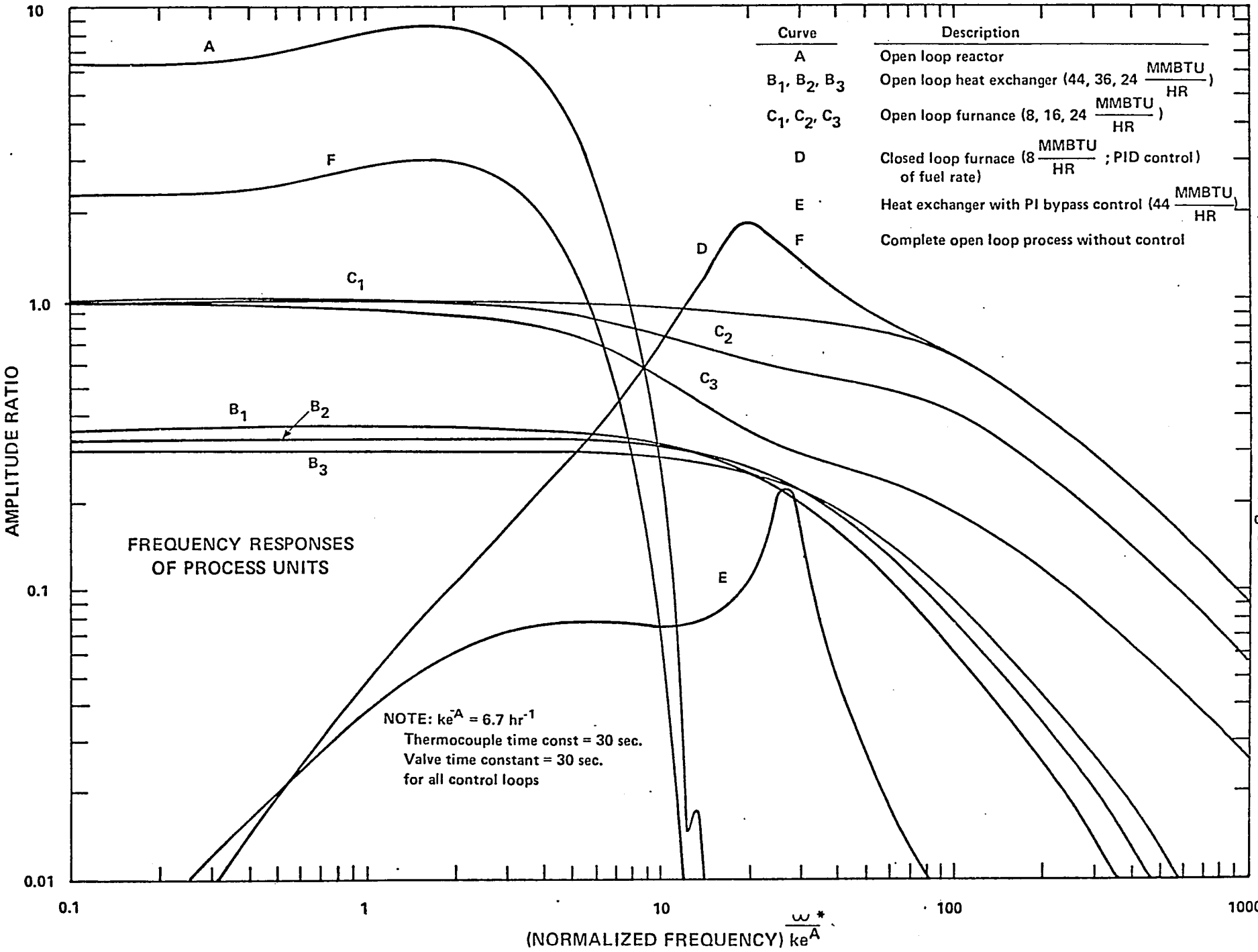
Curve
Description
A
Open loop reactor
B_1, B_2, B_3
Open loop heat exchanger (44, 36, 24 MMBTU/HR)
C_1, C_2, C_3
Open loop furnance (8, 16, 24 MMBTU/HR)
D
Closed loop furnace (8 MMBTU/HR ; PID control of fuel rate)
E
Heat exchanger with PI bypass control (44 MMBTU/HR)
F
Complete open loop process without control
FREQUENCY RESPONSES OF PROCESS UNITS
NOTE: $ke^{-A} = 6.7\ hr^{-1}$
Thermocouple time const = 30 sec.
Valve time constant = 30 sec.
for all control loops
AMPLITUDE RATIO
10
1.0
0.1
0.01
0.1
1
10
100
1000
$\frac{\omega^*}{ke^A}$
(NORMALIZED FREQUENCY)

Figure 4a

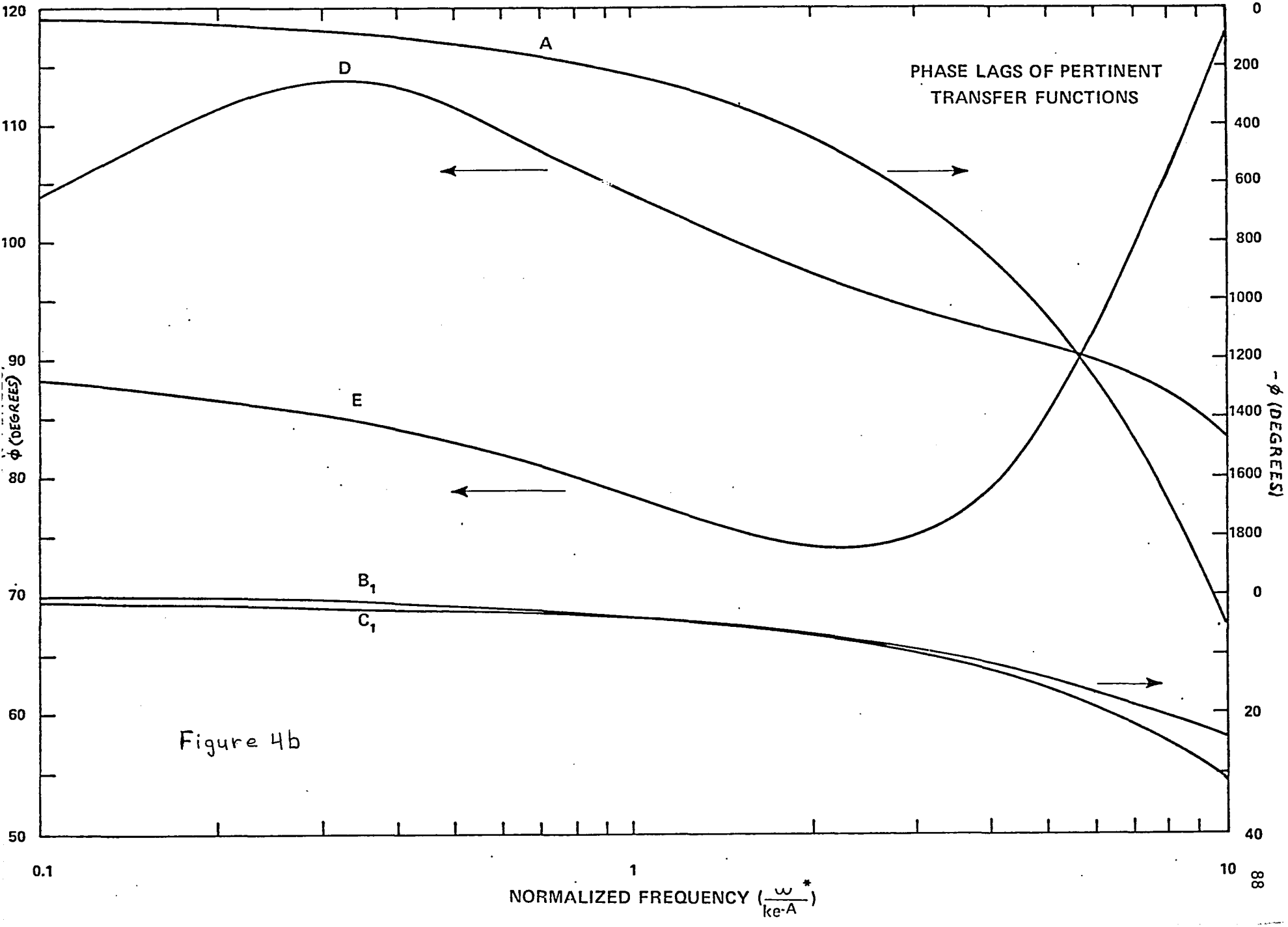
PHASE LAGS OF PERTINENT
TRANSFER FUNCTIONS
A
D
E
B_1
C_1
120
110
100
90
80
70
60
50
0
200
400
600
800
1000
1200
1400
1600
1800
0
20
40
ϕ (DEGREES)
$-\phi$ (DEGREES)
0.1
1
10
NORMALIZED FREQUENCY $(\frac{\omega^*}{k_e \cdot A})$

Figure 4b

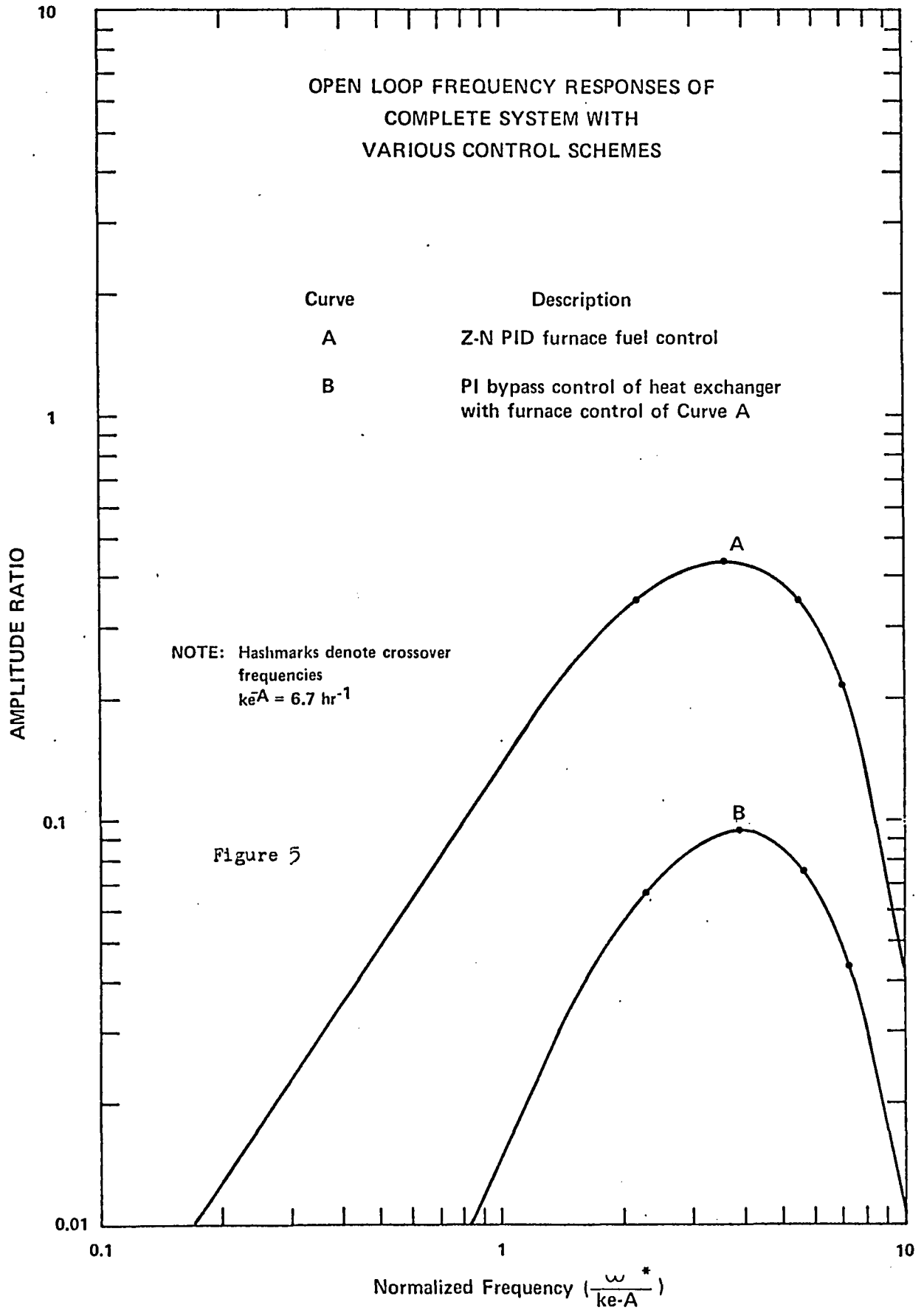
OPEN LOOP FREQUENCY RESPONSES OF
COMPLETE SYSTEM WITH
VARIOUS CONTROL SCHEMES
Curve
Description
A
Z-N PID furnace fuel control
B
PI bypass control of heat exchanger with furnace control of Curve A
NOTE: Hashmarks denote crossover frequencies
$k\bar{e}^A = 6.7\ hr^{-1}$
A
B
AMPLITUDE RATIO
10
1
0.1
0.01
0.1
1
10
Normalized Frequency $(\frac{\omega^*}{ke\text{-}A})$

Figure 5

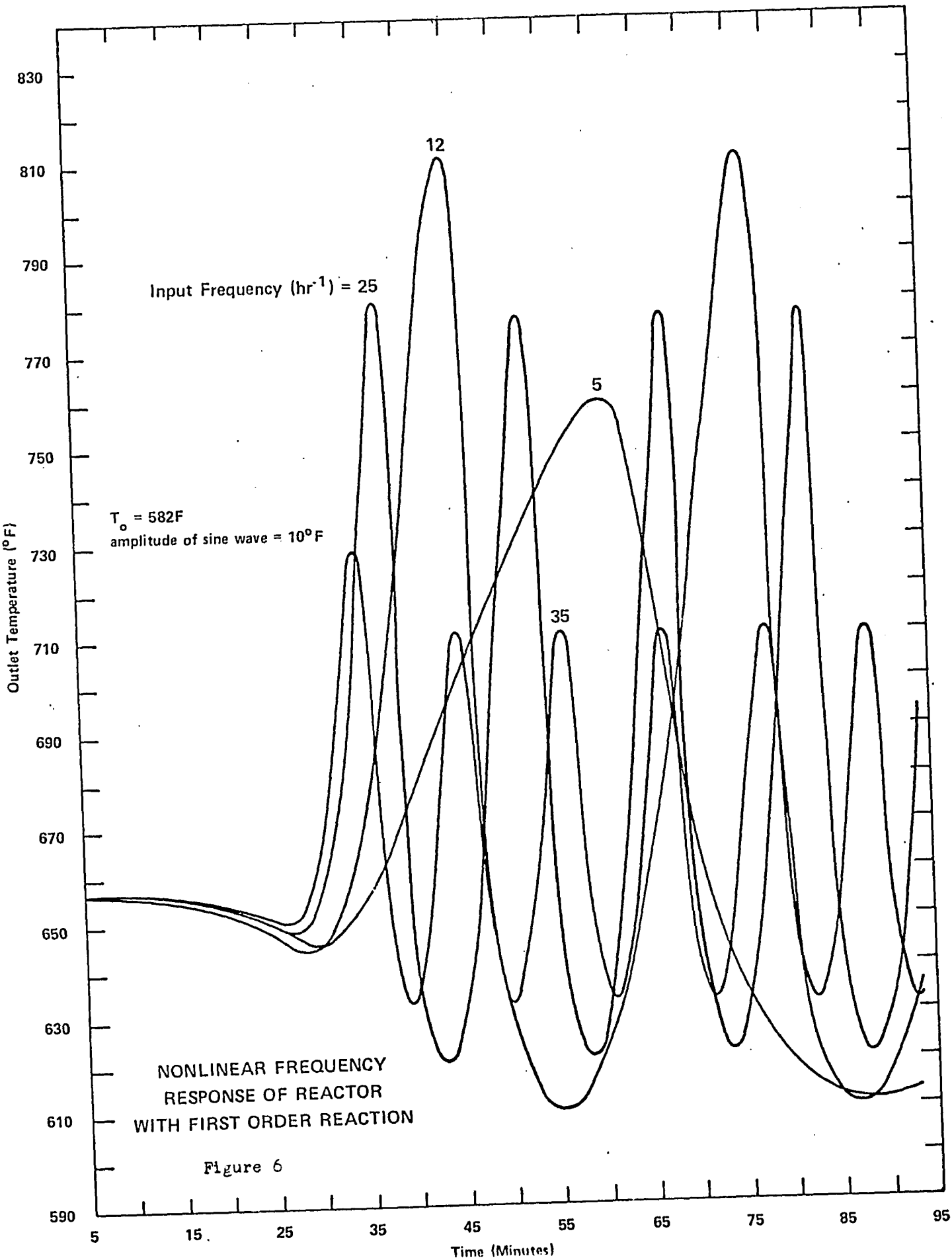

NONLINEAR FREQUENCY RESPONSE OF REACTOR WITH FIRST ORDER REACTION

Figure 6

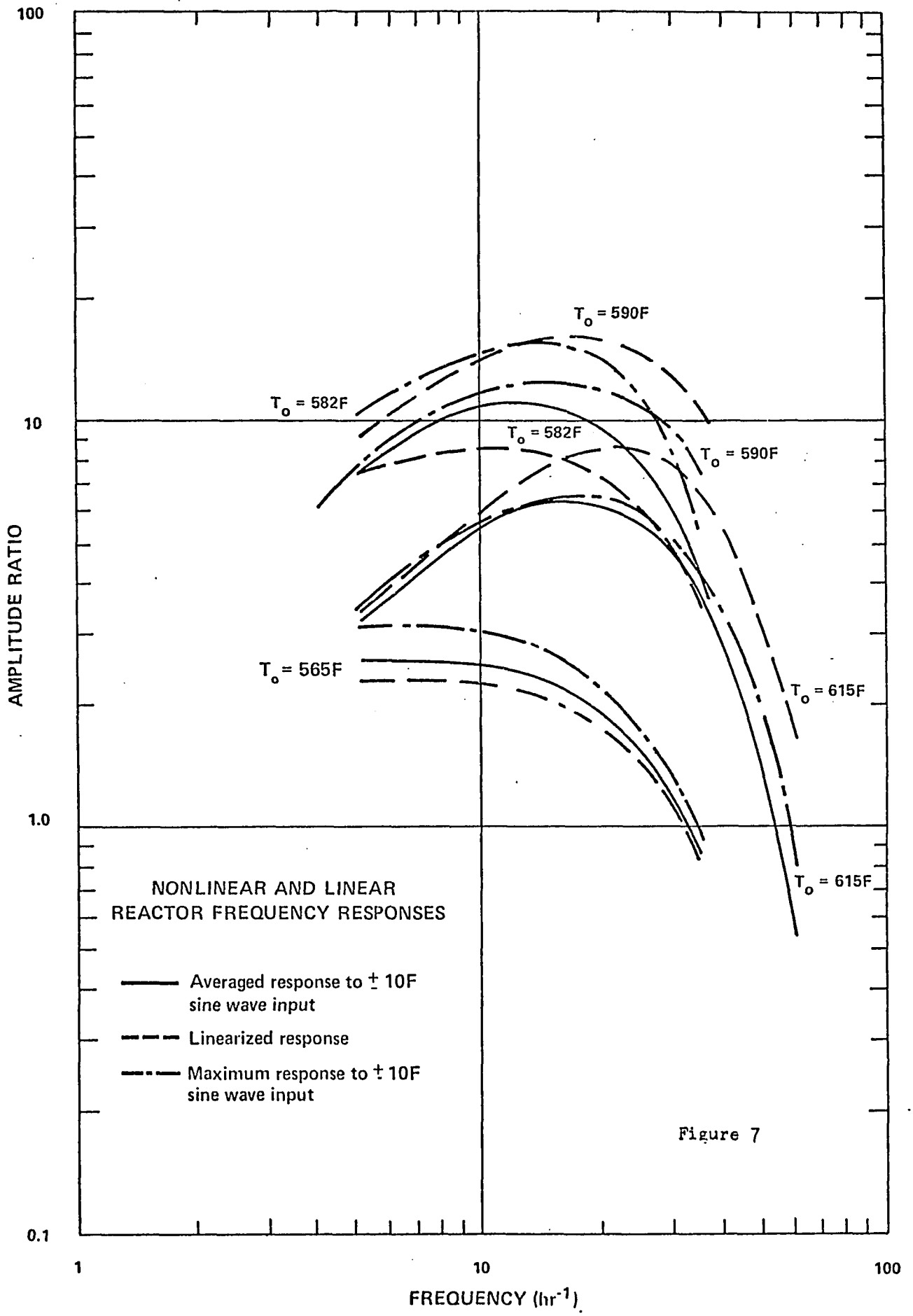
100
10
1.0
0.1
AMPLITUDE RATIO
1
10
100
FREQUENCY (hr^{-1})
T_o = 590F
T_o = 582F
T_o = 582F
T_o = 590F
T_o = 565F
T_o = 615F
T_o = 615F
NONLINEAR AND LINEAR
REACTOR FREQUENCY RESPONSES
Averaged response to ± 10F sine wave input
Linearized response
Maximum response to ± 10F sine wave input

Figure 7

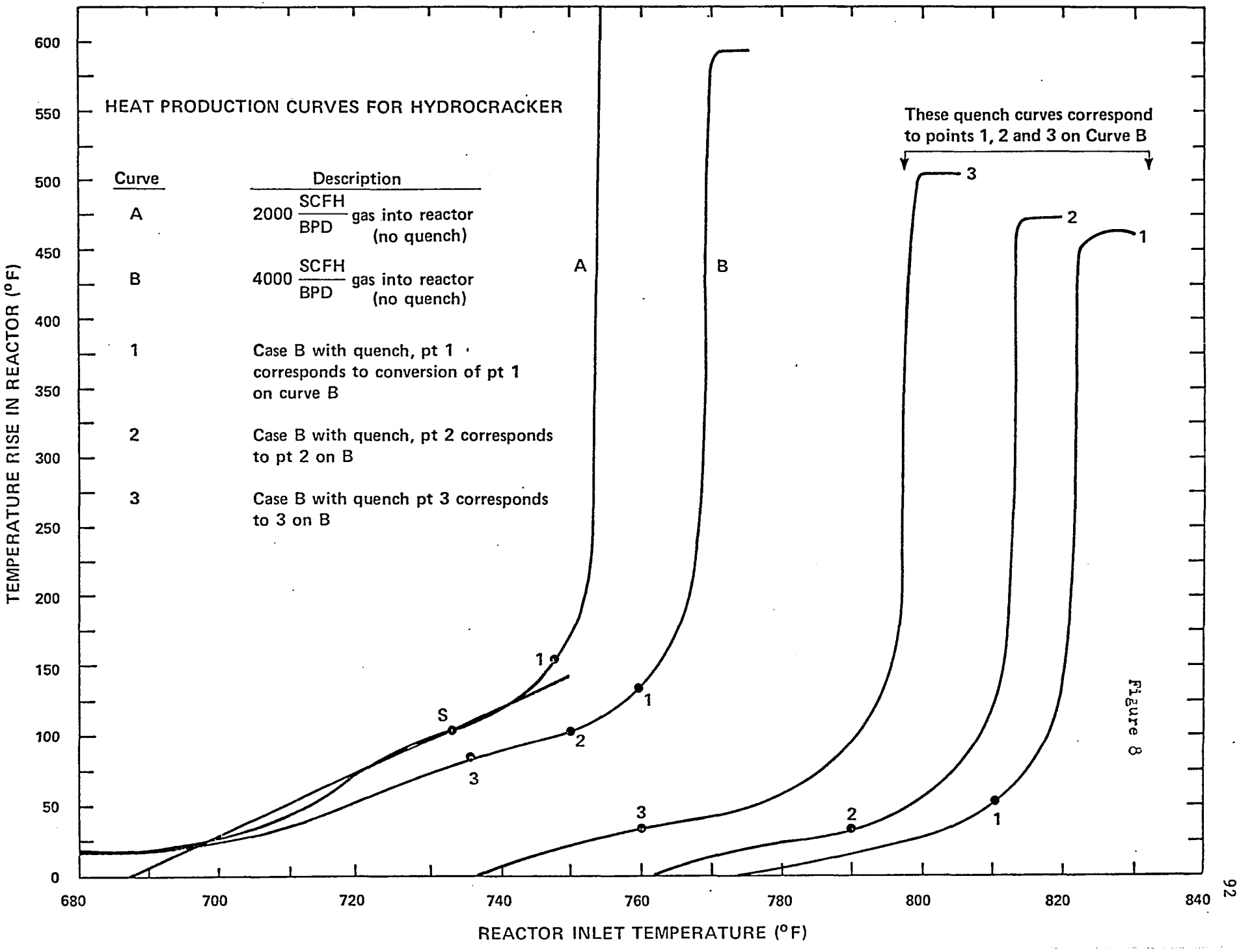
HEAT PRODUCTION CURVES FOR HYDROCRACKER
Curve
Description
A
2000 SCFH/BPD gas into reactor (no quench)
B
4000 SCFH/BPD gas into reactor (no quench)
1
Case B with quench, pt 1 corresponds to conversion of pt 1 on curve B
2
Case B with quench, pt 2 corresponds to pt 2 on B
3
Case B with quench pt 3 corresponds to 3 on B
These quench curves correspond to points 1, 2 and 3 on Curve B
TEMPERATURE RISE IN REACTOR (°F)
REACTOR INLET TEMPERATURE (°F)
600
550
500
450
400
350
300
250
200
150
100
50
0
680
700
720
740
760
780
800
820
840
A
B
S
1
2
3

Figure 8

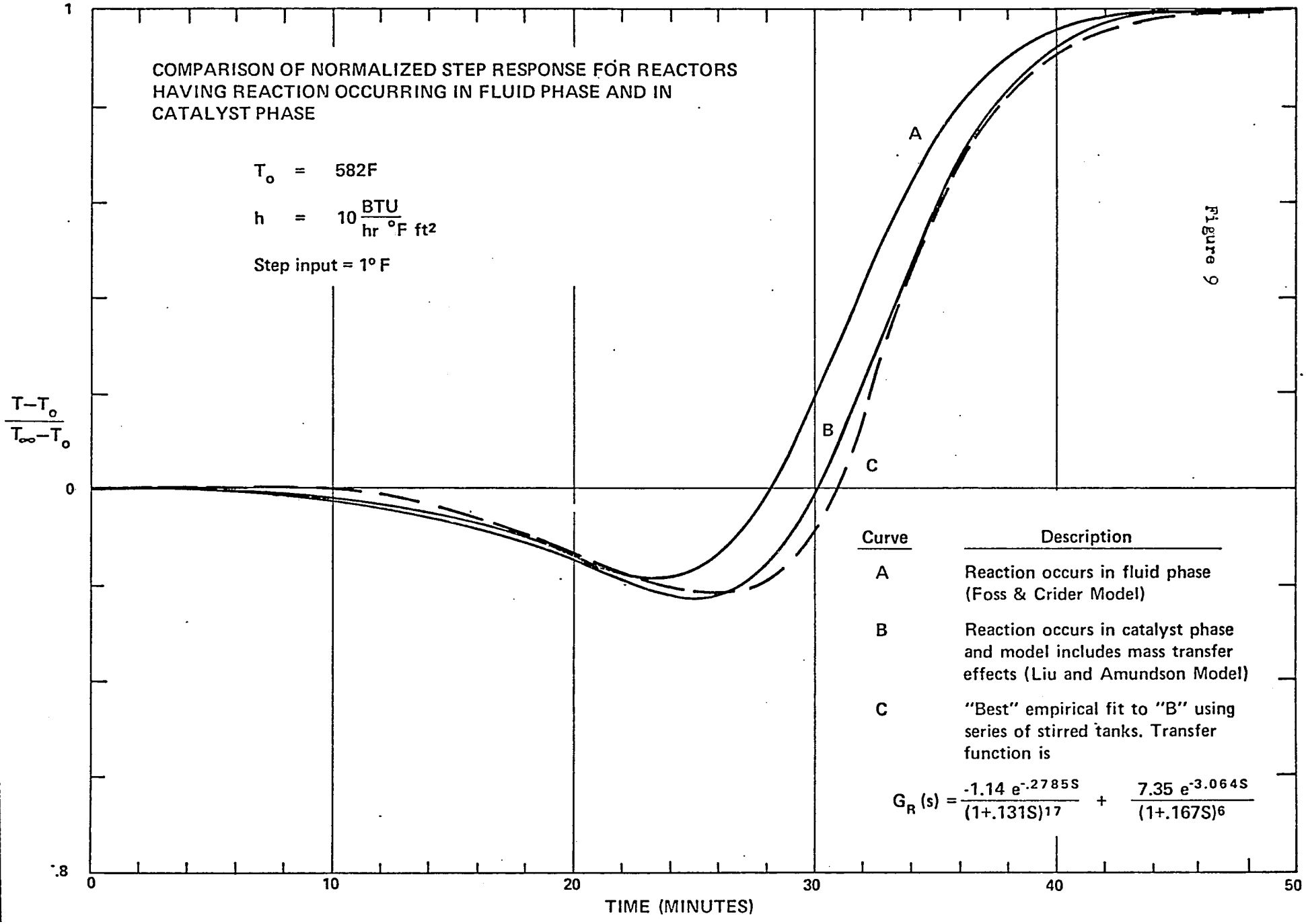
COMPARISON OF NORMALIZED STEP RESPONSE FOR REACTORS HAVING REACTION OCCURRING IN FLUID PHASE AND IN CATALYST PHASE
T_o = 582F
h = 10 BTU / hr °F ft²
Step input = 1° F
A
B
C
Curve
Description
A
Reaction occurs in fluid phase (Foss & Crider Model)
B
Reaction occurs in catalyst phase and model includes mass transfer effects (Liu and Amundson Model)
C
"Best" empirical fit to "B" using series of stirred tanks. Transfer function is
$G_R(s) = \frac{-1.14\, e^{-.2785S}}{(1+.131S)^{17}} + \frac{7.35\, e^{-3.064S}}{(1+.167S)^{6}}$
$\frac{T-T_o}{T_\infty-T_o}$
1
0
-.8
0
10
20
30
40
50
TIME (MINUTES)

Figure 9

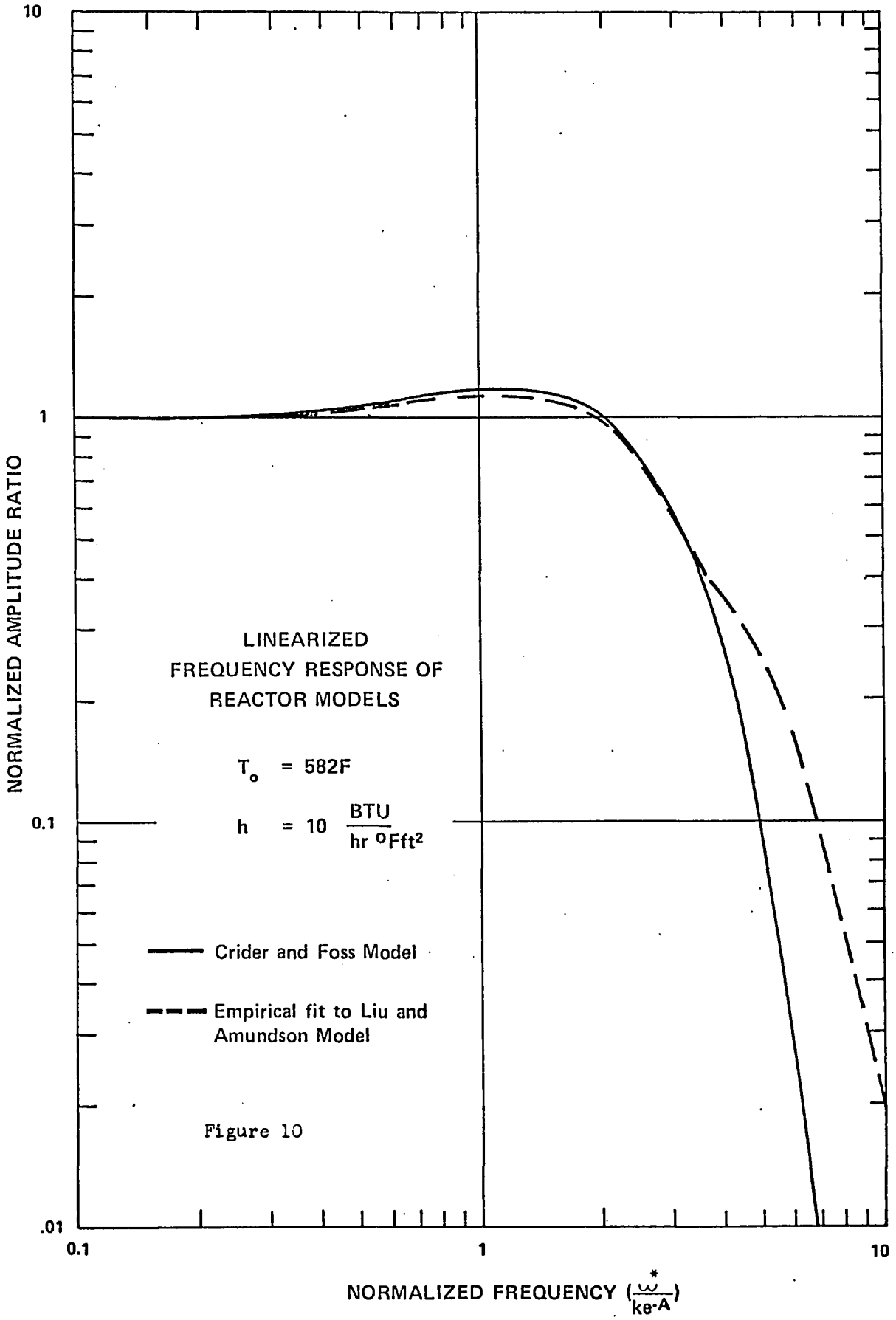
10
1
0.1
.01
0.1
1
10
NORMALIZED AMPLITUDE RATIO
NORMALIZED FREQUENCY $(\frac{\omega^*}{ke\text{-}A})$
LINEARIZED
FREQUENCY RESPONSE OF
REACTOR MODELS
T_o = 582F
h = 10 $\frac{BTU}{hr\ ^oFft^2}$
Crider and Foss Model
Empirical fit to Liu and
Amundson Model

Figure 10

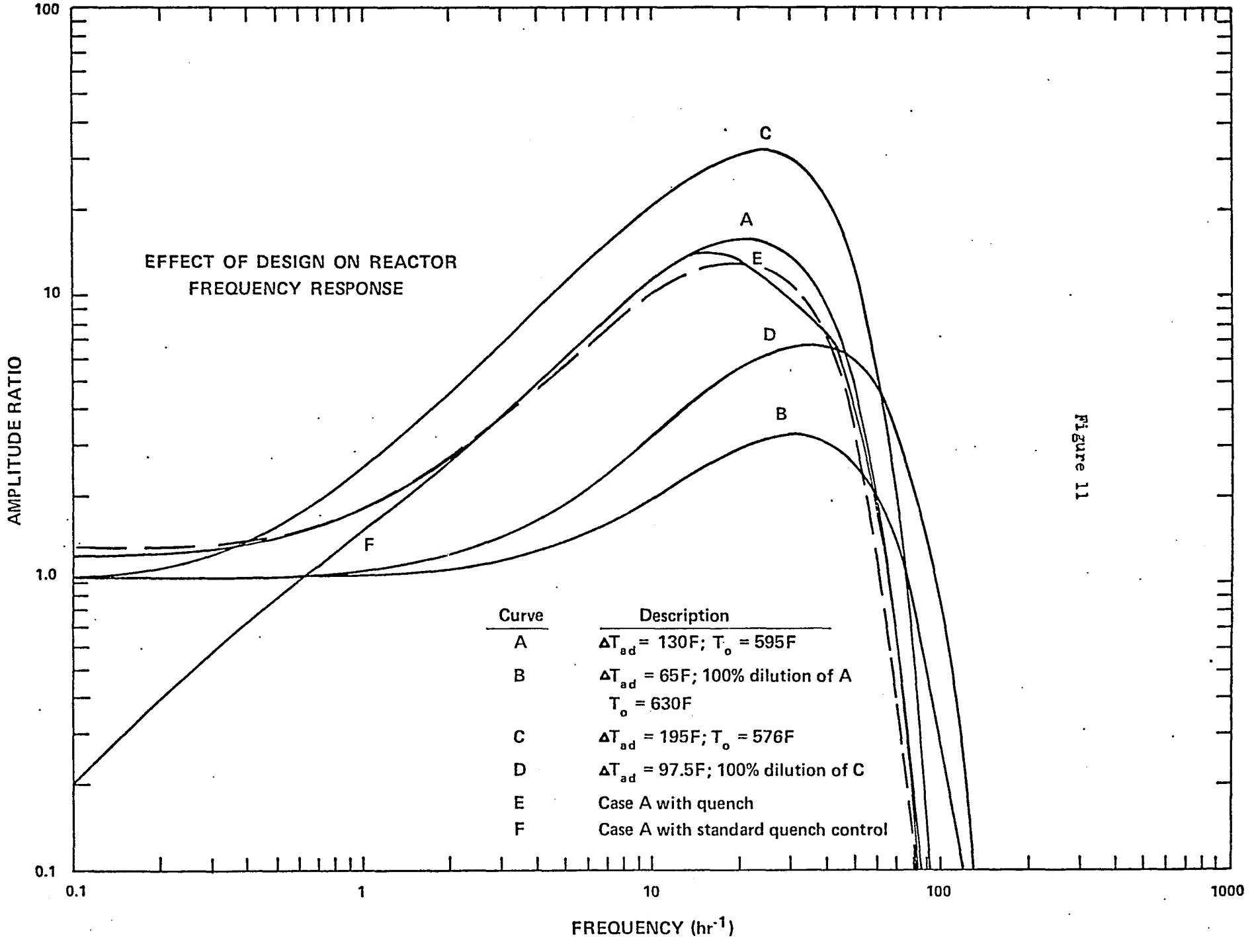
EFFECT OF DESIGN ON REACTOR
FREQUENCY RESPONSE
AMPLITUDE RATIO
FREQUENCY (hr-1)
100
10
1.0
0.1
0.1
1
10
100
1000
C
A
E
D
B
F
Curve
Description
A
ΔTad = 130F; To = 595F
B
ΔTad = 65F; 100% dilution of A
To = 630F
C
ΔTad = 195F; To = 576F
D
ΔTad = 97.5F; 100% dilution of C
E
Case A with quench
F
Case A with standard quench control

Figure 11

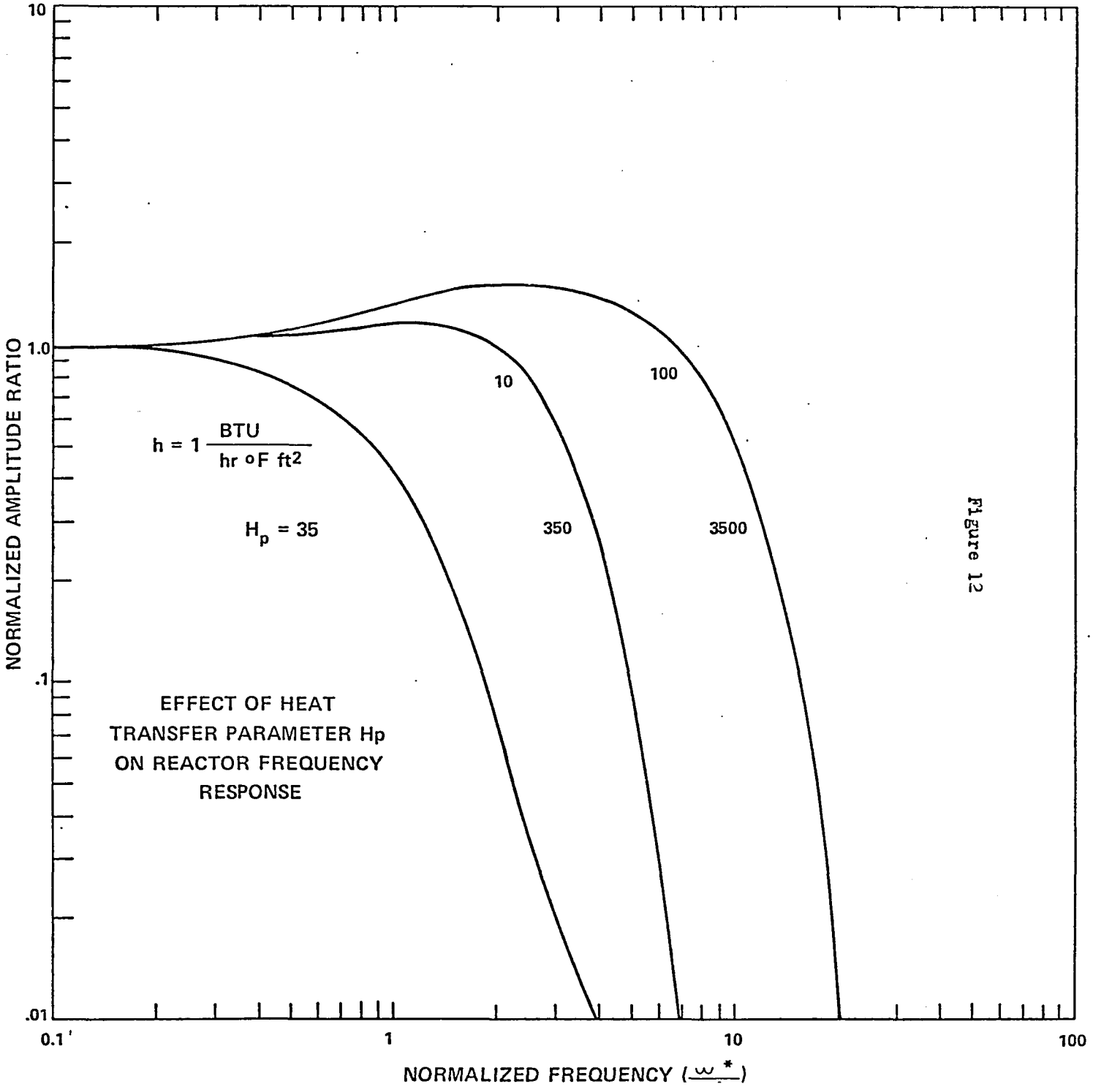
10
1.0
.1
.01
0.1
1
10
100
NORMALIZED AMPLITUDE RATIO
NORMALIZED FREQUENCY ($\frac{\omega}{\omega^*}$)
$h = 1 \frac{BTU}{hr\ ^oF\ ft^2}$
$H_p = 35$
10
100
350
3500
EFFECT OF HEAT TRANSFER PARAMETER Hp ON REACTOR FREQUENCY RESPONSE

Figure 12

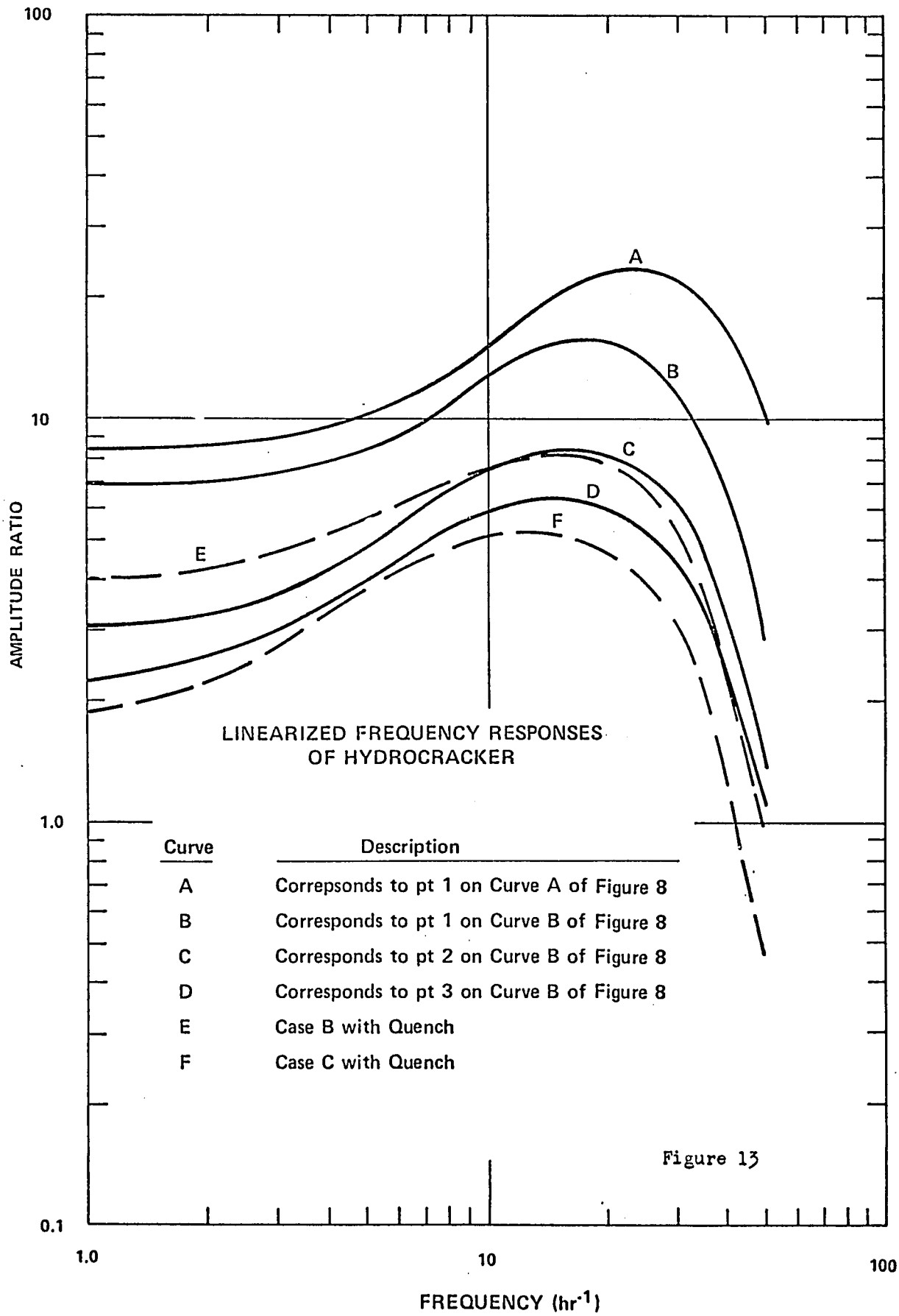

LINEARIZED FREQUENCY RESPONSES OF HYDROCRACKER

Curve	Description
A	Correpsonds to pt 1 on Curve A of Figure 8
B	Corresponds to pt 1 on Curve B of Figure 8
C	Corresponds to pt 2 on Curve B of Figure 8
D	Corresponds to pt 3 on Curve B of Figure 8
E	Case B with Quench
F	Case C with Quench

Figure 13

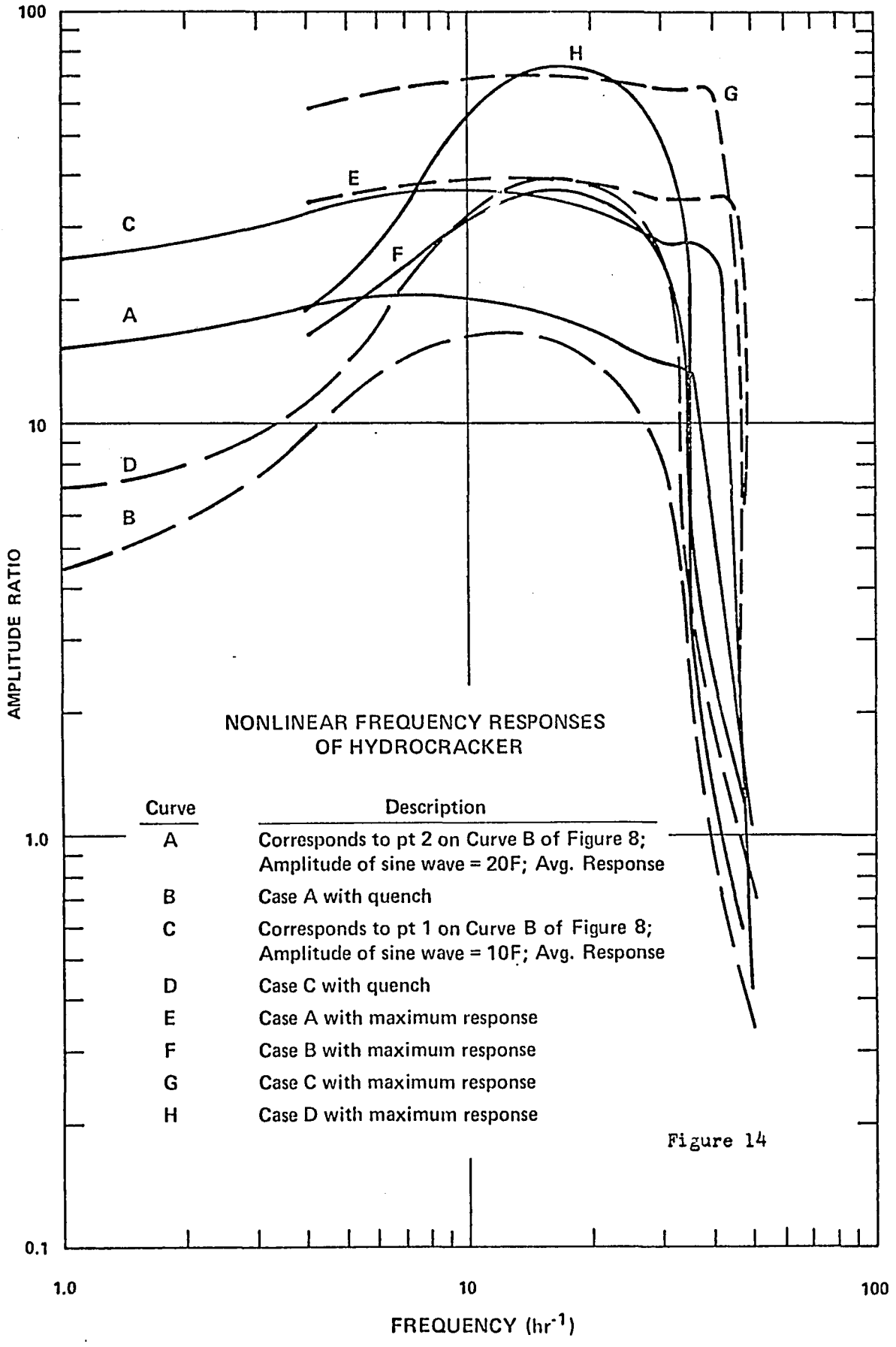
100
10
1.0
0.1
AMPLITUDE RATIO
1.0
10
100
FREQUENCY (hr^{-1})
H
G
E
C
F
A
D
B
NONLINEAR FREQUENCY RESPONSES
OF HYDROCRACKER
Curve
Description
A
Corresponds to pt 2 on Curve B of Figure 8; Amplitude of sine wave = 20F; Avg. Response
B
Case A with quench
C
Corresponds to pt 1 on Curve B of Figure 8; Amplitude of sine wave = 10F; Avg. Response
D
Case C with quench
E
Case A with maximum response
F
Case B with maximum response
G
Case C with maximum response
H
Case D with maximum response

Figure 14

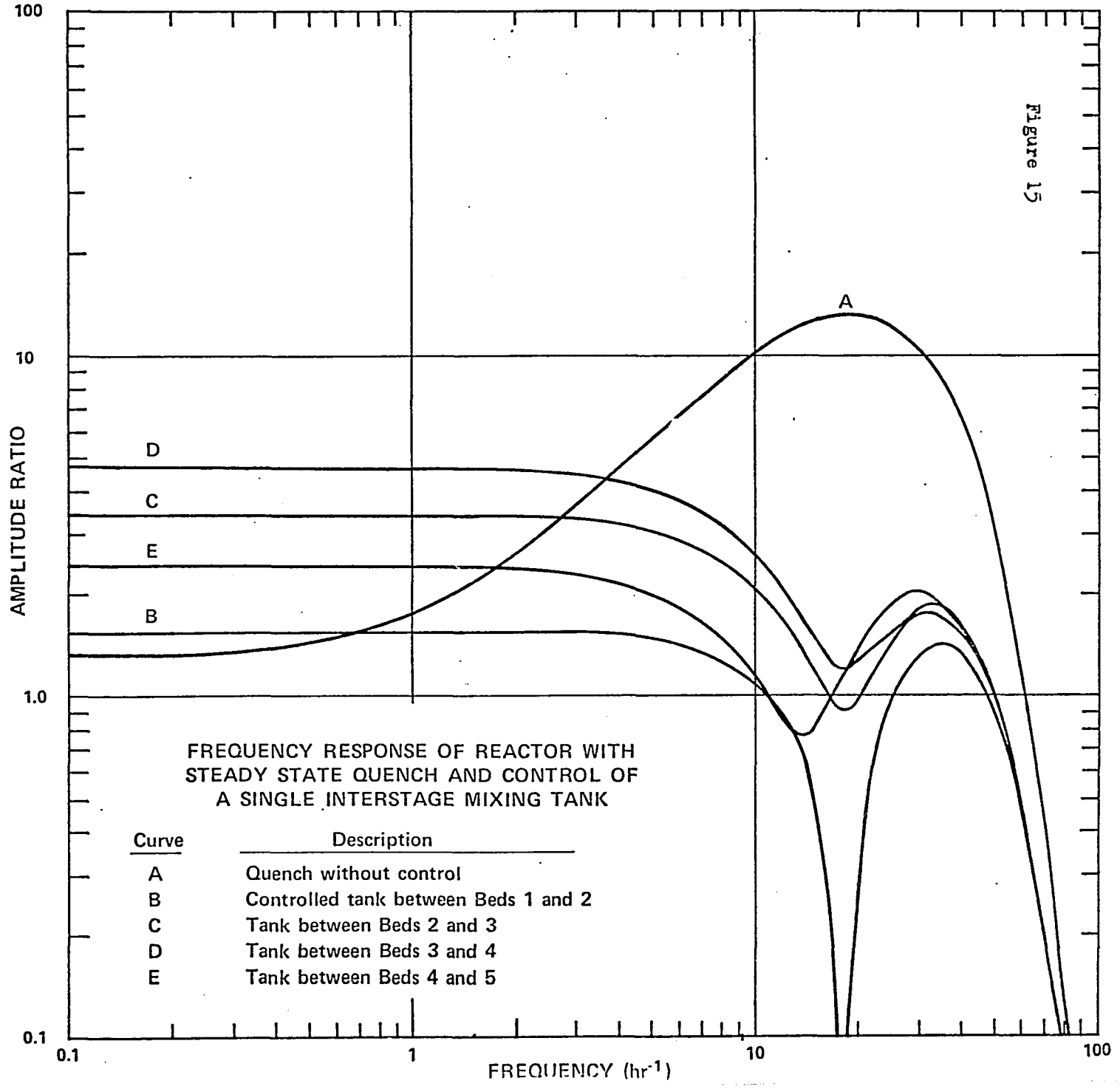
100
10
1.0
0.1
AMPLITUDE RATIO
A
D
C
E
B
0.1
1
10
100
FREQUENCY (hr-1)
FREQUENCY RESPONSE OF REACTOR WITH
STEADY STATE QUENCH AND CONTROL OF
A SINGLE INTERSTAGE MIXING TANK
Curve
Description
A
Quench without control
B
Controlled tank between Beds 1 and 2
C
Tank between Beds 2 and 3
D
Tank between Beds 3 and 4
E
Tank between Beds 4 and 5

Figure 15

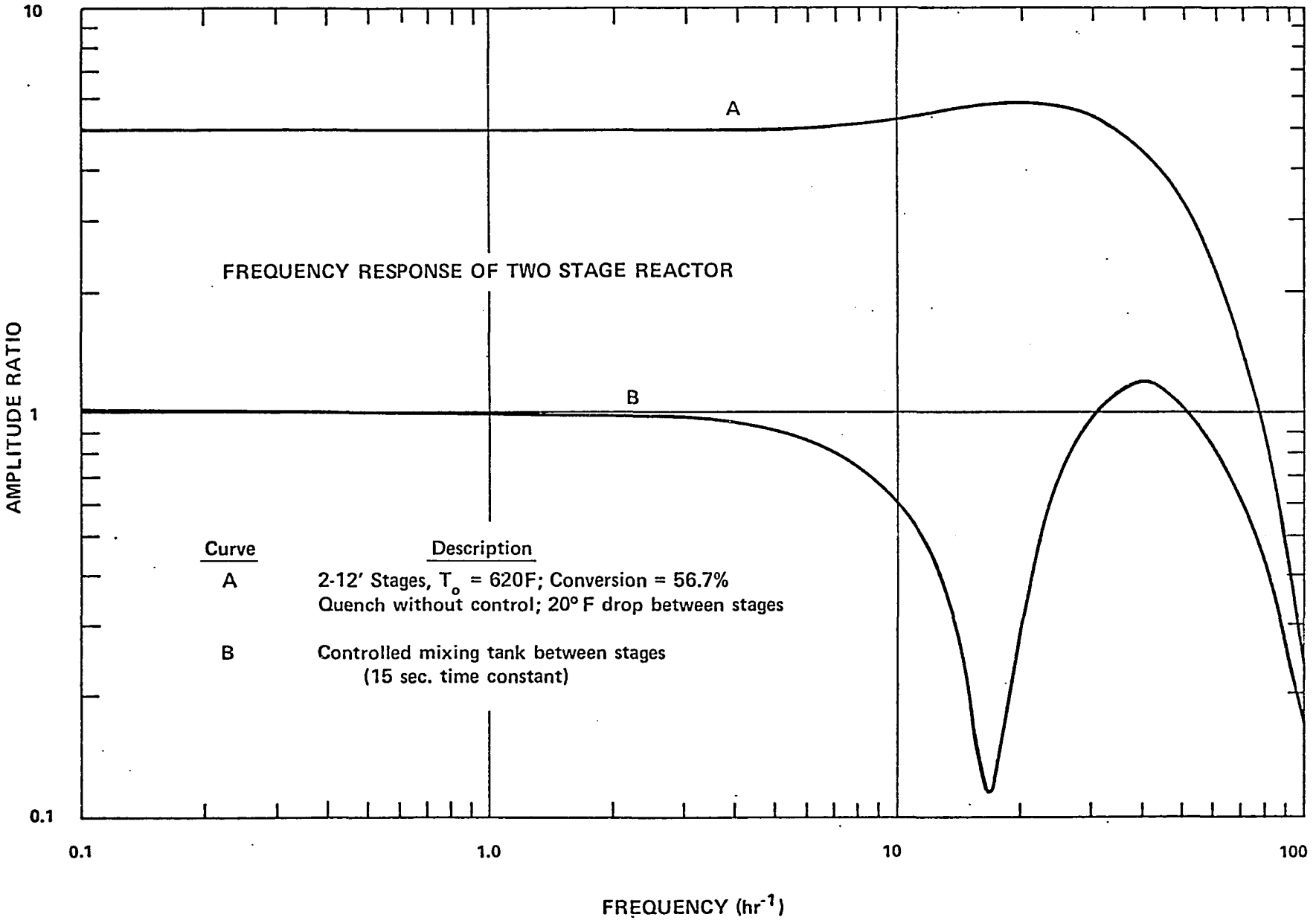
FREQUENCY RESPONSE OF TWO STAGE REACTOR
A
B
Curve
Description
A
2-12' Stages, T_o = 620F; Conversion = 56.7%
Quench without control; 20° F drop between stages
B
Controlled mixing tank between stages
(15 sec. time constant)
AMPLITUDE RATIO
10
1
0.1
0.1
1.0
10
100
FREQUENCY (hr^{-1})

Figure 16

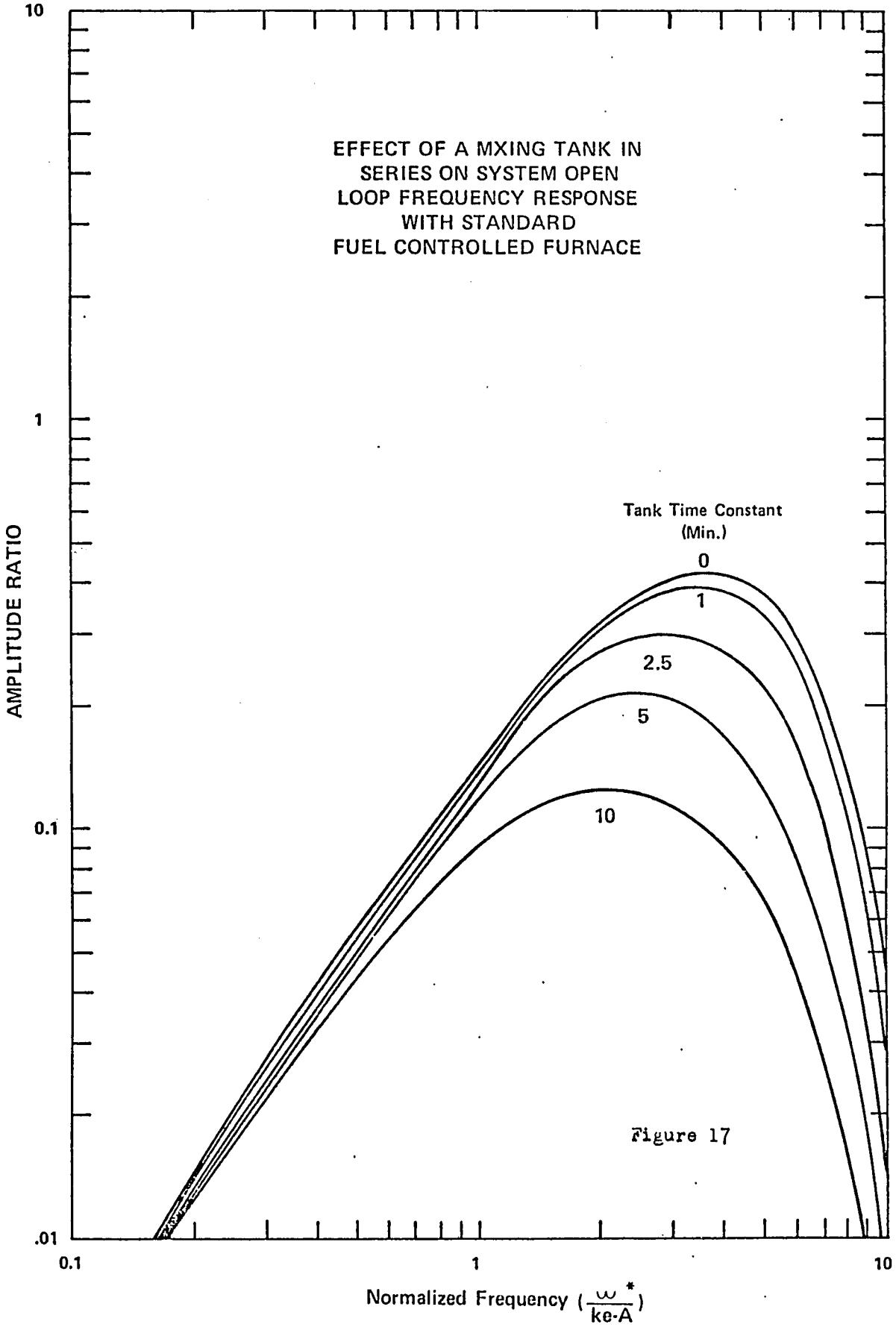
EFFECT OF A MXING TANK IN
SERIES ON SYSTEM OPEN
LOOP FREQUENCY RESPONSE
WITH STANDARD
FUEL CONTROLLED FURNACE
Tank Time Constant
(Min.)
0
1
2.5
5
10
AMPLITUDE RATIO
10
1
0.1
.01
0.1
1
10
Normalized Frequency ($\frac{\omega^*}{ke \cdot A}$)

Figure 17